EVALUATION OF CORN DISTILLER'S DRIED GRAINS WITH SOLUBLES AS A FUNCTIONAL MATERIAL TO REPLACE SYNTHETIC RESIN IN WOOD PARTICLEBOARDS

A Thesis
Submitted to the Graduate Faculty
of the
North Dakota State University
of Agriculture and Applied Science

By

Joshua Dong Xiong Liaw

In Partial Fulfillment of the Requirements
for the Degree of
MASTER OF SCIENCE

Major Program:
Mechanical Engineering

June 2019

Fargo, North Dakota

North Dakota State University
Graduate School

Title

EVALUATION OF CORN DISTILLER'S DRIED GRAINS WITH SOLUBLES AS A FUNCTIONAL MATERIAL TO REPLACE SYNTHETIC RESIN IN WOOD PARTICLEBOARDS

By

Joshua Dong Xiong Liaw

The Supervisory Committee certifies that this ***disquisition*** complies with North Dakota State University's regulations and meets the accepted standards for the degree of

MASTER OF SCIENCE

SUPERVISORY COMMITTEE:

Dr. Dilpreet Bajwa
Chair

Dr. Chad Ulven

Dr. Sreekala Bajwa

Approved:

08/20/2019
Date

Dr. Alan Kallmeyer
Department Chair

ABSTRACT

Corn distiller's dried grains with solubles (DDGS) is mostly marketed as a livestock feed due to its high protein content of 30%. Recently, the proteins in DDGS have shown potential to act as binding agents along with melamine-urea-formaldehyde resin. However, it is unknown if DDGS can be chemically functionalized as a natural binder to replace synthetic resin in particleboard. In this study, several formulations were tested using various concentrations of acetic acid and sodium hydroxide treatments with combinations of temperature, DDGS concentrations, particle sizes, and wax. FTIR results indicated that DDGS proteins were decoupled through acid or alkali treatments, and acid treated DDGS in particleboards displayed higher improvements in internal bond strength as well as the moisture resistance of the particleboards. These results suggest that acid or alkali treated DDGS has potential to act as a natural binder for manufacturing medium-density particleboard.

ACKNOWLEDGEMENTS

It has been an interesting journey to complete my graduate study at NDSU, but overall it has been a rewarding one. I have persevered and managed to overcome many challenges through the help of my committee members, family, and friends. Because of their help, I am proud to acknowledge that the success of this thesis was not wholly my own but also from the contribution of many significant others.

First and foremost, I want to profusely thank my advisor, Dr. Dilpreet Bajwa for his unwavering guidance and support throughout my graduate school career. There were countless times when I underestimated myself but working under his supervision has inspired me to push my limits to achieve my goals. Moreover, his willingness to always be open for critical discussions helped me to overcome numerous obstacles in my research work.

Next, I am not only thankful to Dr. Dilpreet Bajwa but also thankful to my other committee members, Dr. Chad Ulven and Dr. Sreekala Bajwa, for their generosity in allowing me to use their equipment to conduct my research and providing me with valuable input. Their expertise and feedbacks in advising me through this project led to the advancement of my research to replace dangerous synthetic resins with corn DDGS as a binder to manufacture particleboards.

I would also like to thank my research group members Andrew Norris, Jamileh Shojaeiarani, Chad Rehovsky, and Ghazal Vahidi for helping me to drive this project forward. In addition, I appreciate the help of NDSU's statistical consultant Curt Doetkott for kindly assisting me with the statistical analysis part. I must also thank Drew Taylor and Tammi Neville from the NDSU Center for Writers for improving my technical writing skills.

Most importantly, the journey to accomplish this thesis could not have happened without my family members. Therefore, I am deeply grateful to my parents and siblings in Malaysia for providing me with unconditional love, spiritual help, and supporting me through my ups and downs.

Finally, I owe a big thank you to North Dakota Corn Council for funding this project. My success serves as a testament to your generous financial support.

DEDICATION

To my dearest parents and siblings.

Thank you for always being there for me.

TABLE OF CONTENTS

LIST OF TABLES

LIST OF FIGURES

LIST OF ABBREVIATIONS

DSC.....Differential scanning calorimetry.

FTIR.....Fourier transform infrared spectroscopy.

TGA .....Thermogravimetric analysis.

ANOVA .....Analysis of variance.

DDGS.....Distiller's dried grains with solubles.

ANSI .....American National Standards Institute.

ASTM .....American Society for Testing and Materials.

ADF.....Acid detergent fiber.

NDF.....Neutral detergent fiber.

1. INTRODUCTION[1]

Particleboards are one of the most demanded building materials as they can be applied in floor, wall, ceiling panels, counter and desk tops [1]. The history of particleboard manufacturing dates back to the 1950s when manufacturers started utilizing industrial wood residues produced during the production of softwood lumber and plywood [2]. Subsequently, the field continued to expand and the global wood-based panel market size is projected to reach 174.55 billion USD by 2025 [3]. The growth in wood consumption has led to a high worldwide deforestation rate and may result in many devastating effects on our environment [4]. To accommodate the needs of industries, it is crucial to search for new lignocellulosic materials to reduce dependency on wood [5]. Moreover, conventional binders used in engineered wood products are synthetic resins such as urea formaldehyde, phenol formaldehyde, melamine fortified urea formaldehyde, and polymeric diphenylmethane diisocyanate [6]. However, factors such as the carcinogenic nature of formaldehyde emissions and the regulations put in place by agencies like the California Air Resources Board (CARB) have driven manufacturers to seek alternatives to formaldehyde resins [7].

To address the concerns of deforestation and formaldehyde emissions, alternative agriculture residues such as corn distiller's dried grains with solubles (DDGS) is safe and economical, which can potentially be used as a natural binder to eliminate the use of synthetic resin. The cost of DDGS was 4-6 cents per pound, which makes it cheaper than starch, wood fibers, and soy flour [8]. The adhesive properties of DDGS can be derived from its high

[1] Some materials in this thesis are derived from an article by Joshua D. Liaw, Dilpreet S. Bajwa, Jamileh Shojaeiarani, and Sreekala G. Bajwa and accepted for publication in Industrial Crops and Products on June 2019. Joshua D. Liaw had primary responsibility in performing all experiments and analyzing the results. Joshua D. Liaw also drafted and revised all versions of this thesis. Dilpreet S. Bajwa, Jamileh Shojaeirani, and Sreekala G. Bajwa served as proofreader and provided advice for this work, and Dilpreet S. Bajwa also supervised this project.

hydrophobic zein protein content [8], which amounts to 30% protein [9]. A recent study reported that DDGS was added at 5 wt. % together with melamine urea formaldehyde resin at 10 wt. %, and wax at 10 wt. % into particleboard, and resulted in an increase in mechanical properties as well as the moisture resistance of the particleboard [10]. In this case, the proteins of the DDGS were dissociated and reacted with the resin, which improved the mechanical properties, while the results indicated that the improvement in moisture resistance was attributed to the fat component of the DDGS [10]. Furthermore, to utilize the adhesive effect of the protein for bonding and solubilization, the native protein must be denatured to expose more polar groups [11]. Some of the most widely used methods to denature proteins were to expose it to acid or alkali [12], which affects the ability of the protein to come in intimate contact with the wood surface differently [11]. However, it was unknown that if we can use DDGS alone as a natural binder to manufacture formaldehyde free particleboard by denaturing the DDGS protein with acid or alkali.

Thus, the purpose of this study is to identify suitable chemical treatment methods to functionalize the DDGS proteins, while maintaining the properties of the particleboard without the need of dangerous industrial binder. This study investigated the performance of natural binder derived from sodium hydroxide and acetic acid treated DDGS. These formulas were tested at various chemical concentrations with blends of wax for both sodium hydroxide and acetic acid, combined with three temperatures and two DDGS screen sizes. Finally, the results were compared to both ANSI A208.1-2009 standard and manufactured wood particleboard that used two different blends of resin and wax.

1.1. Objectives

The objectives of this research are to understand whether chemically functionalized DDGS with acetic acid or sodium hydroxide can act as natural binder in wood particleboards and to analyze the physical and mechanical properties of medium-density particleboards. A major aspect of this research is to eliminate the use of traditional formaldehyde based resins and develop a safe, strong, and cost effective for industrial applications. This thesis evaluates the following hypotheses:

Hypothesis 1: The protein of the DDGS can be functionalized either with acetic acid or sodium hydroxide as a natural binder in medium-density particleboards.

Hypothesis 2: Higher DDGS concentrations will improve the physical and mechanical properties of the particleboards.

Hypothesis 3: Smaller DDGS particle size will improve the mechanical properties of the particleboards.

2. LITERATURE REVIEW

2.1. Particleboard

2.1.1. Chemical composition of wood

The chemical composition of wood differs with tree part, geographic location, climate, and soil conditions [13]. The two major chemical components in wood are lignin and carbohydrate where the carbohydrate part of wood consists of cellulose and the hemicelluloses [13]. Cellulose, hemicellulose, and lignin of the cell walls are in a 4:3:3 ratio and this ratio can deviate from hardwood, softwood, and herbs [14]. Additionally, cellulose is the strongest polymer in wood and is mainly responsible for giving strength in the wood due to its high degree of polymerization and linear orientation [11]. Each cellulose molecule composed of a linear chain of glucose residues that are covalently bonded to one another and stabilized by hydrogen bonds within the chain [15], as shown in Figure 1. Hemicellulose functions as a link between the cellulose and the amorphous lignin and increases the packing density of the cell wall, whereas lignin is responsible for keeping the fibers together and functions as a stiffening agent for the cellulose molecules [11]. All of these components help in different degrees to the strength of the wood [11].

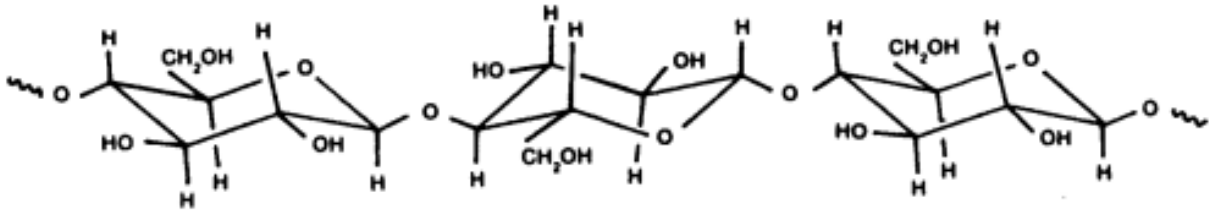

Figure 1. The molecular structure of cellulose. Reprinted with permission from [13]. Copyright 1984, American Chemical Society.

2.1.2. Comparison of manufactured boards

This section discusses the difference between particleboard, fiberboard, plywood, and oriented strand board as defined by ASTM D1554, ASTM D1038, and ASTM D7033. Particleboard is a generic term for a composite material composed of cellulosic materials, in the form of particles and bonded together with some sort of binder, and that may contain additives [16]. Particleboard is often made out of wood that can be in the form of discrete pieces such as chips, curls, flakes, sawdust, shavings, slivers, strands, wood wool, or wood flour; wood flour is particularly important in this study and is defined as a very fine wood that is reduced by a mill until it resembles wheat flour in appearance, and it can pass through a 40-mesh screen [16]. While particleboard is often made out of cellulosic particles, medium-density fiberboard is a composite panel composed of cellulosic fibers bonded together and fiber is differentiated with the slender threadlike elements resulting from mechanical or chemical defiberization, and known as fiber bundles [16]. In contrast to the bundled fibers in medium-density fiberboard, plywood is a crossbanded assembly built with several layers of veneer or veneer in combination with a lumber core bonded with an adhesive [17]. Lastly, oriented strand board is comprised of a mat-formed panel with oriented layers but made up of wood strands bonded with some sort of adhesive under heat and pressure [18]. These wood strands are defined as a small wood particle which has a length-to-width ratio of 2:1 [16].

2.1.3. Particleboard classification and usage

Particleboard has evolved into a highly engineered product that can be used in housing floor application and industrial used for making furniture, cabinets, tables, and countertops [2]. This section discusses classification of particleboard based on its density for different applications. Currently, the densities are defined by ANSI A208.1-2009, where the particleboard

densities are classified as high density (> 800 kg/m^3), medium density (between 640 to 800 kg/m^3), and low density (< 640 kg/m^3). Both high density and medium density particleboards are mainly used in commercial and industrial, whereas low density are used as a door core [19]. Table 1 shows the selected minimum requirements of high density (H), medium density (M), and low density (LD) particleboards on modulus of rupture, modulus of elasticity, internal bond, screw withdrawal, and linear expansion.

Table 1. Properties of the selected grades from ANSI A208.1-2009 [19].

Grade	Physical and Mechanical Properties				
	Modulus of Rupture (N/mm^2)	Modulus of Elasticity (N/mm^2)	Internal Bond (N/mm^2)	Screw Withdrawal (N)	Linear Expansion (max. %)
H-1	14.9	2160	0.81	1600	n/a
H-2	18.5	2160	0.81	1700	n/a
H-3	21.1	2475	0.90	1800	n/a
M-0	7.6	1380	0.31	n/a	n/a
M-1	10.0	1550	0.36	n/a	0.40
M-S	11.0	1700	0.36	800	0.40
LD-1	2.8	500	0.10	360	0.40
LD-2	2.8	500	0.14	520	0.40

2.1.4. Particleboard manufacturing process

The process of manufacturing particleboard begins with using wood residue and passes through several processes to obtain the finished product. These steps include raw material generation, classifying by size, drying, blending with resin and wax, forming, and hot pressing [20]. Figure 2 shows the process flow chart for a typical particleboard plant.

According to Neulicht et al. [20], raw materials such as wood chips, sawdust, and planer shavings are milled by hammermills, flakers, or refiners. The milled particles are screened using gyratory screens or air-classified to separate the core material from the surface material [20].

After separating, the particles are transported to the rotary dryers to reduce the moisture content to between 2 and 8 percent [20]. Next, the core and surface materials are transferred to blenders, and a spray nozzle, tube, or atomizer is used to mix the particles with resin, wax and other additives [20]. The amount of resin depended on the resin type and is typically 8% for urea-formaldehyde but can be as low as 2% for methylene diphenyl diisocyanate (MDI) [21]. Moreover, smaller particles tend to consume more resin due to their high surface-area-to-weight ratio [21].

The two most commonly used resins are phenol-formaldehyde and urea-formaldehyde [20]. Urea-formaldehyde resins are used in particleboards for interior applications whereas phenol-formaldehyde resins are used for exterior applications [20]. Other than the cellulosic material and a bonding system, additive is any material added to particleboard that can enhance the particleboard's dimensional stability, fire retardancy, or other properties [19]. Additives such as waxes are incorporated to improve the moisture resistance of the particleboard under wet conditions, while catalyst is added to accelerate the resin cure time and to minimize the press time [20]. The coated particles are fed to the forming machine to deposit resinated material in the form of a continuous mat [20].

Depending on the application, the type of boards may be a single layer or multi-layer [21]. Though there are two types of boards, multi-layer board is still the more common one [20]. A multi-layered board must be a balanced structure of 3 or 5 layers to prevent distortion or poor properties [21]. The surface layers are made up of fine particles, while coarser particles are used as the core of the board [21]. It is important to note that the overall strength of the board is controlled by the core of the board [22]. Moreover, the flexural strength and modulus of elasticity of the multi-layer board can be increased by changing the properties of its surface and

core layers [20]. Thus, multi-layer board has higher potential to perform better in mechanical properties compared with single layer board.

After forming, the mats are trimmed into its desired lengths and conveyed to the hot press [20]. The trimmed mats are then pressed under heat and pressure to activate the resin to bond the fibers into particleboards [20].

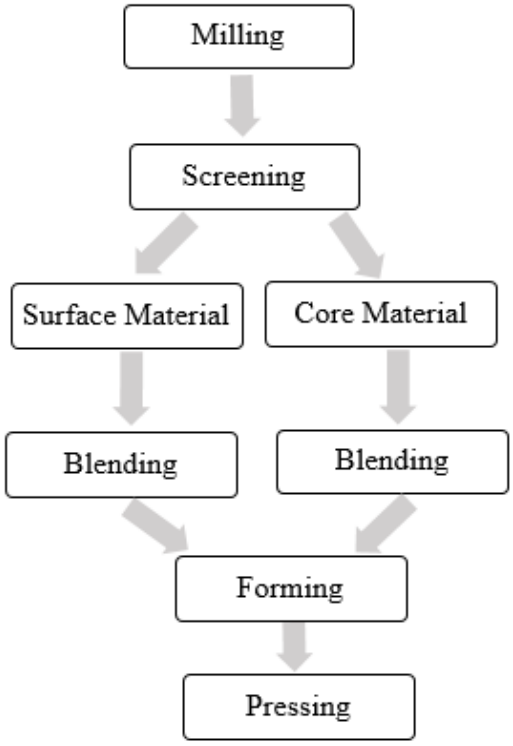

Figure 2. Adapted version of process flow chart for particleboard manufacturing in a typical particleboard plant [20].

2.1.5. Avoiding blow defects during board manufacturing

The board properties are influenced by the press temperature, press time, press pressure, and moisture content. Higher press temperatures and longer press times have shown improvements in physical and mechanical properties because sufficient heat was able to transfer to the core section of the board [23]–[25]. Higher press pressures have also shown improvement in physical and mechanical properties of the board and the density of the board was affected by

the press pressure [26]. One thing to note is that, during hot pressing, the moisture in the board will be converted to vapor and migrates to cooler areas such as the core of the board; this leads to faster heat transfer to the core and the formation of hydrogen bonding among fibers [27], [28]. However, an excessive vapor pressure within the board can cause a blow in the board shortly after leaving the hot press, which happens when the vapor pressure exceeds the internal bond strength of the board [27]. Thus, additional press time is needed to relieve the vapor pressure before the board can be taken out of the hot press safely [27]. It is important to ensure that the press time is adequate, because excessive press time can cause issues with overcuring that will lower the internal bond strength of the board and decrease the rate of production [22].

2.1.6. Industrial resin for boards

The most commonly used binders in wood panel industry are petroleum-derived resins such as urea formaldehyde, melamine urea formaldehyde, and phenol formaldehyde [29]. Urea formaldehyde binder was determined by the California Air Resources Board to be significant source of formaldehyde emission because urea formaldehyde was able to cure throughout its lifetime and emitting formaldehyde in the environment after the wood composite panels were manufactured [7]. In contrast, phenol formaldehyde emits 90% less formaldehyde than urea formaldehyde, and phenol formaldehyde was suitable for exterior use due to its better water resistance than urea formaldehyde [7]. In 2004, the International Agency for Research on Cancer has classified formaldehyde as a known carcinogen [29]. To minimize formaldehyde emissions from wood products, the California Air Resources Board has regulated the formaldehyde emissions to be no higher than 0.06 ppm for both particleboard and medium density fiberboard whereas 0.05 ppm for hardwood plywood [30].

2.2. Corn DDGS

2.2.1. Corn kernel components

The two major components of corn kernel are the endosperm and germ, both of which consist of starch and oil, as shown in Figure 3. Around 75% of the protein can be found in the endosperm tissue and the remainder can be found between the germ and bran [31].

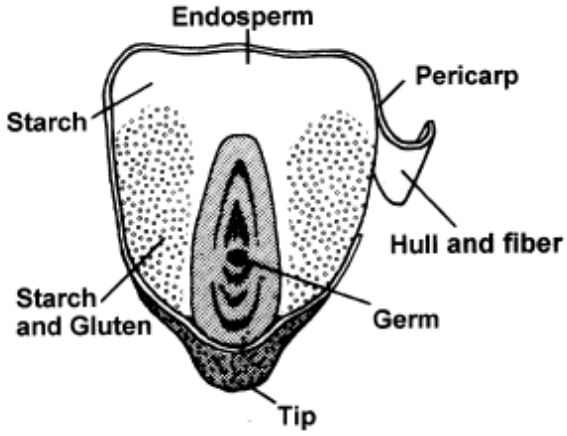

Figure 3. Cross-section of corn kernel. Reprinted with permission from [31]. Copyright 2001, Elsevier.

Table 2 shows the four major classes of protein and one of the dominant proteins in corn is zein, while both albumins and globulins are mainly located in the germ. This thesis emphasized the importance of zein because zein is the main protein that is found in both corn and DDGS [32].

Table 2. Distribution of protein fractions in corn [31].

Protein	*Whole kernel %*	*Endosperm %*	*Germ %*
Albumins	8	4	30
Globulins	9	4	30
Glutelin	40	39	25
Zein	39	47	5

The structure of the zein protein is globular [33]. Zein can be classified as α, β, and γ and located in the corn endosperm where the α-zein is the most abundant, which accounts for up to 85% of the total zein [34]. Figure 4 shows the tertiary structure of zein, where the tandem repeating units form helices connected by glutamine-rich loops [35]. The glutamine-rich loops located at the top and bottom are hydrophilic, whereas the α-helix sides have a hydrophobic nature [34]. This means that zein is classified as amphilic because it possesses both hydrophilic and hydrophobic characteristics [36]. However, more than 50% of zein's amino acid residues are hydrophobic [37], whereas their hydrophilic residues only account for up to 26% [31]. Thus, the highly hydrophobic zein protein found in DDGS may improve the water resistance properties of the particleboards.

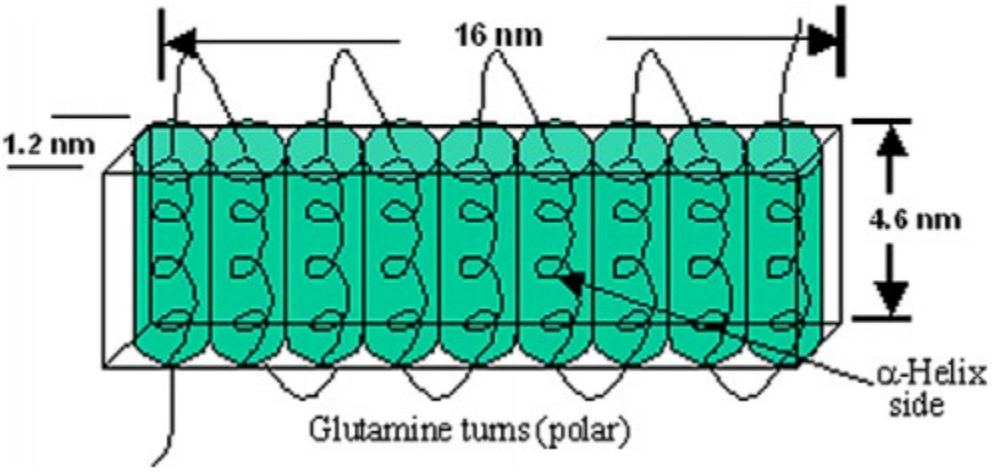

Figure 4. α-zein structural model. Reprinted with permissions from [34] and [35]. Copyrights 2008 and 1997, Elsevier.

2.2.2. DDGS from corn-ethanol production

In 2017, the U.S. was the world's largest producer of ethanol, which produced 15.8 billion gallons [38]. The vast majority of U.S. ethanol is derived from corn [38]. The two common techniques used to produce fuel ethanol from corn grains are the wet milling process and the dry-grind process [39]. The most widely used method in the U.S. for corn-ethanol

production is the dry-grind process, also referred as dry milling [39]. In the corn dry milling process, corn is hammer milled into a medium-to-fine grind meal [39]. The corn meal is then mixed with water to form slurry [39]. In the liquefaction step, the starch is hydrolyzed into dextrin with an alpha amylase enzyme to produce mash [39]. The mash is cooked, cooled and sent for fermentation to convert the dextrose to ethanol by yeast [39]. The co-products for dry milling process are distiller's grains, distiller's grains with solubles, and carbon dioxide [39]. Corn ethanol production can generate roughly a third of a kilogram each of ethanol, DDGS, and carbon dioxide when 1 kg of corn is utilized [40]. The high protein in DDGS makes it suitable to be marketed as animal feed [41].

2.2.3. Properties of DDGS

The rapid growth in the ethanol industry led to substantial research on determining the physical properties of DDGS [42]. This is essential because the physical properties vary among ethanol processing plants and at a given plant over time [42]. Table 3 summarizes some physical properties of DDGS.

Table 3. Physical properties of DDGS [42].

Physical Property	Range
Moisture content (%)	13.2-21.2
Water activity (-)	0.53-0.63
Thermal conductivity (W/m°C)	0.06-0.08
Thermal resistivity (m°C/W)	13.1-15.6
Thermal diffusivity (mm2/s)	0.13-0.15
Bulk density (kg/m3)	389.3-501.5
Angle of repose (°)	26.5-34.2

Other than the physical properties as mentioned in Table 1, another important physical property of DDGS is particle size. This is because particle size will influence the other physical

properties such as the bulk density, angle of repose, compressibility, heat transfer characteristics, and flowability properties of DDGS [43]. The particle size of DDGS can range from less than 0.1 mm to more than 2 mm in diameter [43]. In general, milling DDGS particles down to smaller sizes will lead to higher surface area and a greater number of contact points between particles [43]. Figure 5 and Figure 6 show that the surface layer of DDGS particles consist mainly protein and fat compared with carbohydrate, and protein and fat in DDGS particles can act as a natural adhesive [44].

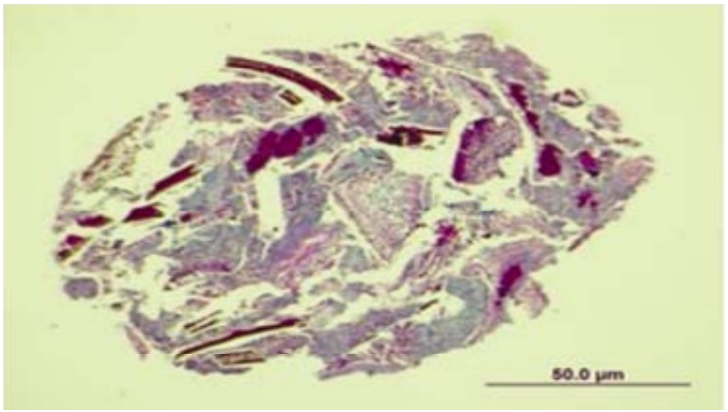

Figure 5. Cross-sectional image of stained DDGS particles where the carbohydrate is represented by dark purple and protein by pink color. Reprinted with permission from [44]. Copyright 2009, John Wiley and Sons.

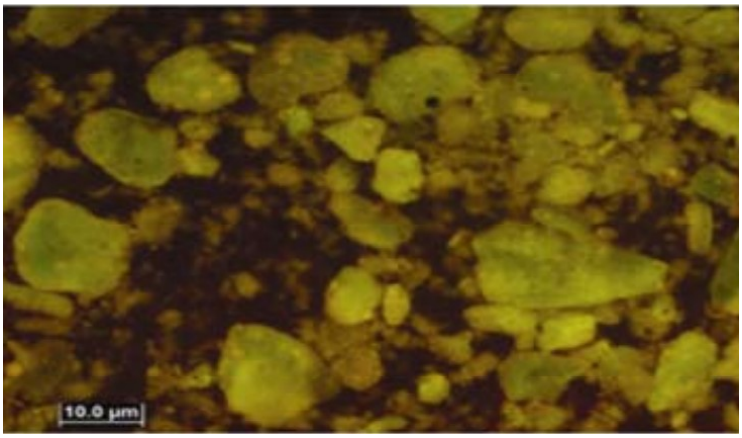

Figure 6. Surface fat globules of DDGS particles. Reprinted with permission from [44]. Copyright 2009, John Wiley and Sons.

2.2.4. Proteins as adhesives

Factors such as the carcinogenic nature of formaldehyde [29] and strict limits imposed by the California Air Resources Board on formaldehyde emissions from wood products [30] have expensive compliance, testing, and certification requirements [45]. Thus, green protein-based adhesives have gained considerable amount of attention [45]–[47].

The adhesive effect or functionality of proteins are determined from the protein structure itself, which will be discussed as follows. Proteins are large and complex structures made up of basic molecular building blocks known as amino acids [48]. As shown in Figure 7, amino acids are combined together by peptide bonds to form a primary protein structure; this structure is known as a polypeptide chain [48], shown in Figure 8. Due to secondary interactions such as hydrogen bonding, electrostatic forces, van der Waals forces, hydrophobic interactions, and disulphide linkages, the polypeptide chains display specific configurations [48]. These interactions form higher-level structures of proteins, and the structures are secondary, tertiary, and quaternary [48].

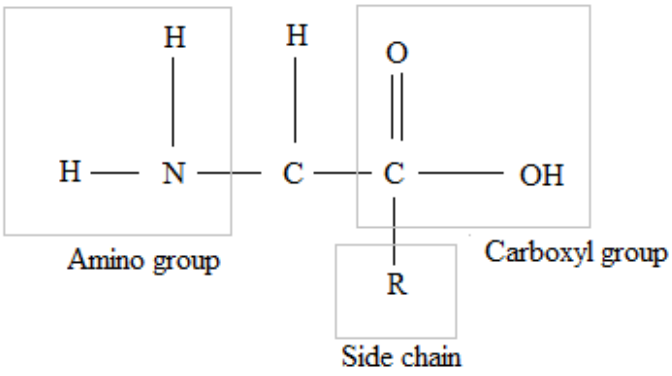

Figure 7. Adapted structure of an amino acid [49].

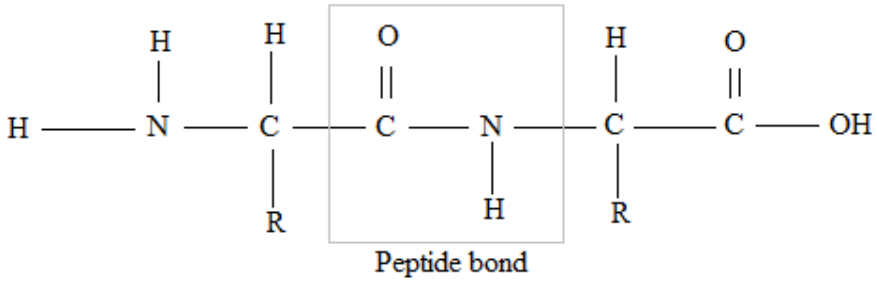

Figure 8. Adapted structure showing linkage between two amino acids to form a peptide bond [49].

The secondary structure of protein is made up of alpha helices and beta sheets. The occurrence of alpha helices and beta sheets are the result of amino acids in a polypeptide chain linked by several hydrogen bonds [48].

The tertiary structure of a protein is represented by the three-dimensional structure of a protein and associates the spatial arrangement of polypeptide chains through coiling an uncoiling [48]. The tertiary structure shows the interactions between alpha helices and beta sheets through covalent disulfide bonds, electrostatic and hydrophobic interactions, and hydrogen bonding [48].

The quaternary structure is the highest-level structure of the protein. This structure is made up of two or more polypeptide chains that are bonded together by noncovalent or covalent interactions [48].

The protein structure can be unfolded in a process called denaturation, which involves disruption of both hydrogen bonds and electrostatic interactions between amino acids [50]. Though this process disrupts the internal bonds in the protein, it also exposes them to allow the protein to adhere to surrounding materials, such as wood [11]. Acid-induced protein unfolding occurs between pH 2 and pH 5 and base induced involves pH 10 or higher [50]. For DDGS in particular, a patent specified by Mohanty et al. [51] had successfully developed an adhesive by hydrolyzing the grains with an aqueous sodium hydroxide solution and cooking it in a pressure

cooker, washing it with water, filtering it using a Buckner funnel, and boiling it to obtain a concentrated suspension. Finally, a brown and viscous concentrated suspension was tested to have a lap shear strength of around 123 psi [51]. However, there are a lot of processes involve in making DDGS as adhesive, and these processes are not ideal to be used in DDGS wood particleboard manufacturing.

2.2.5. Solubility of zein protein

The solubility and chemical reactivity of zein are determined by its functional groups of amines, amides, hydroxyls, carboxylates and phenols [36]. These different types of functional groups allow zein to be physically and chemically modified to improve its functional properties [36]. Generally, zein is water-insoluble due to the presence of hydrocarbon groups in zein's side chains, but zein becomes soluble in water in the presence of high concentrations of alkali at pH 11 or above, alcohols, and other organic solvents [31], [36]. These organic solvents can be classified as primary solvents, secondary solvents, and ternary solvents [52]. A primary solvent is a compound that could dissolve zein in a concentration of more than 10% [52]. Acetic acid is classified as primary solvent because it can interact with the amino acids of zein to dissolve both the polar and nonpolar amino acids in zein [52]. Furthermore, the solubility of zein in water can be improved by either acid or alkali deamidation to convert the glutamine and asparagine amino acids to the acid or salt forms [31]. Previous study indicated that deamidation decreased the number of hydrogen bonds in protein and led to protein unfolding [53].

3. MATERIALS AND METHODS

3.1. Materials

Pine wood flour of 2020-grade was obtained from American Wood Fibers (Wausau, WI, USA). The particle size distribution for wood flour is shown in Table 4, and the wood flour had an average size of 425 µm.

Table 4. Particle size distribution for wood flour.

U.S. Standard Sieve No. and Micron Equivalent	Wood Flour Content, %
No. 20 (850 µm)	< 1
No. 40 (425 µm)	68-74
No. 60 (250 µm)	23-27
Pan (< 250 µm)	2-4

DDGS was supplied by Blue Flint Ethanol plant (Underwood, ND, USA). Unprocessed DDGS was milled with screen sizes of 120 µm and 250 µm in a Retsch Rotor Beater Mill SR300 (Newtown, PA, USA) as illustrated in Figure 9. The moisture content of the wood flour and DDGS were at 8% and 7%, respectively.

Figure 9. Retsch Rotor Beater Mill SR300.

The particle size distribution for DDGS at screen sizes of 120 µm and 250 µm are shown in Table 5. Both the sodium hydroxide (NaOH) pellets with ≥ 90 % NaOH concentration and reagent grade glacial acetic acid were purchased from the Department of Chemistry and Biochemistry at North Dakota State University (Fargo, ND, USA), and the supplier for these products is MilliporeSigma (Burlington, MA, USA). The distilled water was obtained from the Department of Chemistry and Biochemistry at North Dakota State University (Fargo, ND, USA). The wax emulsion called Transseal Pre-Wax was purchased from Wood Finishers Depot (Baytown, TX, USA) and manufactured by Groco Specialty Coatings (Dallas, TX, USA). Phenol formaldehyde resin with 25-50% by weight of phenol-formaldehyde polymer sodium salt was obtained from Hexion Inc. (Columbus, OH, USA).

Table 5. Particle size distribution for DDGS.

U.S. Standard Sieve No. and Micron Equivalent	DDGS Content, % (120 µm screen size)	DDGS Content, % (250 µm screen size)
No. 60 (250 µm)	0.3-1.2	7.4-8.7
No. 80 (180 µm)	6.2-17.7	19.1-23.0
No. 100 (150 µm)	2.9-12.2	12.4-13.1
Pan (< 150 µm)	73.8-87.3	56.6-59.6

3.2. Board processing

To reduce the formation of clumps during the chemical treatment process, different DDGS concentrations at 10 wt. %, 25 wt. %, and 50 wt. % were dispersed in the pine wood flour matrices of 90 wt. %, 75 wt. %, and 50 wt. %, respectively, by hand mixing the dried particles. Next, concentrated acetic acid or sodium hydroxide was dissolved in water to achieve the desired concentration. The protein decoupling process was initiated by hand mixing the desired concentration of chemical solution to both DDGS and wood flour particles at a ratio of 2:8. The treated particles were blended, mixed, and agitated for seven minutes in the Patterson Kelley

Twin Shell Dry Blender (East Stroudsburg, PA, USA), as shown in Figure 10, to obtain uniform mixtures.

Figure 10. Twin Shell Dry Blender.

In addition to using the blender, samples that contain wax combinations were prepared by using a Vaper HVLP Spray Gun (Renton, WA, USA) to spray a Northern Industrial Cement Mixer Model 998252 (Burnsville, MN, USA), as shown in Figure 11 and Figure 12. The control samples were prepared differently by spraying the cement mixer using a spray gun with combinations of 12 wt. % phenol formaldehyde resin and 10 wt. % wax. These percentages were calculated based on Equations (1) and (2).

$$\%\, resin\ = \frac{mass\ of\ resin}{mass\ of\ dried\ particles} \times 100\ \% \tag{1}$$

$$\%\, wax\ = \frac{mass\ of\ wax}{mass\ of\ dried\ particles} \times 100\ \% \tag{2}$$

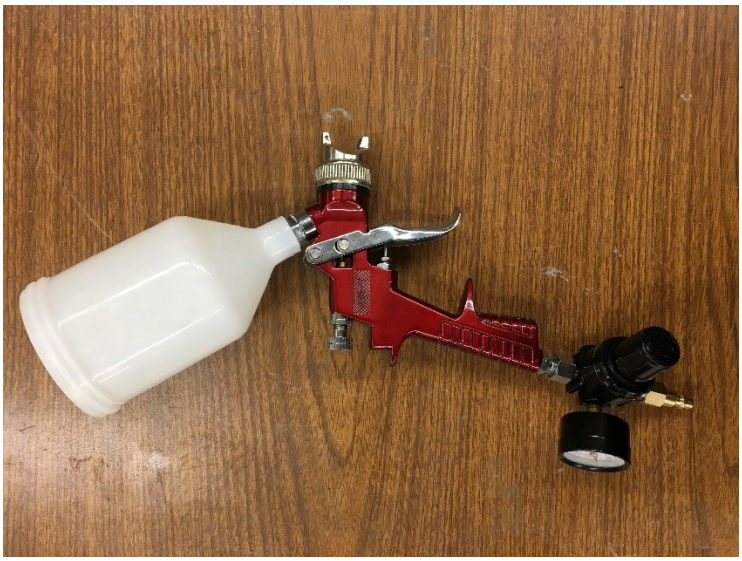

Figure 11. Spray gun.

Figure 12. Cement mixer.

The samples were then placed into a mold, as shown in Figure 13, and then pressed into medium-density particleboards using a hydraulic hot press, Carver Hot Press Model 4122 (Wabash, IN, USA), shown in Figure 14. A pressure of 3.80 MPa (18 metric tons) was applied to the samples in the initial phase of the experiment, and a pressure of 4.65 MPa (22 metric tons) was applied to the samples in the final phase. The total press time was 12 minutes, and the applied pressure was released every 4 minutes to reduce built-up pressure. The dimensions of

each medium density particleboard were 305 mm (length) × 153 mm (width) × 6 mm (nominal thickness).

Figure 13. Mold for manufacturing particleboard.

Figure 14. Hot press.

3.3. Chemical treatment characterization

3.3.1. Composition analysis

Composition analysis was performed on untreated DDGS particles, 12.8 M acetic acid treated DDGS particles, and 8.0 M sodium hydroxide treated DDGS particles to determine the nitrogen, crude protein, neutral detergent fiber (NDF), acid detergent fiber (ADF), fat, and lignin contents of the samples. These DDGS particles consisted of DDGS particles that were milled with screen size of 250 μm. The chemically treated samples were oven dried at 30℃ for about 48 hours prior to test. The tests were performed by the Department of Animal Sciences at North Dakota State University. The Association of Analytical Community's (AOAC) methods were followed for crude protein test (2001.11), both fiber and lignin tests (973.18), and crude fat test (920.39), and the ANKOM method was used for NDF and ADF analyses.

3.3.2. Thermogravimetric analysis (TGA)

Thermogravimetric analysis was performed on untreated DDGS particles, 12.8 M acetic acid treated DDGS particles, and 8.0 M sodium hydroxide treated DDGS particles to analyze the degradation temperature and the rate of degradation of the samples. These DDGS particles consisted of DDGS particles that were milled with screen size of 250 μm. The chemically treated samples were oven dried at 30℃ for about 48 hours prior to test. The analysis was conducted using a TA Q500 TGA (New Castle, DE, USA). The temperature was increased at a rate of 10℃/min from 25℃ to 400℃. The experiments were carried out under nitrogen gas with a flow rate of 60 ml/min.

3.3.3. Differential scanning calorimetry (DSC)

Differential scanning calorimetry was performed on untreated DDGS particles, 12.8 M acetic acid treated DDGS particles, and 8.0 M sodium hydroxide treated DDGS particles to

analyze the melting peak and glass transition temperature of the samples. These DDGS particles consisted of DDGS particles that were milled with screen size of 250 μm. The chemically treated samples were oven dried at 30℃ for about 48 hours prior to test. The analysis was conducted using a TA Q1000 DSC (New Castle, DE, USA). The temperature was ramped at a rate of 10℃/min from -20℃ to 190℃. The experiments were carried out under nitrogen gas with a flow rate of 50 ml/min.

3.3.4. Fourier transform infrared spectroscopy (FTIR)

Fourier transform infrared spectroscopy was performed on untreated DDGS particles, 12.8 M acetic acid treated DDGS particles, and 8.0 M sodium hydroxide treated DDGS particles to determine the difference in functionality between chemically treated DDGS and untreated DDGS. These DDGS particles consisted of DDGS particles that were milled with screen size of 250 μm. The chemically treated samples were oven dried at 30℃ for about 48 hours prior to test. The analysis was conducted using a Thermo Scientific Nicolet 8700 FTIR spectrometer (Waltman, MA, USA). All of the samples were mixed with KBr and pressed at 2 tons using a Specac Mini-Pellet Press (Limited, UK) to form disc-shaped specimens.

3.4. Physical and mechanical testing

Samples from the initial phase testing and final phase testing were cut according to the patterns provided in Figure 15 and Figure 16, respectively; these patterns were adapted from ASTM D1037-12 [54]. The initial phase tests include density, static bending, and internal bond, while the final phase tests include density, static bending, internal bond, hardness, screw withdrawal, water absorption, and linear expansion. The initial phase tests were performed to determine the preferred temperature and chemical concentrations. These preferred parameters were then incorporated in the final phase testing.

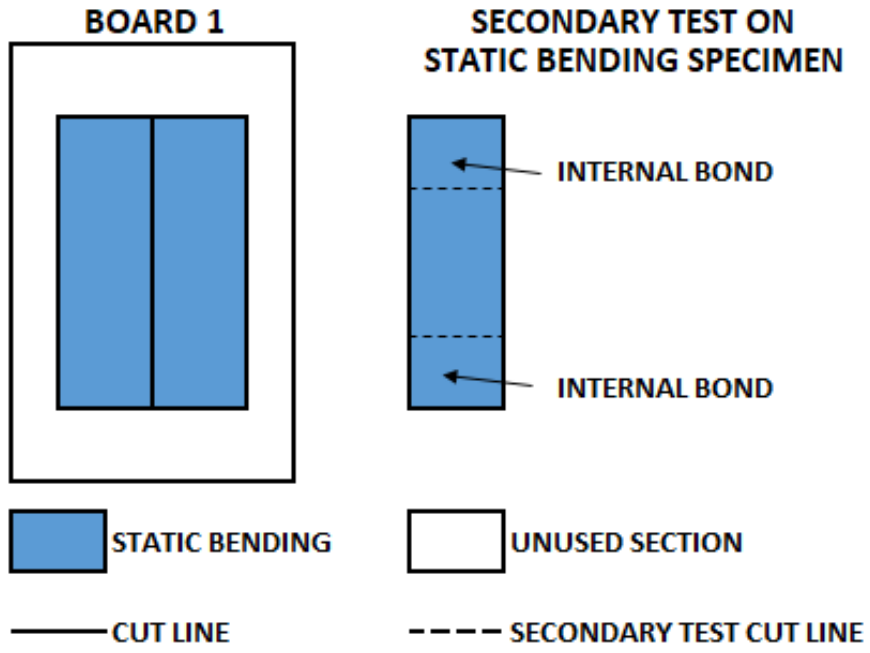

Figure 15. Particleboard cut out patterns for initial phase testing.

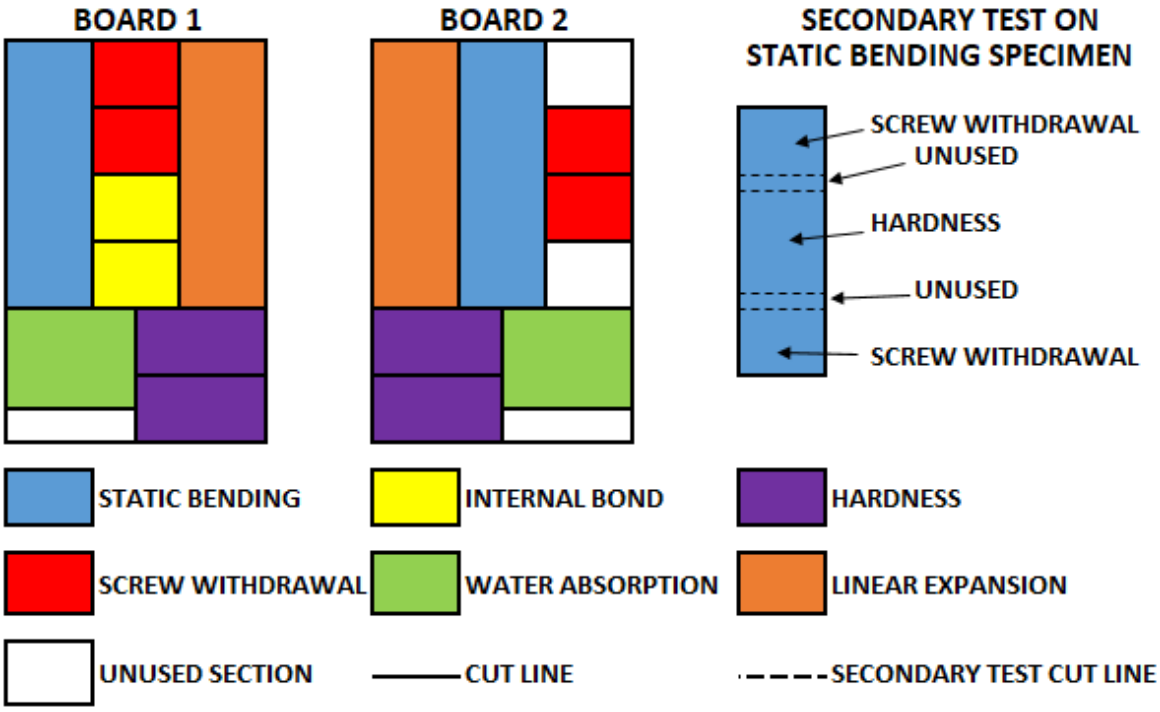

Figure 16. Particleboard cut out patterns for final phase testing.

The statically-bent samples from the initial phase of the experiment were reused for internal bond test, while statically-bent samples from the final phase of the experiment were reused for hardness and screw withdrawal tests. The reused samples for internal bond and screw withdrawal tests were cut adequately far from the fracture point of the statically-bent samples except for hardness. The reused samples for hardness test were cut in a way that the hardness indentation points were far enough from the fracture point of the statically-bent samples, as shown in Figure 17, to prevent any influence from the statically-bent samples.

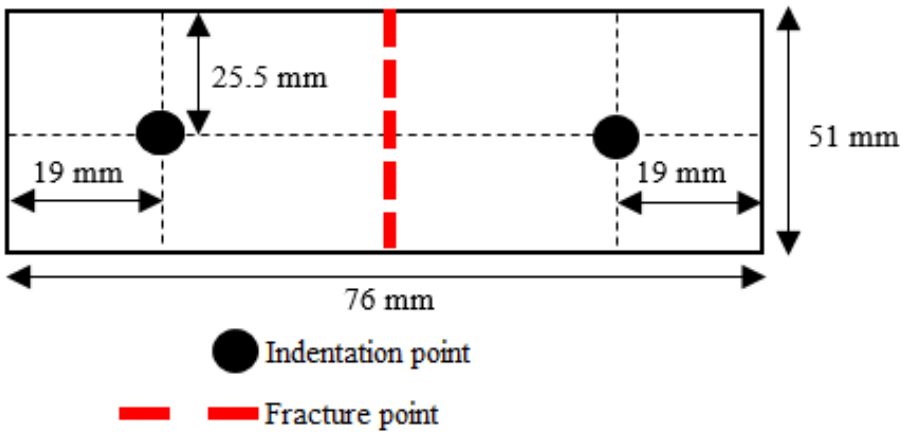

Figure 17. Fracture point of a statically-bent sample.

It should be noted that a batch consisted of a board in the initial phase, while two boards were produced from a batch in the final phase to speed up the manufacturing process. Two batches were manufactured for both the initial and final phases of this experiment.

3.4.1. Density

The density test was adapted from ASTM D2395-17 [55]. The mass was measured by weighing the mass of the entire panel to ±0.1 g. The volume was determined from the mean of three lengths, three widths, and four thickness measurements. The dimensions were measured to ±0.01 mm. The density was then calculated based on Equation (3).

$$\rho = \frac{M}{LWT} \tag{3}$$

Where ρ represents density in kg/m^3, M represents mass in kg, L represents length in m, W represents width in m, and T represents thickness in m.

3.4.2. Water absorption

A water absorption test was used to determine the resilience of a board to absorb water when submerged horizontally in a water bath at 20 ± 1°C. This test was adapted from ASTM D1037-12 [54]. The water absorption test was conducted using a 2-plus-22-hour method. The dry specimen dimensions were 76 mm × 76 mm × approximately 6 mm manufactured thickness. The dry specimen was submerged in water for 2 hours, drained for 10 minutes, and then, their mass, length, width, and thickness were obtained. After the 2-hour measurements were obtained, the specimen was submerged for an additional 22 hours, and the procedures of draining and measuring were repeated. For both time points, percent change in mass and percent change in volume were calculated based on Equations (4) and (5).

$$\%\ Change\ in\ Mass = \frac{M_f - M_i}{M_i} \times 100 \tag{4}$$

$$\%\ Change\ in\ Volume = \frac{V_f - V_i}{V_i} \times 100 \tag{5}$$

Where M_i and V_i are the initial mass and initial volume, respectively, and M_f and V_f are the final mass and final volume, respectively. The initial mass and initial volume measured the dry mass and dry volume, respectively, whereas the final mass and final volume measured the submerged mass and submerged volume, respectively.

The volume is calculated based on Equation (6).

$$V = LWT \tag{6}$$

Where V represents the volume, L represents the length, W represents the width, and T represents the thickness of the samples measured at the midpoint of all four sides. Four samples were tested for each unique formulation.

3.4.3. Linear expansion

Linear expansion test was used to determine the dimensional stability of a board in the presence of high humidity. The linear expansion test was adapted from ASTM D1037-12 [54]. The test was conducted using a Binder Humidity Chamber model KBF 115-UL (Tuttlingen, Germany). The dry specimen dimensions were 195 mm × 50 mm × approximately 6 mm manufactured thickness. The specimen was first condition to achieve practical equilibrium at 50% relative humidity, and a temperature of 20 ± 3℃ and the length of the specimen was measured to 0.02 mm. Practical equilibrium is defined as not having a mass change of more than 0.05% in a 24-hour period. After the measurements were obtained for 50% relative humidity, the specimen was exposed to 80% relative humidity and temperature of 20 ± 3℃, and the procedures of achieving practical equilibrium and obtaining measurements were repeated. The specimen lengths were calculated based on Equation (7).

$$\%\ Change\ in\ Length = \frac{L_f - L_i}{L_i} \times 100 \quad (7)$$

Where L_i is the initial length and L_f is the final length. Four samples were tested for each unique formulation. Figure 18 displays the placement of the samples in the humidity chamber.

Figure 18. Linear expansion test.

3.4.4. Static bending

A three-point static bending test was conducted to determine the flexural properties of the particleboards, specifically on the modulus of rupture and modulus of elasticity. The static bending test was adapted from ASTM D1037-12 [54]. The test was conducted using a TestResources Model 312 Frame (Shakopee, MN, USA). The specimen dimensions were 195 mm × 51 mm × approximately 6 mm manufactured thickness. The span length and crosshead rate were calculated in accordance to the standard with values of 144 mm and 2.88 mm/min, respectively. The crosshead rate was calculated based on Equation (8).

$$N = \frac{zL^2}{6d} \tag{8}$$

Where N represents the crosshead rate in mm/min, z represents the outer fiber strain rate of 0.005 mm/mm/min, L represents the span length in mm, and d represents the thickness in mm.

The modulus of rupture and modulus of elasticity were calculated based on Equation (9) and Equation (10), respectively.

$$R_b = \frac{3P_{max}L}{2bd^2} \quad (9)$$

$$E = \frac{L^3}{4bd^3}\frac{\Delta P}{\Delta y} \quad (10)$$

Where R_b represents the modulus of rupture in MPa, E represents the modulus of elasticity in MPa, P_{max} represents the maximum load in N, L represents the span length in mm, b represents the width in mm, d represents the thickness in mm, and $\Delta P/\Delta y$ represents the slope of the straight line portion of the load-deflection curve in N/mm. Four static bending samples were tested for each unique formulation. Figure 19 displays the fixture and loading conditions used for all static bending tests.

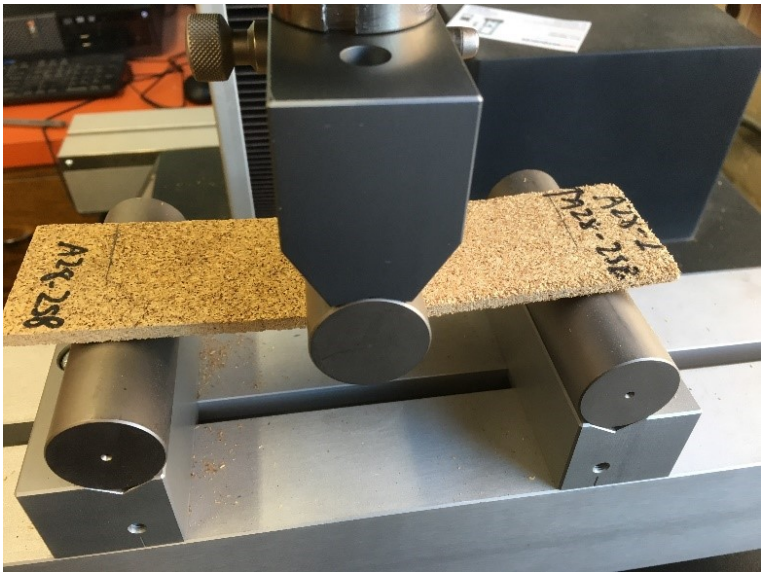

Figure 19. Three-point static bending test.

3.4.5. Internal bond

Internal bond or tension perpendicular to the surface test was conducted to determine the cohesion of the panel. The internal bond test was adapted from ASTM D1037-12 [54]. The specimen dimensions were 51 mm × 51 mm × approximately 6 mm manufactured thickness was glued to the loading blocks using a hot melt adhesive provided by Masonite PrimeBoard in

Wahpeton, North Dakota. The adhesive was melted using a hot plate and applied to the surface of the blocks. The melted glued was allowed to cool for at least an hour before applying to the second surface.

The test was conducted using a TestResources Model 312 Frame (Shakopee, MN, USA). The crosshead rate used in this test was 1 mm/min, which was deviated from the constant strain rate of 0.08 cm/cm as specified by the standard. This change was due to the unavailability of a suitable extensometer to test at a constant strain rate. It should be noted that adhesive failures between the loading block and the adhesive were discarded and excluded in the analysis. The internal bond strength was calculated based on Equation (11).

$$IB = \frac{P_{max}}{ab} \tag{11}$$

Where IB represents the internal bond strength, P_{max} represents the maximum load in N, a represents the width in mm, and b represents the length in mm. Six internal bond samples were tested for each unique formulation in the initial phase, and eight samples in the final phase. Figure 20 displays the fixture and loading blocks used for all internal bond tests.

Figure 20. Internal bond test.

3.4.6. Screw withdrawal

Screw withdrawal test was conducted to measure the ability of the particleboard to resist screw pullout. The screw withdrawal test was adapted from ASTM D1037-12 [54]. The specimen dimensions were 51 mm × 51 mm × quadruple the manufactured thickness. The additional thickness was achieved by gluing four specimens together using a Weldwood contact cement as required by the standard. The specimen was predrilled to form a lead hole of 3.2 mm and a depth of 17 mm. After predrilling, a Number 10 screw was screwed into the lead hole.

The test was conducted using a TestResources Model 312 Frame (Shakopee, MN, USA). The specimen was tested at a crosshead rate of 1.5 mm/min, and the maximum load of screw withdrawal was recorded. This test was performed with four replicates for each unique formulation. Figure 21 displays the configuration used for all screw withdrawal tests.

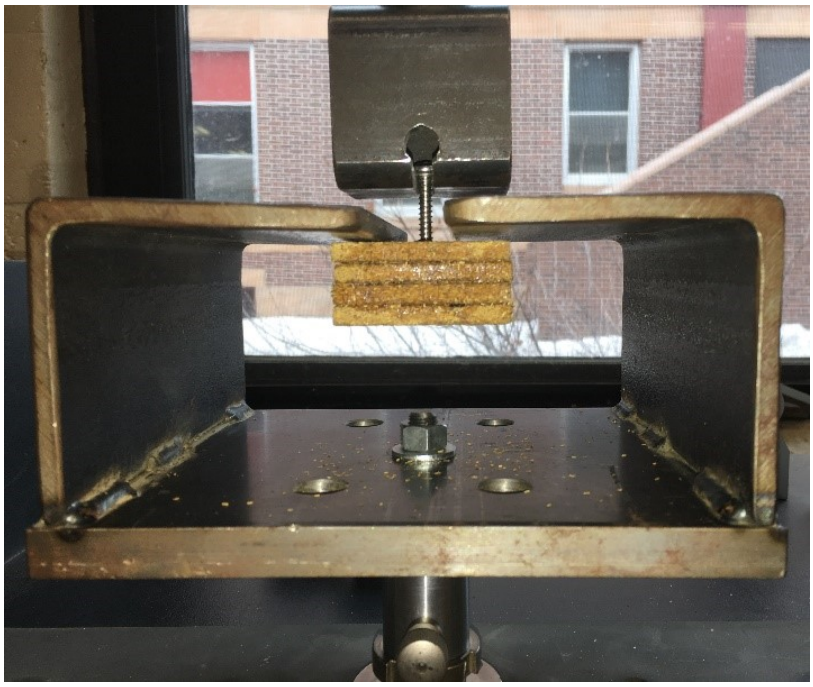

Figure 21. Screw withdrawal test.

3.4.7. Hardness

Hardness test was conducted to measure the ability of the particleboard to resist indentation. The hardness test was adapted from ASTM D1037-12. The specimen dimensions were approximated to 76 mm × 51 mm × triple the manufactured thickness. The additional thickness was achieved by gluing three specimens together using Weldwood contact cement as prescribed by the standard. Though the standard called for a Janka-ball method in which the test will be stopped when the ball has penetrated to a depth of one-half its diameter, this test was modified slightly to use a ball of 19 mm that only penetrated to a depth of 4.75 mm. This was done to prevent the Janka-ball from indenting deeper than the manufactured thickness, so the modified depth was half the required depth; this modified depth can be found from similar studies [56], [57]. Two penetrations were performed in each specimen as shown in Figure 22.

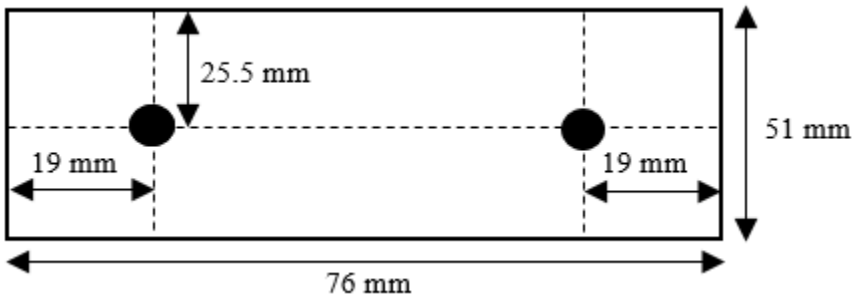

Figure 22. Indentation points of a hardness specimen.

The test was conducted using a TestResources Model 312 Frame (Shakopee, MN, USA). The specimen was tested at a crosshead rate of 6 mm/min, and the maximum load of hardness was recorded. Four hardness specimens were tested for each unique formulation. Figure 23 displays the configuration used for all hardness tests.

Figure 23. Hardness test.

4. DESIGN OF EXPERIMENT

4.1. Design of experiment

This experiment was divided into two different phases: an initial phase and a final phase. The initial phase of the experiment was performed to determine the interaction of both temperature and chemical concentration on the flexural properties and internal bond strength of the particleboards. A screen size of 250 µm and a DDGS loading concentration of 50 wt. % were held constant throughout the initial phase. In total, twelve different blends comprised of *1 particle size × 1 DDGS loading concentration × 2 chemical treatments × 3 temperatures* as well as *1 particle size × 1 DDGS loading concentration × 2 chemical treatments × 3 chemical concentrations* were studied, shown in Table 6 and Table 7, respectively. For each of these six different blends, two boards were manufactured per blend for a total of twelve.

Table 6. The number of boards manufactured for each formulation of temperature and chemical treatment.

	Chemical treatment	
Press temperature	12.8 M Acetic acid	2.0 M Sodium hydroxide
170℃	2	2
180℃	2	2
190℃	2	2

Table 7. The number of boards manufactured for each formulation of acid and alkaline concentrations hot pressed at 190℃.

Chemical treatment	Acetic acid			Sodium hydroxide		
Chemical concentration	8.0 M	11.0 M	12.8 M	2.0 M	5.0 M	8.0 M
Number of boards	2	2	2	2	2	2

Once the initial phase was completed and the mechanical properties were determined, the final phase of the experiment was conducted to investigate the effect of screen size and DDGS

loading concentration on the physical and mechanical properties of particleboards. In this final phase, the chemical treatments used for DDGS particles were 12.8 M acetic acid and 8.0 M sodium hydroxide, the screen sizes used to micronize DDGS particles were 120 and 250 μm, the DDGS loading concentrations were 10, 25, and 50 wt. %, and the press temperature was 190℃. In total, four boards for each of twelve different blends comprised of *2 particle sizes × 3 DDGS loading concentrations × 2 chemical treatments* were manufactured, shown in Table 8.

Table 8. The number of boards manufactured for each formulation of DDGS concentration and screen size.

	Screen size	
DDGS concentration	120 μm	250 μm
10 wt. %	4/chemical treatment	4/chemical treatment
25 wt. %	4/chemical treatment	4/chemical treatment
50 wt. %	4/chemical treatment	4/chemical treatment

Since the sodium hydroxide treated DDGS blend samples had weak water resistance properties, 10 wt. % wax was added to the particleboards. Hence, another four different blends comprised of *2 particle sizes × 1 DDGS concentration × 2 chemical treatments × 1 wax* were studied, as shown in Table 9. In each case, four boards were manufactured per blend for a total of sixteen.

Table 9. The number of boards manufactured with addition of wax for each formulation of DDGS concentration and screen size.

	Screen size	
DDGS concentration	120 μm	250 μm
50 wt. %	4/chemical treatment	4/chemical treatment

In addition to the initial and final phases, two control sets were manufactured; the first used wood flour and 12 wt. % phenol formaldehyde, while the second used wood flour, 12 wt. %

phenol formaldehyde, and 10 wt. % wax. The control boards were produced without using DDGS filler, and four control boards were manufactured per blend for a total of eight.

4.2. Data analysis

The five methods used to evaluate the results were interval plot, analysis of variance (ANOVA), interaction plot, Tukey's test, and tabular additive weighting method.

All statistical analyses were performed using Minitab 19. ANOVA was conducted to compare the means of the groups. If the ANOVA results indicated that the interaction effects were significant, the main effects cannot be interpreted alone, thus an interaction plot was used as a visual representation to interpret the interaction effects. Moreover, a Tukey's test was run on those ANOVA results to determine whether the means of different samples were significantly different.

4.2.1. Interval plot

Interval plots are a useful tool to compare the means of groups. This plot displays a 95% confidence interval for the mean of each group and a red dotted line indicates the minimum requirements of the physical and mechanical properties for medium-density particleboards as prescribed in ANSI A208.1-2009 standard [19].

4.2.2. Analysis of variance (ANOVA)

ANOVA is a useful method to evaluate the effects of two or more factors on the response and was used to evaluate the test results at the 0.05 level of significance. To analyze a two-factor factorial design involves partitioning the sum of squares total (SST) into four parts. These four parts include the sum of squares due to factor A (SSA), the sum of squares due to factor B (SSB), the sum of squares due to the interaction between factors A and B (SSAB), and the sum of squares error (SSE).

As defined by *Applied Statistics for Engineers and Scientists* [58], r is the number of levels of factor A, c is the number of levels of factor B, n' is the number of replication, n is the total number of observation, and X_{ijk} is the value of the kth observation for level i of factor A and level j of factor B.

The SST is the total variation of all observations and is defined in Equation (12).

$$SST = \sum_{i=1}^{r}\sum_{j=1}^{c}\sum_{k=1}^{n'}\left(X_{ijk} - \bar{\bar{X}}\right)^2 \tag{12}$$

Where $\bar{\bar{X}}$ is the overall mean and is defined in Equation (13).

$$\bar{\bar{X}} = \frac{\sum_{i=1}^{r}\sum_{j=1}^{c}\sum_{k=1}^{n'} X_{ijk}}{rcn'} \tag{13}$$

The SSA is the differences between the various levels of factor A and the overall mean, and SSA is defined in Equation (14).

$$SSA = cn'\sum_{i=1}^{r}\left(\bar{X}_{i..} - \bar{\bar{X}}\right)^2 \tag{14}$$

Where $\bar{X}_{i..}$ is the mean of the ith level of factor A and is defined in Equation (15).

$$\bar{X}_{i..} = \frac{\sum_{j=1}^{c}\sum_{k=1}^{n'} X_{ijk}}{cn'} \tag{15}$$

For i = 1, 2, …, r.

The SSB is the differences between the various levels of factor B and the overall mean, and SSB is defined in Equation (16).

$$SSB = rn'\sum_{j=1}^{c}\left(\bar{X}_{.j.} - \bar{\bar{X}}\right)^2 \tag{16}$$

Where $\bar{X}_{.j.}$ is the mean of the jth level of factor B and is defined in Equation (17).

$$\bar{X}_{,j,} = \frac{\sum_{i=1}^{r}\sum_{k=1}^{n'} X_{ijk}}{cn'} \tag{17}$$

For j = 1, 2, …, c.

The interaction effect between factors A and B is defined in Equation (18).

$$SSAB = n' \sum_{i=1}^{r}\sum_{j=1}^{c}\left(X_{ij.} - \bar{X}_{i..} - \bar{X}_{.j.} + \bar{\bar{X}}\right)^2 \tag{18}$$

The SSE is defined in Equation (19).

$$SSE = \sum_{i=1}^{r}\sum_{j=1}^{c}\sum_{k=1}^{n'}\left(X_{ijk} - \bar{X}_{ij}\right)^2 \tag{19}$$

Where $\bar{X}_{ij.}$ is the mean of the cell ij, the combination of the ith level of factor A and the jth level of factor B, and $\bar{X}_{ij.}$ is defined in Equation (20).

$$\bar{X}_{ij,} = \sum_{k=1}^{n'} \frac{X_{ijk}}{n'} \tag{20}$$

The mean square values are computed by dividing the sum of square values by the degree of freedom as shown in Equations (21), (22), (23), and (24).

$$MSA = \frac{SSA}{r-1} \tag{21}$$

$$MSB = \frac{SSB}{c-1} \tag{22}$$

$$MSAB = \frac{SSAB}{(r-1)(c-1)} \tag{23}$$

$$MSE = \frac{SSE}{rc(n'-1)} \tag{24}$$

Factors A and B are tested using hypothesis testing. The null and alternative hypotheses are:

$$H_0: \mu_1 = \mu_2 = \cdots = \mu_r$$

$$H_1: Not\ all\ \mu_i\ are\ equal$$

The F test for factor A main effect is calculated in Equation (25).

$$F = \frac{MSA}{MSE} \tag{25}$$

Likewise, the F test for factor B main effect is calculated in Equation (26).

$$F = \frac{MSB}{MSE} \tag{26}$$

The F test for interaction effect is determined in Equation (27).

$$F = \frac{MSAB}{MSE} \tag{27}$$

The hypothesis testing is performed once the F-values are established. The null hypothesis is rejected when $F > \mathrm{F}_{\alpha=0.05}$ as shown in Equations (28), (29), and (30), and this implies that the main effect or interaction effect is not significant.

$$F = \frac{MSA}{MSE} > \mathrm{F}_{\alpha=0.05} \tag{28}$$

$$F = \frac{MSB}{MSE} > \mathrm{F}_{\alpha=0.05} \tag{29}$$

$$F = \frac{MSAB}{MSE} > \mathrm{F}_{\alpha=0.05} \tag{30}$$

4.2.3. Interaction plot

An interaction plot is used as a visual representation to determine the existence of interaction. This method, defined by *Applied Statistics for Engineers and Scientists* [58], was used to evaluate the test results. Parallel lines signify that there is no interaction between factors, while intercepting lines signify an interaction between factors is significant. More intercepting lines in the result indicated a stronger interaction effect.

4.2.4. Tukey's test

Tukey's Pairwise Comparison test was conducted to compare all pairs of treatment means. This method, defined by *Design and Analysis of Experiments* [59] was used to test all pairwise mean comparisons as follows:

$$H_0: \mu_i = \mu_j$$

$$H_1: \mu_i \neq \mu_j$$

For these two hypotheses, $i \neq j$, H_0 is the null hypothesis, and H_1 is the alternative hypothesis.

For equal sample sizes, Tukey's test states that two means are significantly different when the absolute value of sample difference is greater than Equation (31).

$$T = q_\alpha(a, f)\sqrt{\frac{MS_E}{n}} \tag{31}$$

Tukey's test for unequal sample sizes is defined in Equation (32).

$$T = \frac{q_\alpha(a, f)}{\sqrt{2}}\sqrt{MS_E\left(\frac{1}{n_i} + \frac{1}{n_j}\right)} \tag{32}$$

Where $q_\alpha(a, f)$ value is obtained from the Studentized range statistic table, α=0.05 which corresponds to 95 % confidence interval, MS_E is the mean square error, and n is the number of samples.

4.2.5. Tabular additive weighting method

The tabular additive weighting method was used to decide the best alternative based on multiple criteria. This method, defined by *Systems Engineering and Analysis* [60], was used to analyze the test results by comparing different alternatives with respect to each criteria. Using this method, a weight (W) is assigned to each criterion; the total weights assigned for internal bond strength and flexural strength are 60% and 40%, respectively. Since this project

emphasized the importance of functionalized DDGS as a natural binder to bond with the wood flour, a higher weight is assigned to internal bond strength. After assigning a weight to each criterion, the performance rating (R) is ranked ordinally for each criterion with respect to each alternative. The performance rating (R) is ranked between 1 and 3 and were assigned to the flexural and internal bond strength, where 3 represents the highest performance, 2 represents the intermediate performance, and 1 represents the lowest performance. Finally, the totals of W × R are used in comparing the alternatives, where the highest W × R values indicated the best alternative.

5. RESULTS AND DISCUSSION

5.1. Chemical treatment characterization and analysis results

5.1.1. Composition analysis

Composition analysis was performed to determine the nitrogen, crude protein, neutral detergent fiber (NDF), acid detergent fiber (ADF), lignin, and crude fat contents. Previous work verified that 0.1 M sodium hydroxide treatment led to solubilization of DDGS fiber, which resulted in loss of protein, starch, hemicellulose, lignin, and fat contents in the DDGS [61]. In this study, Table 10 shows that alkali treatment of 8.0 M degraded and solubilized both the protein and fat components in the DDGS, while the protein and fat contents in 12.8 M acetic acid treated DDGS are not noticeably different than the untreated DDGS. In comparison to the untreated DDGS, both acid and alkali treated DDGS display lower percentages of NDF and ADF. The lower percentage of NDF is attributed to the degradation of cellulose, hemicellulose, and lignin, and the lower percentage of ADF is attributed to the degradation of lignin and cellulose.

Table 10. Composition analysis of untreated and treated DDGS particles.

Component	Nitrogen %	Protein %	NDF %	ADF %	Lignin %	Fat %
DDGS, 250, untreated	5.30	33.15	45.30	15.30	2.06	8.71
DDGS, 250, 12.8 M acetic acid	5.38	33.62	41.90	14.90	2.05	8.13
DDGS, 250, 8.0 M sodium hydroxide	4.63	28.91	25.50	9.65	0.65	4.33

5.1.2. Thermogravimetric analysis (TGA)

Thermogravimetric analysis was performed to investigate the behaviors of treated and untreated DDGS particles at high temperatures, as shown in Figure 24.

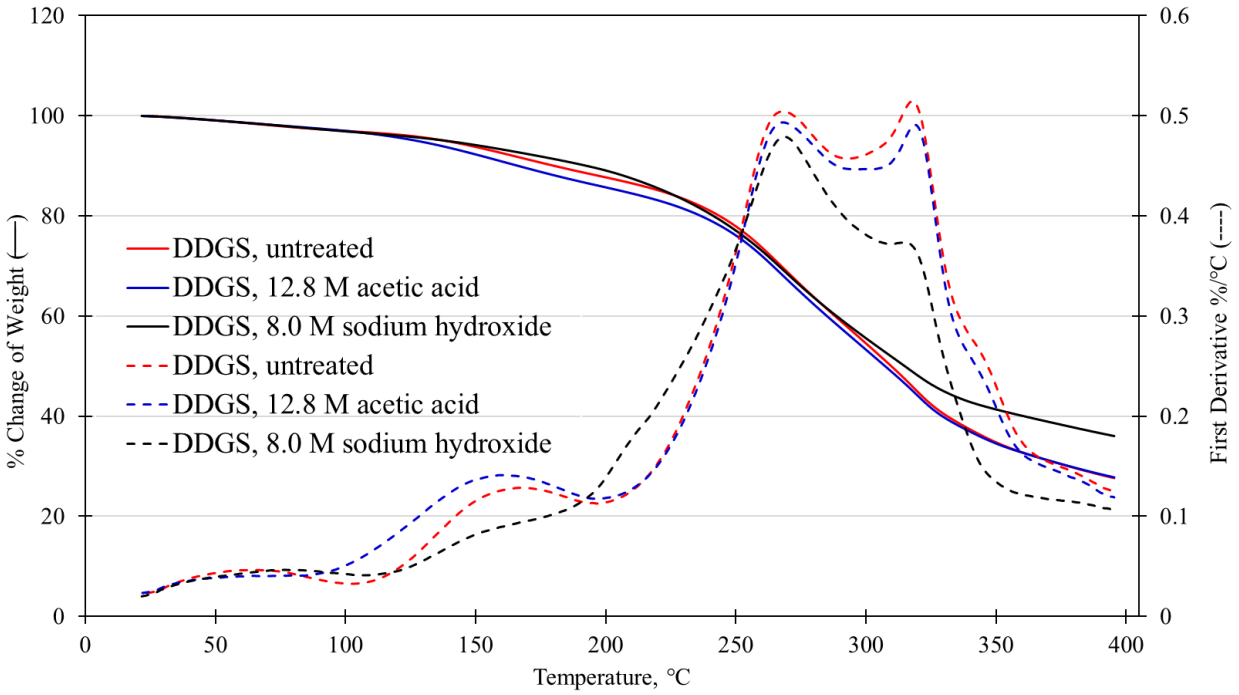

Figure 24. Thermogravimetric analysis of untreated and treated DDGS particles.

The weight loss at temperatures below 100°C is attributed to the loss of moisture in all samples and is considered negligible.

The local maxima of the first derivative curves occur between 100°C and 200°C, which relates to the initial degradation of DDGS components. These components include protein, starch, fat, hemicellulose, cellulose, and lignin [62]. The temperature range of the local maxima corresponds to a similar study [10]. To maintain about 90% of DDGS weight in the percentage change of weight curves, the press temperature should not exceed 200°C, which confers with the similar study [10]. Pressing the wood composite at the right temperature is crucial to prevent loss of mechanical properties.

Between 250°C and 350°C of the first derivative cures, all samples display their mass decomposition of major components of DDGS, and the range is similar to the previous study [10]. These major components include protein, hemicellulose, cellulose, and lignin [10], [63].

Among the DDGS samples, both acid treated and untreated DDGS particles exhibit higher degradation rate than alkali treated. This trend relates to the previous study that better heat stability is achieved with a lower protein content in DDGS [64]. As observed in the composition analysis in Table 10, alkali treated DDGS have a protein content of 28.91%, which is numerically lower than both untreated DDGS and acid treated DDGS of 33.15% and 33.62%, respectively.

Overall, acid treated and untreated DDGS samples display similar decomposition behavior, while alkali treated DDGS samples have better thermal stability. Thus, the presence of DDGS protein in samples may influence their degradation behaviors.

5.1.3. Differential scanning calorimetry (DSC)

The effect of untreated and treated DDGS particles on the glass transition and melting peak temperatures were analyzed using DSC, as shown in Figure 25. Untreated, acid treated, and alkali treated DDGS particles display glass transition temperatures of 53.50℃, 63.93℃, and 60.05℃, respectively. The higher glass transition temperatures of treated DDGS might be attributed to its lower fat contents [6].

The untreated, acid treated, and alkali treated DDGS particles have melting peaks at 110.59℃, 125.04℃, and 122.38℃, respectively. Among samples, chemically treated DDGS particles have higher melting temperatures than untreated DDGS. These melting peaks fall within the initial degradation range from the TGA, between 100℃ and 200℃, in Figure 24, and these melting peaks possibly demonstrated on both the denaturation temperatures of proteins and degradation temperatures of DDGS components. The higher melting temperatures of treated DDGS samples were possibly due to the denaturation and solubilization of protein during acid or alkali treatment process, which may result in the change of DDGS composition and protein

structure. Thus, the higher melting temperature of treated DDGS could possibly means that chemically treated DDGS samples have been denatured to potentially act as a natural binder.

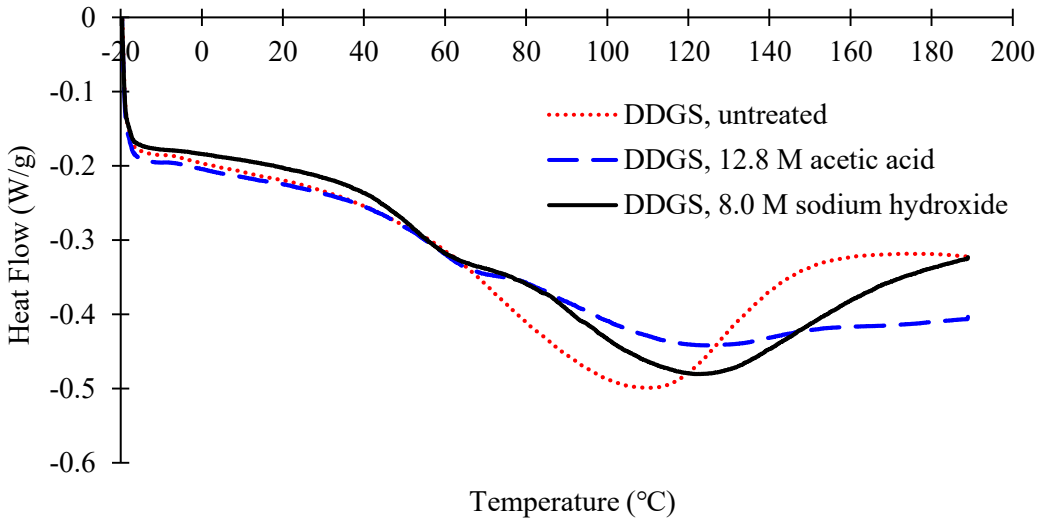

Figure 25. Differential scanning calorimetry results of untreated and treated DDGS particles.

5.1.4. Fourier transform infrared spectroscopy (FTIR)

Figure 26 shows the FTIR spectrum of untreated DDGS and treated DDGS particles. The broad peaks in the 3500-3200 cm^{-1} region represent the –OH and –NH stretching, whereas the peaks in the 2950-2500 cm^{-1} region represent the –CH stretching. The –OH and –NH stretching are identified as carbohydrates and protein, respectively, while the –CH stretching is identified as lipids [65]. Next, the peaks in the 1500-1000 cm^{-1} region represent the CHO bond of carbohydrates [66]. The peaks in the region of 1700-1500 cm^{-1} region represent the protein amide I and II [67], while the peaks in the 1700-1800 cm^{-1} region represent the –C=O stretching. Moreover, the peaks in the 600-700 cm^{-1} region show the P-S and P=S stretching [6]. The –C=O and P-S/P=S stretching are identified as lignin and protein, respectively [6].

From all these peaks, a noticeably different in terms of peak intensity fell within the 1700-1500 cm^{-1} region. The peaks in this region show weaker peak intensities of treated DDGS

than untreated DDGS. The weaker peak intensities of protein amide I and II may be attributed to the unfolded proteins of acid or alkali treated DDGS.

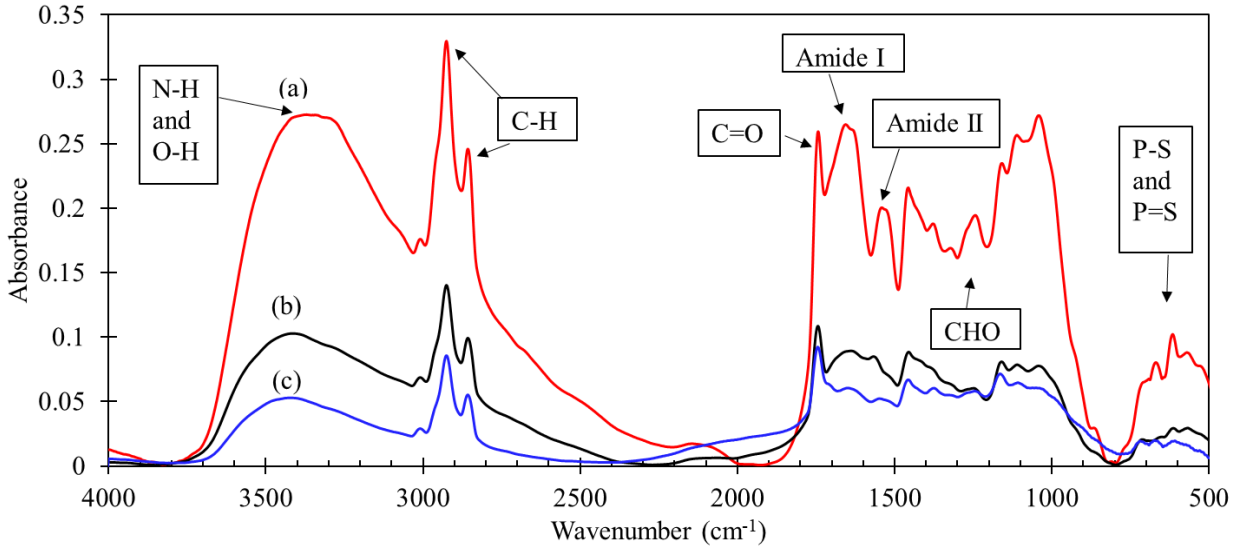

Figure 26. FTIR spectrum of (a) untreated DDGS particles, (b) 8.0 M sodium hydroxide treated DDGS particles, and (c) 12.8 M acetic acid treated DDGS particles.

5.2. Initial phase of mechanical testing

The initial mechanical tests were performed on the samples to understand the effect of press temperature and chemical concentration on both the internal bond and flexural strengths of particleboards. The preferred temperature and chemical concentrations were selected based on the weighting method and were then used in the final phase of this research.

5.2.1. Density results

The medium-density of the particleboards as defined by ANSI A208.1 standard was between 640 kg/m^3 and 800 kg/m^3 [19]. The target density of the particleboards was 720 kg/m^3 which is the middle limit of medium-density particleboards. The density results are shown in Figure 27 and Figure 28. When comparing the density to the ANSI A208.1 standard, all formulations fall within the medium-density particleboard category.

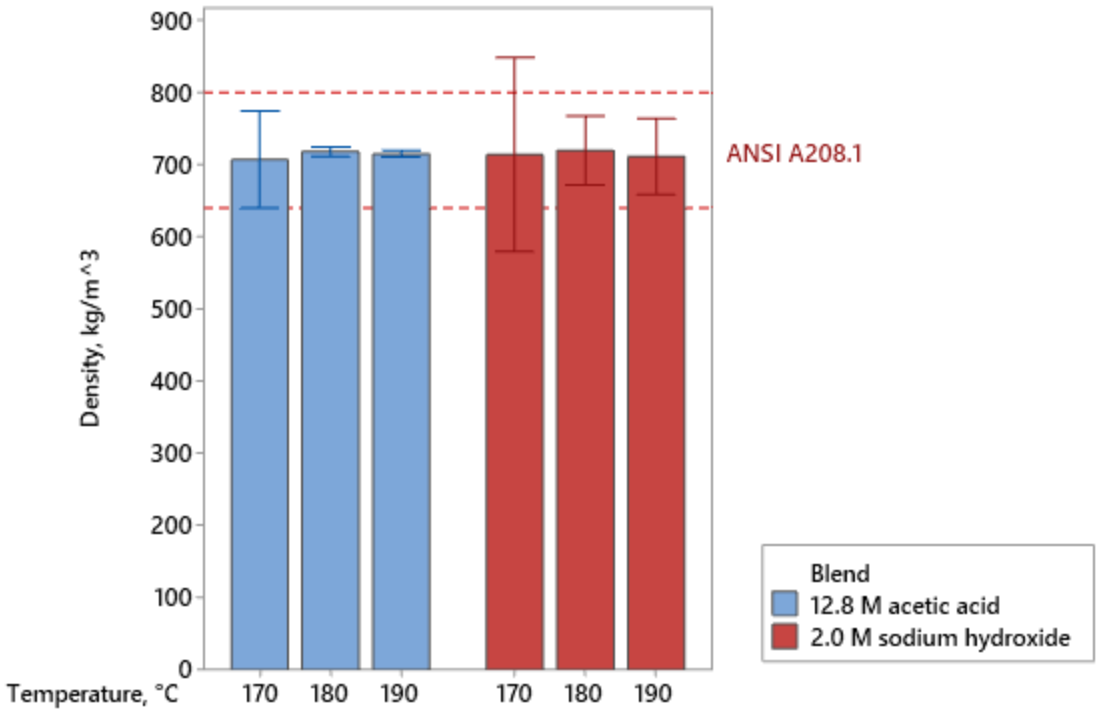

Figure 27. Density of particleboards at various press temperatures.

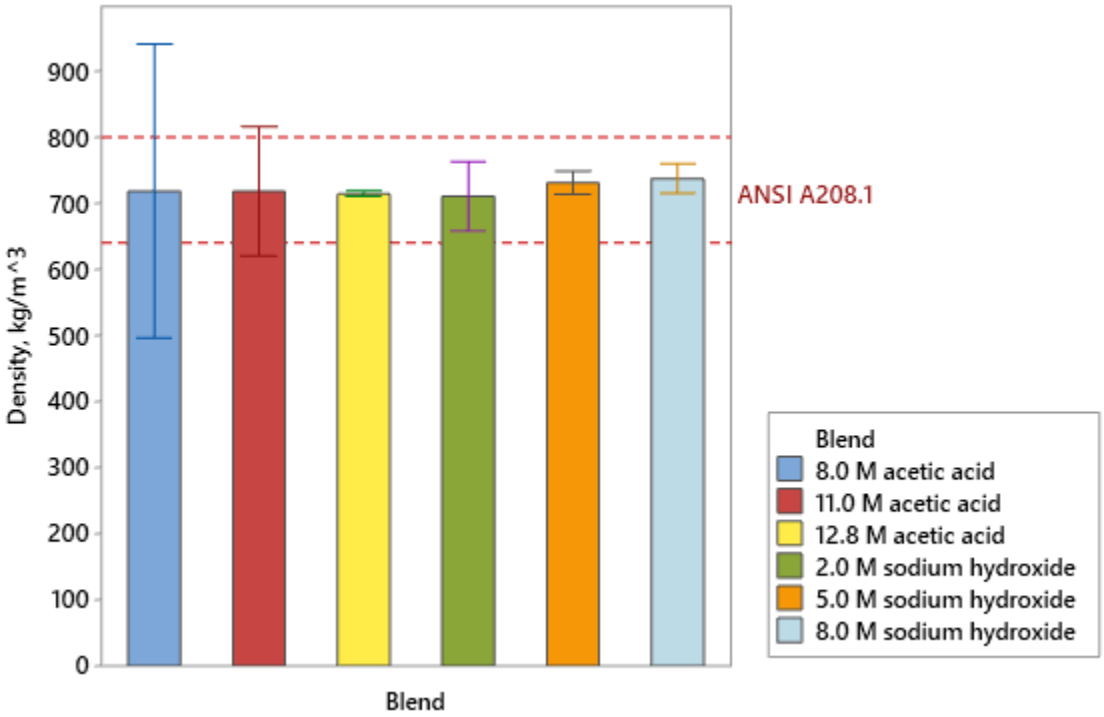

Figure 28. Density of particleboards at various chemical concentrations.

5.2.2. Relationship between temperature and mechanical properties of particleboards

The samples were hot-pressed at 170℃, 180℃, and 190℃ to study the effect of temperature on the modulus of rupture of particleboards, as shown in Figure 29, where high modulus of rupture is desired. Tisserat et al. reported that the superior modulus of rupture of fiberboard pressed at 185℃ was attributed to the plasticization of DDGS [6]. Furthermore, the plasticization occurred when the samples had a smooth tactile feel on their surface, which imitated a wood composite manufactured with a thermoset or thermoplastic resin [6]. In this study, the modulus of rupture of the samples pressed at 190℃ are superior to those pressed at 170℃ and 180℃, which may be attributed to a higher plasticization of the particleboards while limited plasticization occurred below 190℃. However, the flexural samples failed to meet the requirements of the ANSI A208.1-2009 standard.

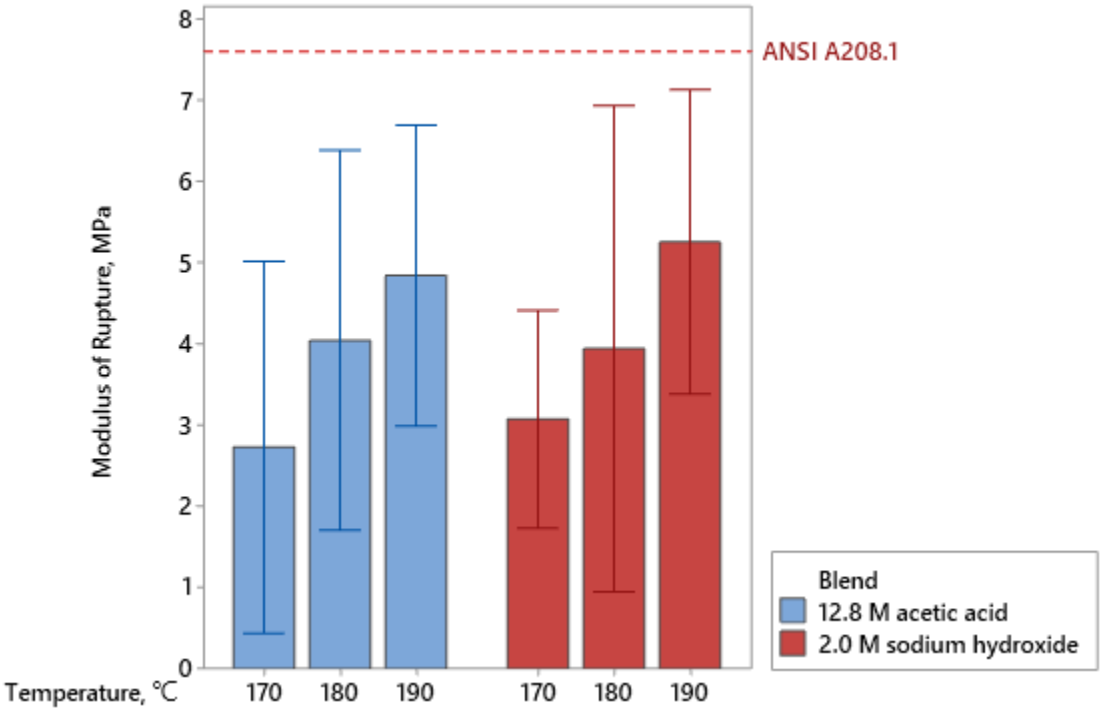

Figure 29. Relationship between temperature and modulus of rupture of particleboards.

The highest internal bond strengths for 2.0 M sodium hydroxide and 12.8 M acetic acid treatments are achieved at 190℃ and 180℃, respectively, as shown in Figure 30. The decrease in internal bond strength of acetic acid treatment at 190℃ may be due to the brittleness and degradation of the DDGS. However, no clear trend is visible based on increasing or decreasing the temperature of sodium hydroxide treated DDGS. This is likely due to the small number of temperatures that are tested. The results in Figure 30 show that the samples have met the internal bond strength requirement of ANSI A208.1-2009 standard.

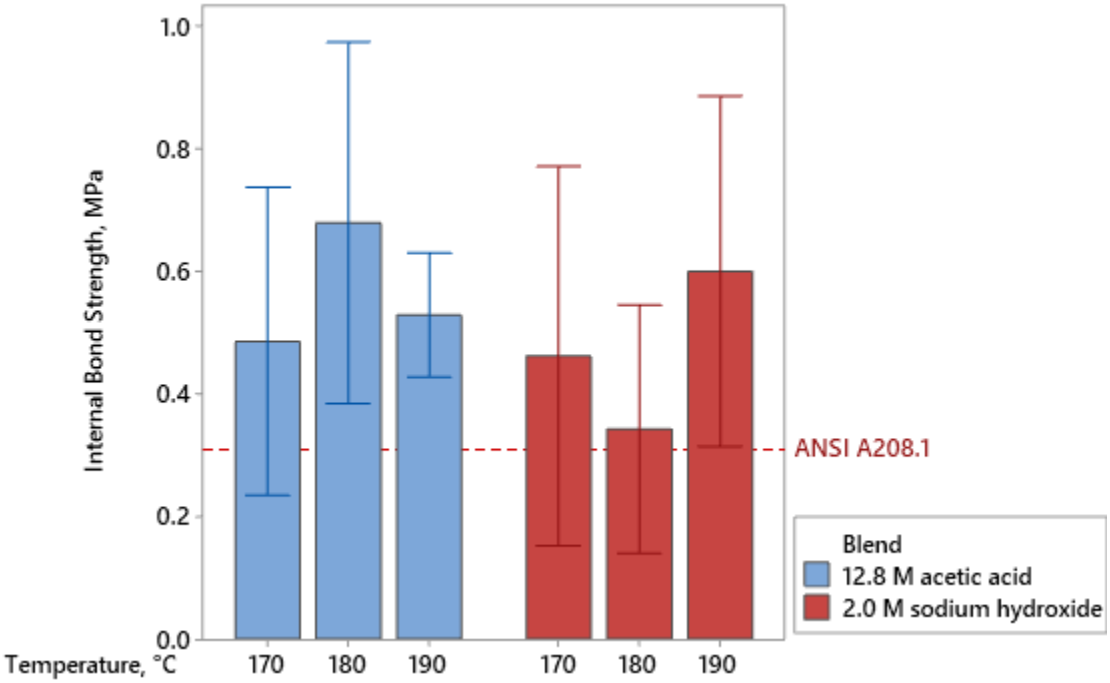

Figure 30. Relationship between temperature and internal bond strength of particleboards.

5.2.3. Relationship between chemical concentration and mechanical properties of particleboards

Figure 31 depicts the relationship between chemical concentration and flexural strength of particleboards. The highest flexural strengths are achieved with 2.0 M sodium hydroxide and 12.8 M acetic acid. No clear trend is visible based on increasing or decreasing chemical

concentration, which is likely due to the small number of molarities that were tested. A previous study shows that weak acid treatment led to the hydrolysis of hemicellulose that resulted in increasing porosity of the lignocellulosic biomass, while alkaline treatment led to the removal of lignin [68]. Thus, higher chemical concentration of acid treated DDGS can possibly lead to better penetration of acid into the composite and may be able to enhance the binding properties of DDGS particles with wood flour.

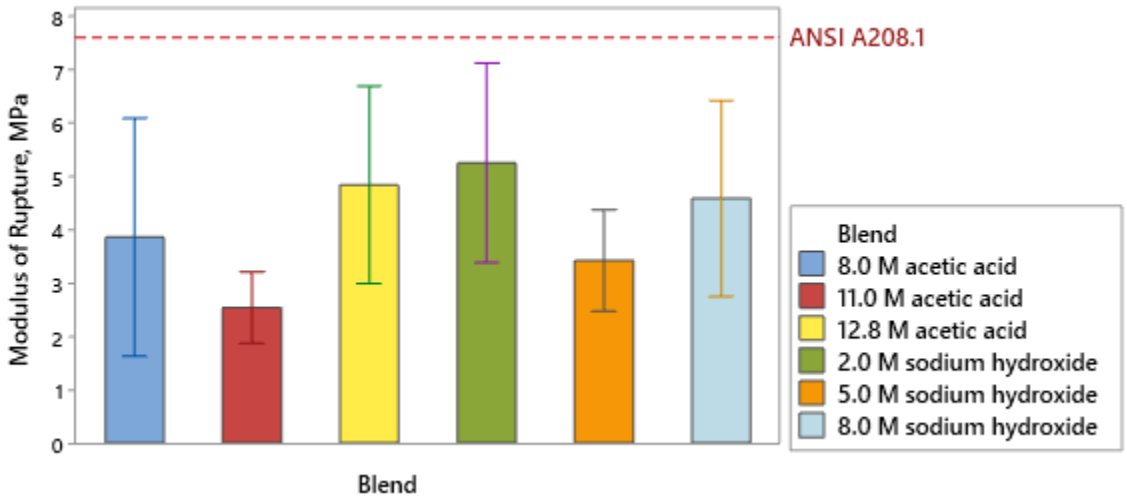

Figure 31. Relationship between chemical concentration and flexural strength of particleboards.

Figure 32 shows that the internal bond strengths of particleboards increase with increasing concentration of sodium hydroxide, where 8.0 M alkali treated DDGS displays a relatively high internal bond strength. The high internal bond strength may be attributed to the DDGS proteins being denatured and may lead to greater hydrolysis of DDGS proteins as the concentration of sodium hydroxide increases. The higher concentrations of sodium hydroxide treated samples lead to better bonding between wood flour and DDGS particles. However, with acid treated DDGS, the highest internal bond strength is achieved at 11.0 M acetic acid treatment. This may be attributed to the increase in chemical acidity from 8.0 M to 11.0 M that enhance the internal bond strengths of the samples because of better penetration of acid or alkali

into the composite. However, no clear trend is visible based on increasing or decreasing chemical concentration. This is likely due to the small number of molarities that were tested.

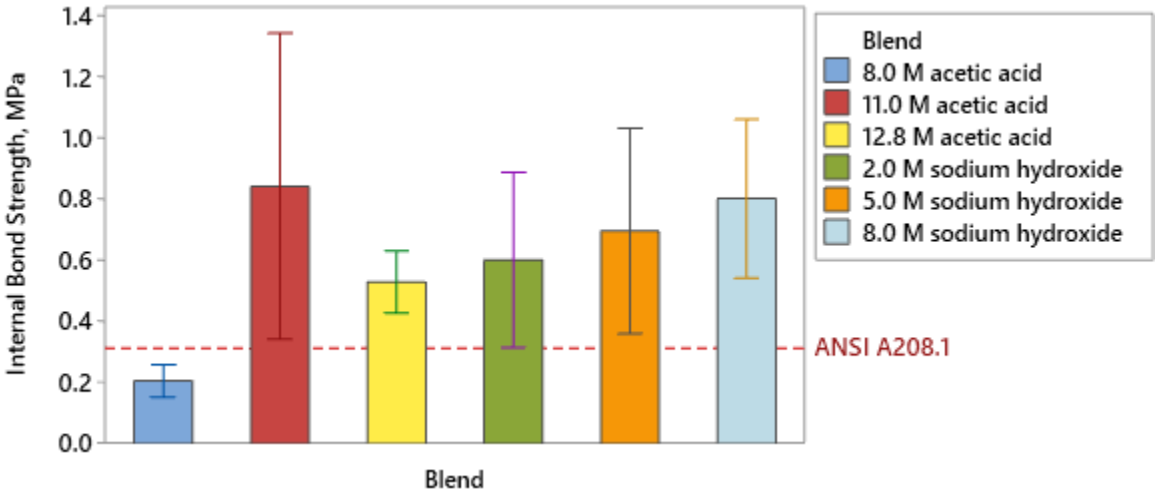

Figure 32. Relationship between chemical concentration and internal bond strength of particleboards.

5.2.4. Tabular additive weighting method

Table 11, Table 12, Table 13, and Table 14 illustrate a tabular additive weighting method. The performance rating (R) was ranked between 1 and 3 and were assigned to the flexural and internal bond strength results in Figure 29, Figure 30, Figure 31, and Figure 32. The totals of W × R are used in comparing the alternatives, where the highest W × R values indicated the best alternative.

From Table 11 and Table 12, the preferred press temperatures are 180°C and 190°C, respectively. Even though the preferred press temperature is 180°C in Table 11, 190°C is chosen because of the small difference of 0.2 in sums of W × R between 180°C and 190°C alternatives, while in Table 12 there is a larger difference of 1.6 which shows processing at 190°C produces superior mechanical properties. For convenience purposes, 190°C press temperature is selected as the preferred temperature for all treatments. From Table 13 and Table 14, 12.8 M and 8.0 M

are selected as the preferred concentration for acetic acid and sodium hydroxide, respectively.

Those molarities are selected due to their high values in sums of W × R.

Table 11. Selection of the preferred press temperature from the mechanical testing of 12.8 M acetic acid treatment. The preferred temperature is underlined.

Alternative\ Criterion	Weight (W)	170°C		180°C		190°C	
		Rating (R)	W × R	Rating (R)	W × R	Rating (R)	W × R
Internal bond strength	0.6	1	0.6	3	1.8	2	1.2
Flexural strength	0.4	1	0.4	2	0.8	3	1.2
Sum	**1.0**		**1.0**		**2.6**		**2.4**

Table 12. Selection of the preferred press temperature from the mechanical testing of 2 M sodium hydroxide treatment. The preferred temperature is underlined.

Alternative\ Criterion	Weight (W)	170°C		180°C		190°C	
		Rating (R)	W × R	Rating (R)	W × R	Rating (R)	W × R
Internal bond strength	0.6	2	1.2	1	0.6	3	1.8
Flexural strength	0.4	1	0.4	2	0.8	3	1.2
Sum	**1.0**		**1.6**		**1.4**		**3.0**

Table 13. Selection of the preferred chemical concentration from the mechanical testing of acetic acid treatment at various concentrations. The preferred chemical concentration is underlined.

Alternative\ Criterion	Weight (W)	8.0 M		11.0 M		12.8 M	
		Rating (R)	W × R	Rating (R)	W × R	Rating (R)	W × R
Internal bond strength	0.6	1	0.6	3	1.8	2	1.2
Flexural strength	0.4	2	0.8	1	0.4	3	1.2
Sum	**1.0**		**1.4**		**2.2**		**2.4**

Table 14. Selection of the preferred chemical concentration from the mechanical testing of sodium hydroxide treatment at various concentrations. The preferred chemical concentration is underlined.

Alternative\ Criterion	Weight (W)	2.0 M		5.0 M		8.0 M	
		Rating (R)	W × R	Rating (R)	W × R	Rating (R)	W × R
Internal bond strength	0.6	1	0.6	2	1.2	3	1.8
Flexural strength	0.4	3	1.2	1	0.4	2	0.8
Sum	**1.0**		**1.8**		**1.6**		**2.6**

5.3. Final phase of physical and mechanical testing

Initial phase of mechanical testing indicated that 12.8 M and 8.0 M were selected as the preferred concentration for acetic acid and sodium hydroxide, respectively, while the preferred press temperature was at 190℃. These preferred concentrations and press temperature were applied in this section to understand the physical and mechanical behaviors of particleboards.

5.3.1. Density results

The medium-density of the particleboards as defined by ANSI A208.1 was between 640 kg/m^3 and 800 kg/m^3 [19]. The target density of the particleboards is 720 kg/m^3, which is the middle limit of medium-density particleboards and all formulations fall within the medium-density particleboard category, as shown in Figure 33.

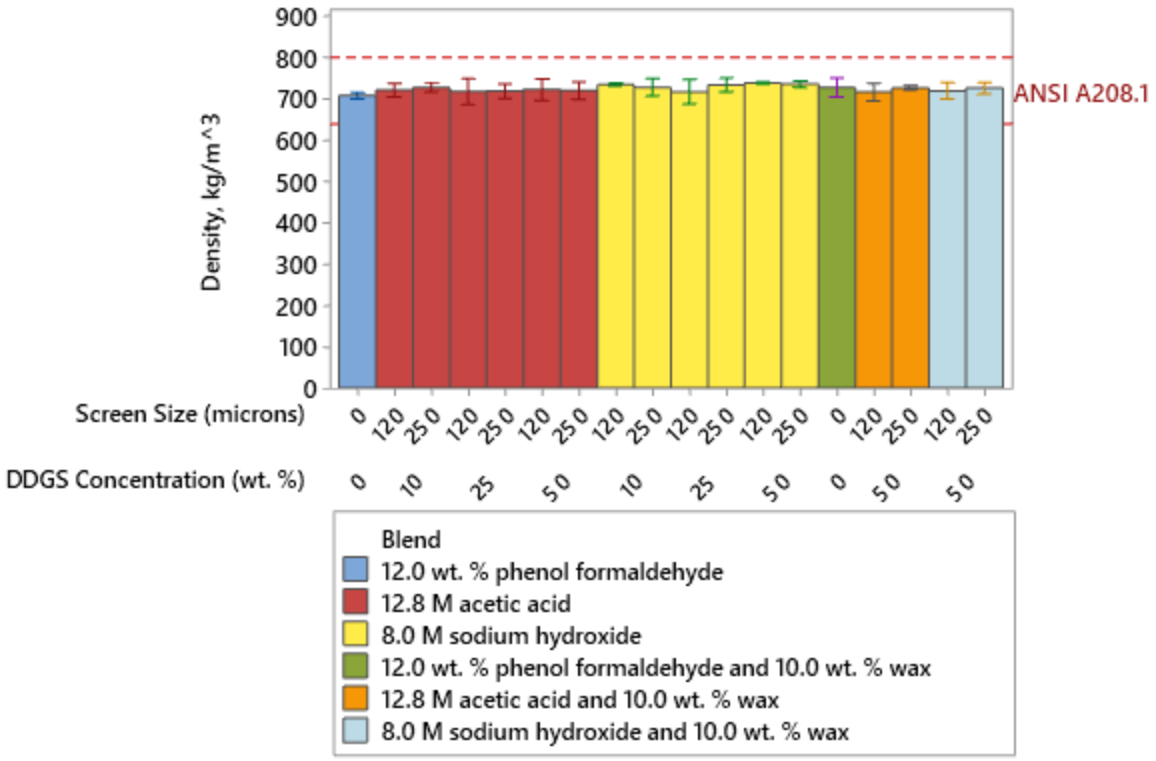

Figure 33. Density of particleboards.

The factor information displays the specific blends, screen sizes, and DDGS concentrations performed using a three-way ANOVA model, as shown in Table 15. The three-way interaction between blend, screen size, and DDGS concentration is not significant, as shown in Table 16. Moreover, all the other interaction effects in the three-way ANOVA model are not significant; therefore, the interactions in Figure 34 can be ignored.

Table 15. Factor information for three-way ANOVA on density.

Factor	Levels	Values
Blend	2	12.8 M acetic acid, 8.0 M sodium hydroxide
Screen Size	2	120, 250
DDGS Concentration	3	10, 25, 50

Table 16. A three-way ANOVA for density.

Source	DF	SS	MS	F	P
Blend	1	1209.12	1209.12	8.16	0.007
Screen Size	1	51.56	51.56	0.35	0.559
DDGS Concentration	2	446.14	223.07	1.5	0.236
Blend*Screen Size	1	1.44	1.44	0.01	0.922
Blend*DDGS Concentration	2	216.91	108.46	0.73	0.488
Screen Size*DDGS Concentration	2	271.52	135.76	0.92	0.409
Blend*Screen Size*DDGS Concentration	2	453.55	226.78	1.53	0.23
Error	36	5336.6	148.24		
Total	47	7986.84			
S	12.1753	**R-sq**	33.18%	**R-sq (adj)**	12.77%

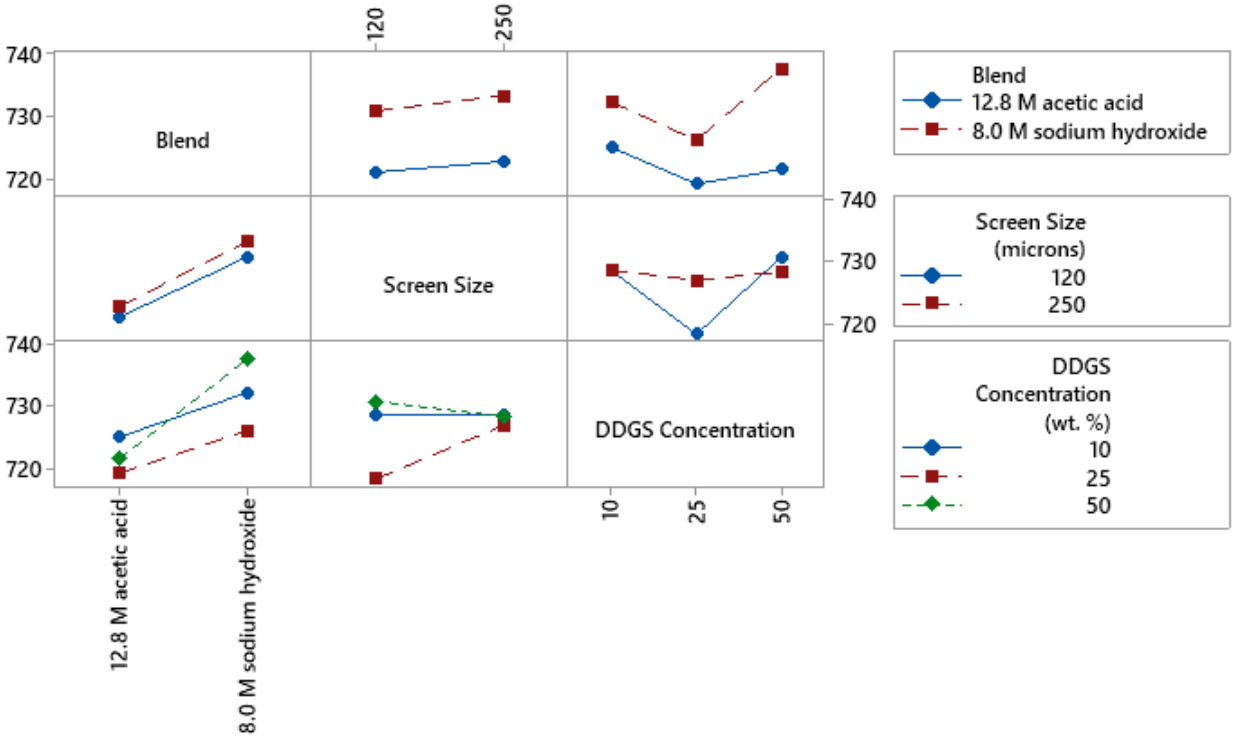

Figure 34. Interaction plot of blend, screen size, and DDGS concentration for density.

Since the interaction effect is not significant; therefore, a three-way ANOVA test on main effects will be interpreted, and blend is the only main effect being significant. Thus, a separate ANOVA model was run on blend followed by post hoc Tukey test to determine whether the means are significantly different. The results indicated that 8.0 M sodium hydroxide is not significantly different as most blends but significantly different from both 12.8 M acetic acid and 12 wt. % phenol formaldehyde, as shown in Table 17.

Table 17. Tukey pairwise comparison showing the influence of blend on the density.

Blend	N	Mean	Grouping	
8.0 M sodium hydroxide	24	732.02	A	
12.0 wt.% phenol formaldehyde and 10.0 wt.% wax	4	727.88	A	B
8.0 M sodium hydroxide and 10.0 wt.% wax	8	723.19	A	B
12.8 M acetic acid and 10.0 wt.% wax	8	721.99	A	B
12.8 M acetic acid	24	721.98		B
12.0 wt.% phenol formaldehyde	4	708.44		B
Means that do not share a letter are significantly different.				

5.3.2. Water absorption results

The water absorption test was tested using a 2-plus-22-hour method to obtain the physical behavior of the sample in both short term of 2 hours and long term of 24 hours bases. This section does not include analysis on 8.0 M sodium hydroxide because the samples broke apart after being submerged for 2 hours. Thus, no meaningful data can be obtained from the 8.0 M sodium hydroxide blend, and 10 wt. % wax was added to improve the moisture resistance of this blend. By adding wax to the combination of 8.0 M sodium hydroxide and 50 wt. % DDGS, meaningful results were obtained. The highest DDGS concentration was chosen to include wax because the results of acetic acid blend show that the water resistance properties of the boards increase with increasing DDGS concentration. Thus, 10 wt. % wax was added to both acetic acid and sodium hydroxide blends that contain 50 wt. % DDGS for further analysis.

5.3.2.1. 2-hour percentage change in volume test

The 2-hour percentage change in volume of each particleboard was measured and is summarized in Figure 35, where low percentage change in volume is desired.

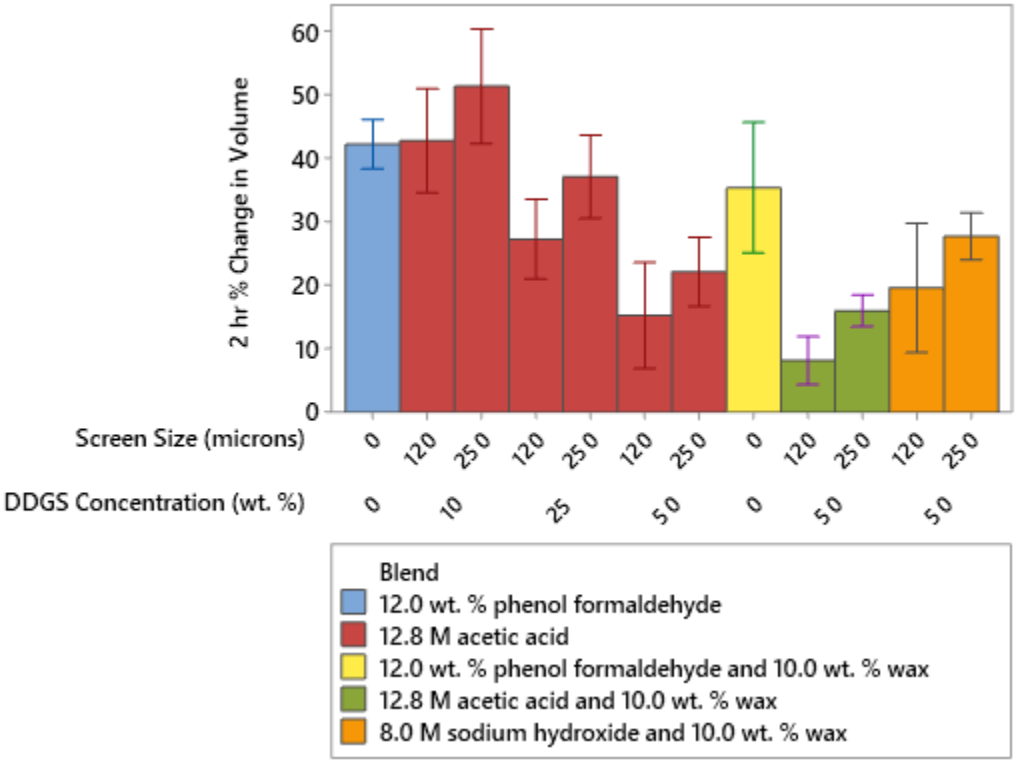

Figure 35. 2-hour percentage change in volume of particleboards.

The factor information displays the specific screen sizes and DDGS concentrations that were performed using a two-way ANOVA model, as shown in Table 18. The interaction effect in the two-way ANOVA model is not significant in Table 19, and this is supported by the parallel profiles in Figure 36; thus the interaction effect can be ignored. Since the interaction effect is not significant; therefore, the two-way ANOVA test on main effect can be interpreted, where screen size and DDGS concentration are significant. The main effects indicated that either smaller screen size or larger DDGS concentrations lead to better water resistance properties of particleboards.

Table 18. Factor information on two-way ANOVA for 2-hour percentage change in volume.

Factor	Levels	Values
Screen Size	2	120, 250
DDGS Concentration	3	10, 25, 50

Table 19. A two-way ANOVA for 2-hour percentage change in volume.

Source	**DF**	**SS**	**MS**	**F**	**P**
Screen Size	1	425.98	425.98	19.58	0
DDGS Concentration	2	3228.55	1614.28	74.19	0
Screen Size*DDGS Concentration	2	8.98	4.49	0.21	0.815
Error	18	391.63	21.76		
Total	23	4055.15			
S	4.66447	**R-sq**	90.34%	**R-sq (adj)**	87.66%

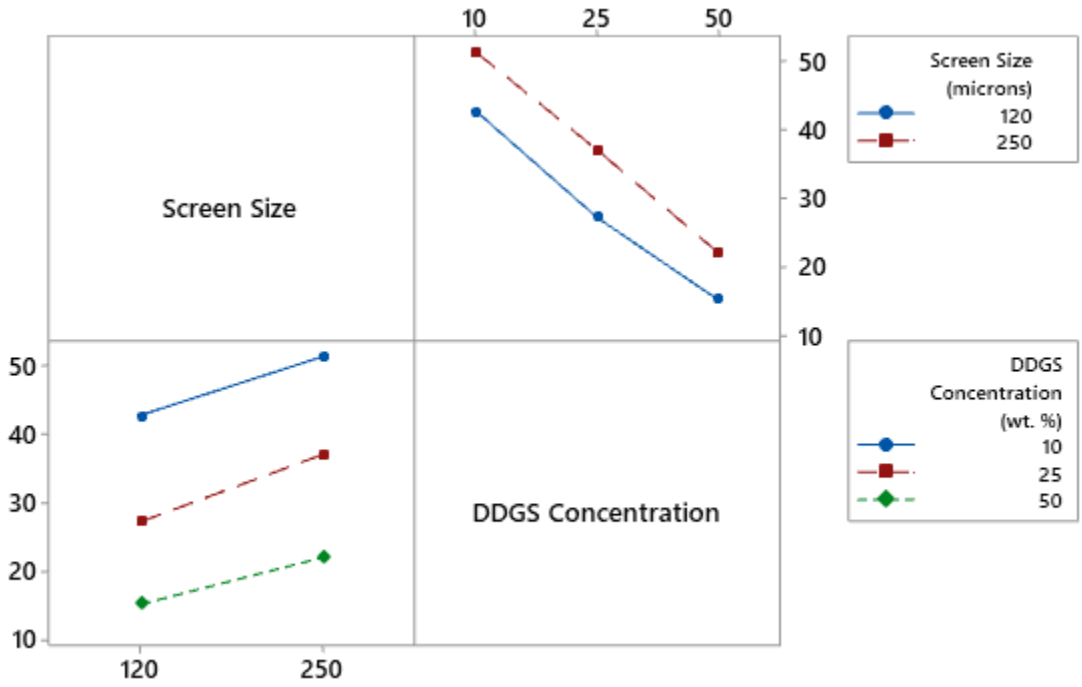

Figure 36. Interaction plot of screen size, and DDGS concentration for 2-hour percentage change in volume.

Blend was not included in a two-way ANOVA; thus, a separate ANOVA model was run on blend-only followed by post hoc Tukey test to determine whether the means are significantly different. 12.8 M acetic acid is significantly different than 12.8 M acetic acid and 10 wt. % wax in Table 20, and this implies that the addition of wax into particleboards lead to better water resistance property compared to without wax.

Table 20. Tukey pairwise comparison showing the influence of blend on the 2-hour percentage change in volume.

Blend	N	Mean	Grouping		
12.0 wt.% phenol formaldehyde	4	42.33	A		
12.0 wt.% phenol formaldehyde and 10.0 wt.% wax	4	35.48	A	B	
12.8 M acetic acid	24	32.72	A	B	
8.0 M sodium hydroxide and 10.0 wt.% wax	8	23.71		B	C
12.8 M acetic acid and 10.0 wt.% wax	8	12.13			C
Means that do not share a letter are significantly different.					

5.3.2.2. 2-hour percentage change in mass test

The 2-hour percentage change in mass of each particleboard was measured and is summarized in Figure 37, where low percentage change in mass is desired.

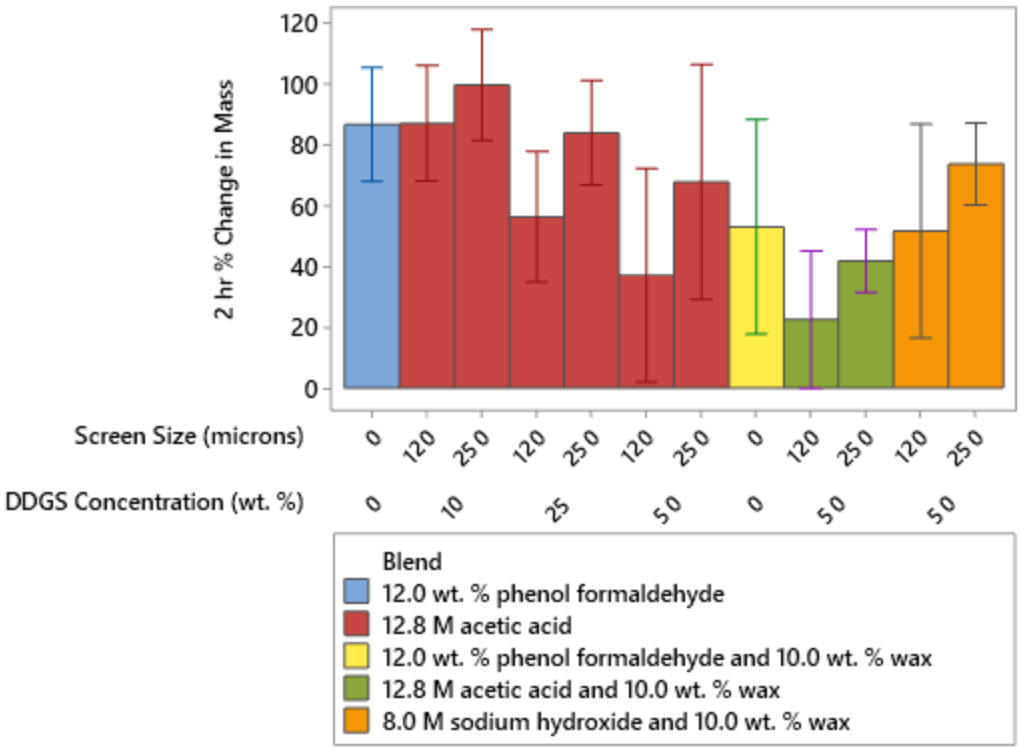

Figure 37. 2-hour percentage change in volume of particleboards.

The factor information displays the specific screen sizes and DDGS concentrations that were performed using a two-way ANOVA model, as shown in Table 21. The interaction effect in the two-way ANOVA model is not significant in Table 22, and this is supported by the parallel profiles in Figure 38; thus the interaction effect can be ignored. Since the interaction effect is not significant; therefore, a two-way ANOVA test on main effect can be interpreted, where screen size and DDGS concentration are significant. The main effects indicated that either smaller screen size or larger DDGS concentrations lead to better water resistance of the particleboards.

Table 21. Factor information on two-way ANOVA for 2-hour percentage change in mass.

Factor	Levels	Values
Screen Size	2	120, 250
DDGS Concentration	3	10, 25, 50

Table 22. A two-way ANOVA for 2-hour percentage change in mass.

Source	DF	SS	MS	F	P
Screen Size	1	3345.5	3345.5	12.16	0.003
DDGS Concentration	2	6743.5	3371.7	12.25	0
Screen Size*DDGS Concentration	2	375.4	187.7	0.68	0.518
Error	18	4953.9	275.2		
Total	23	15418.3			
S	16.5897	**R-sq**	67.87%	**R-sq (adj)**	58.94%

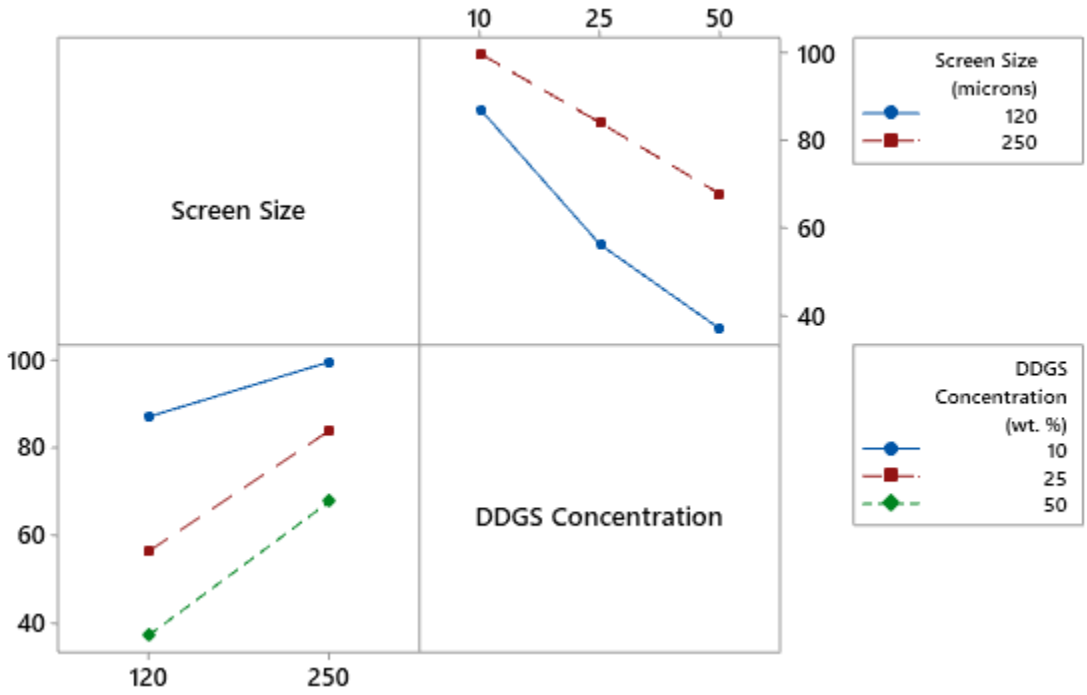

Figure 38. Interaction plot of screen size, and DDGS concentration for 2-hour percentage change in mass.

Blend was not included in a two-way ANOVA model; therefore, a separate ANOVA model was run on blend followed by post hoc Tukey test to determine whether the means are significantly different. 12.8 M acetic acid is significantly different than 12.8 M acetic acid and 10 wt. % wax in Table 23, and this implies that the addition of wax into particleboards lead to a better water resistance property compared to without wax.

Table 23. Tukey pairwise comparison showing the influence of blend on the 2-hour percentage change in mass.

Blend	N	Mean	Grouping	
12.0 wt.% phenol formaldehyde	4	86.71	A	
12.8 M acetic acid	24	72	A	
8.0 M sodium hydroxide and 10.0 wt. % wax	8	62.69	A	B
12.0 wt.% phenol formaldehyde and 10.0 wt. % wax	4	53.1	A	B
12.8 M acetic acid and 10.0 wt. % wax	8	32.2		B
Means that do not share a letter are significantly different.				

5.3.2.3. 24-hour percentage change in volume test

The 24-hour percentage change in volume of each particleboard was measured and is summarized in Figure 39, where low percentage change in volume is desired.

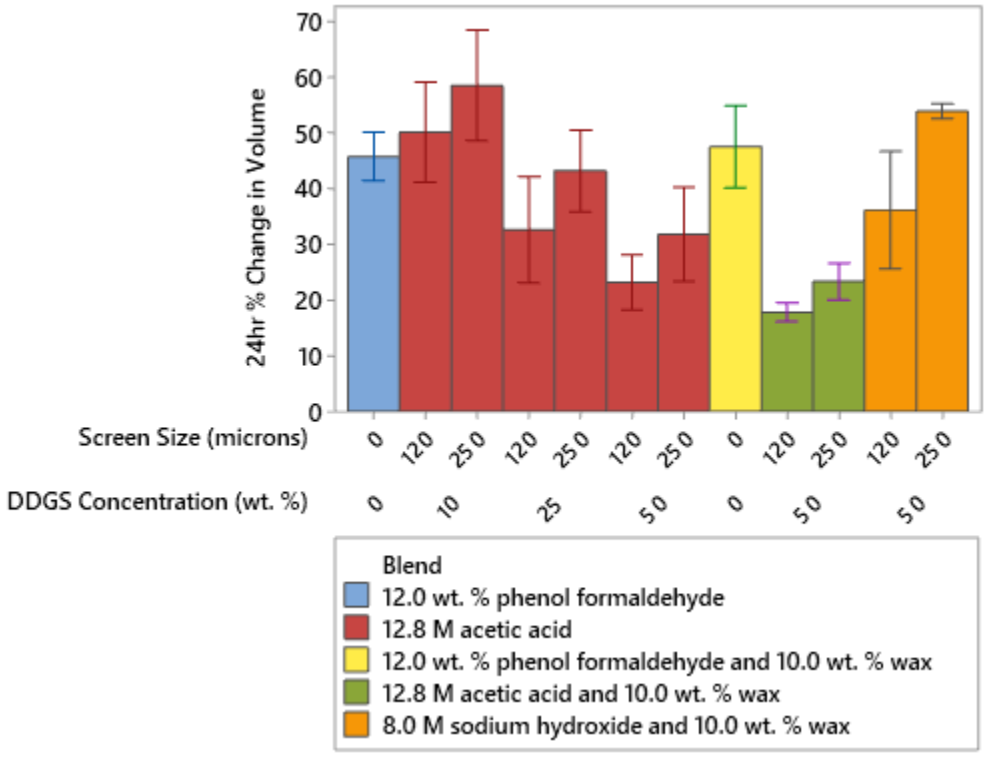

Figure 39. 24-hour percentage change in volume of particleboards.

The factor information displays the specific screen sizes and DDGS concentrations that were performed using a two-way ANOVA model, as shown in Table 24. The interaction effect in

the two-way ANOVA model is not significant in Table 25, and this is supported by the parallel profiles in Figure 40; thus, the interaction effect can be ignored. Since the interaction effect is not significant; therefore, a two-way ANOVA test on main effect can be interpreted, where screen size and DDGS concentration are significant. The main effects indicated that either smaller screen size or larger DDGS concentrations lead to better water resistance of the particleboards.

Table 24. Factor information on two-way ANOVA for 24-hour percentage change in volume.

Factor	Levels	Values
Screen Size	2	120, 250
DDGS Concentration	3	10, 25, 50

Table 25. A two-way ANOVA for 24-hour percentage change in volume.

Source	**DF**	**SS**	**MS**	**F**	**P**
Screen Size	1	507.09	507.09	18.31	0
DDGS Concentration	2	2934.23	1467.11	52.96	0
Screen Size*DDGS Concentration	2	5.71	2.86	0.1	0.903
Error	18	498.6	27.7		
Total	23	3945.64			
S	5.2631	**R-sq**	87.36%	**R-sq (adj)**	83.85%

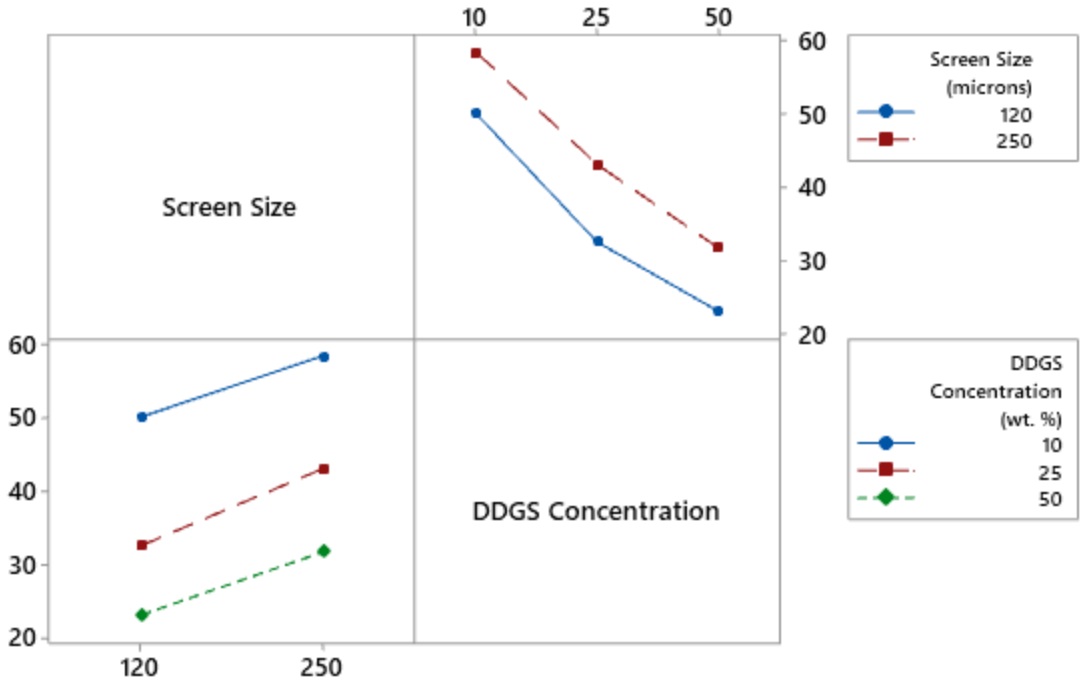

Figure 40. Interaction plot of screen size and DDGS concentration for 24-hour percentage change in volume.

Blend was not included in a two-way ANOVA model; therefore, a separate ANOVA model was run on blend followed by post hoc Tukey test to determine whether the means are significantly different. The Tukey test revealed that 12.8 M acetic acid is significantly different than other blends in Table 26, and this implies that the addition of wax into particleboards lead to a better water resistance property compared to without wax. Overall, 12.8 M acetic acid and 10 wt. % wax blend outperformed the control combinations of 12 wt. % phenol formaldehyde and 10 wt. % wax.

Table 26. Tukey pairwise comparison showing the influence of blend on the 24-hour percentage change in volume.

Blend	N	Mean	Grouping	
12.0 wt.% phenol formaldehyde and 10.0 wt.% wax	4	47.55	A	
12.0 wt.% Phenol formaldehyde	4	45.82	A	
8.0 M sodium hydroxide and 10.0 wt.% wax	8	45.06	A	
12.8 M acetic acid	24	39.95	A	
12.8 M acetic acid and 10.0 wt.% wax	8	20.59		B
Means that do not share a letter are significantly different.				

5.3.2.4. 24-hour percentage change in mass test

The 24-hour percentage change in mass of each particleboard was measured and is summarized in Figure 41, where low percentage change in mass is desired.

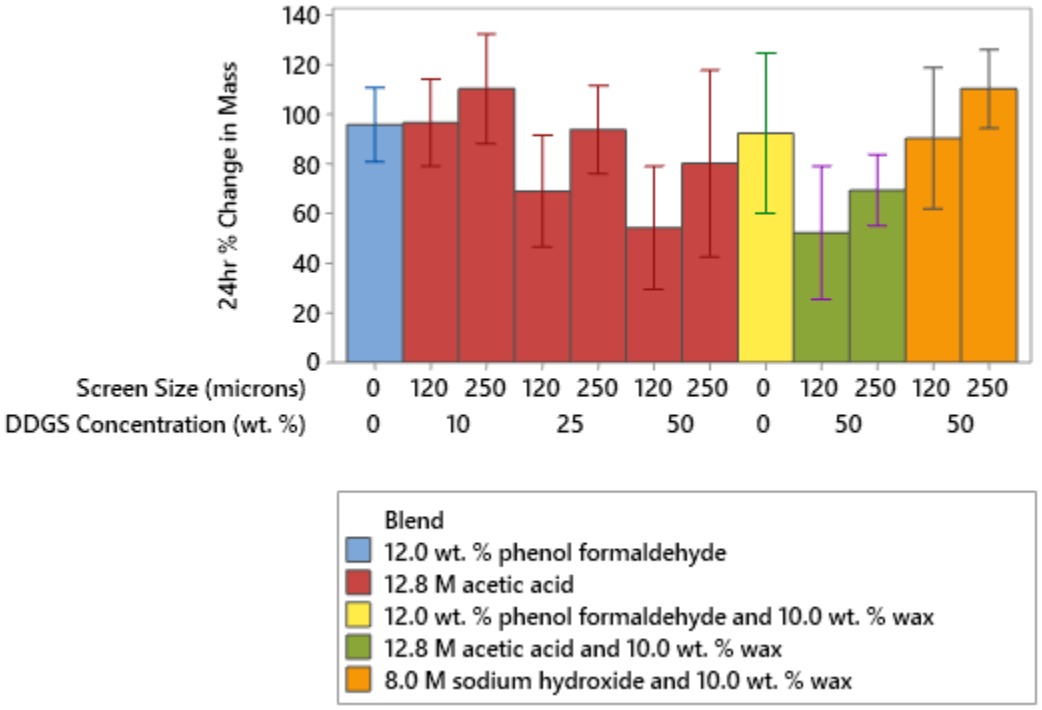

Figure 41. 24-hour percentage change in mass of particleboards.

The factor information displays the specific screen sizes and DDGS concentrations that were performed using a two-way ANOVA model, as shown in Table 27. The interaction effect in

the two-way ANOVA model is not significant in Table 28, and this is supported by the parallel profiles in Figure 42; thus, the interaction effect can be ignored. Since the interaction effect is not significant; therefore, a two-way ANOVA test on main effect can be interpreted, where screen size and DDGS concentration are significant. The main effects indicated that either smaller screen size or larger DDGS concentrations lead to better water resistance of the particleboards.

Table 27. Factor information on two-way ANOVA for 24-hour percentage change in mass.

Factor	Levels	Values
Screen Size	2	120, 250
DDGS Concentration	3	10, 25, 50

Table 28. A two-way ANOVA for 24-hour percentage change in mass.

Source	**DF**	**SS**	**MS**	**F**	**P**
Screen Size	1	2743.9	2743.93	11.43	0.003
DDGS Concentration	2	5322.9	2661.44	11.09	0.001
Screen Size*DDGS Concentration	2	184	92.01	0.38	0.687
Error	18	4320	240		
Total	23	12570.9			
S	15.492	**R-sq**	65.63%	**R-sq (adj)**	56.09%

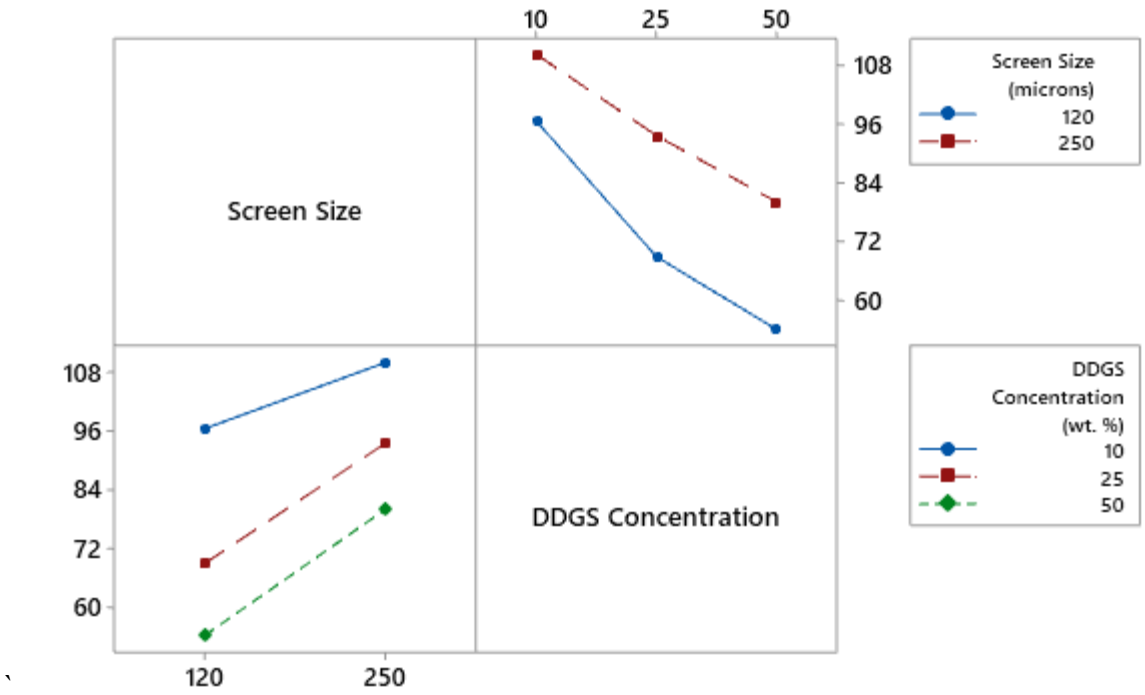

Figure 42. Interaction plot of screen size and DDGS concentration for 24-hour percentage change in mass.

Since blend was not included in a two-way ANOVA model; thus, a separate ANOVA model was run on blend followed by post hoc Tukey test to determine whether the means are significantly different. The Tukey test revealed that 12.8 M acetic acid and 10 wt. % wax is significantly different than 8.0 M sodium hydroxide and 10 wt. % wax in Table 29, and this implies that 12.8 M acetic acid and 10 wt. % wax is more water resistant compared to 8.0 M sodium hydroxide and 10 wt. % wax.

Table 29. Tukey pairwise comparison showing the influence of blend on the 24-hour percentage change in mass.

Blend	N	Mean	Grouping	
8.0 M sodium hydroxide and 10.0 wt.% wax	8	100.24	A	
12.0 wt.% phenol formaldehyde	4	95.66	A	B
12.0 wt.% phenol formaldehyde and 10.0 wt.% wax	4	92.3	A	B
12.8 M acetic acid	24	83.92	A	B
12.8 M acetic acid and 10.0 wt.% wax	8	60.76		B
Means that do not share a letter are significantly different.				

5.3.3. Linear expansion results

The percentage change in length of each particleboard was measured and is summarized in Figure 43, where low percentage change in length is desired. When comparing the linear expansion results to the ANSI A208.1 standard, all formulations do not fulfill the standard requirement except for acetic acid treated particleboards at 120 microns screen size and 10 wt. % DDGS concentration. It should be noted that no linear expansion value was provided in the standard for medium-density particleboards at grade M-0, thus the most common required linear expansion percentage was used and that being no greater than 0.4%.

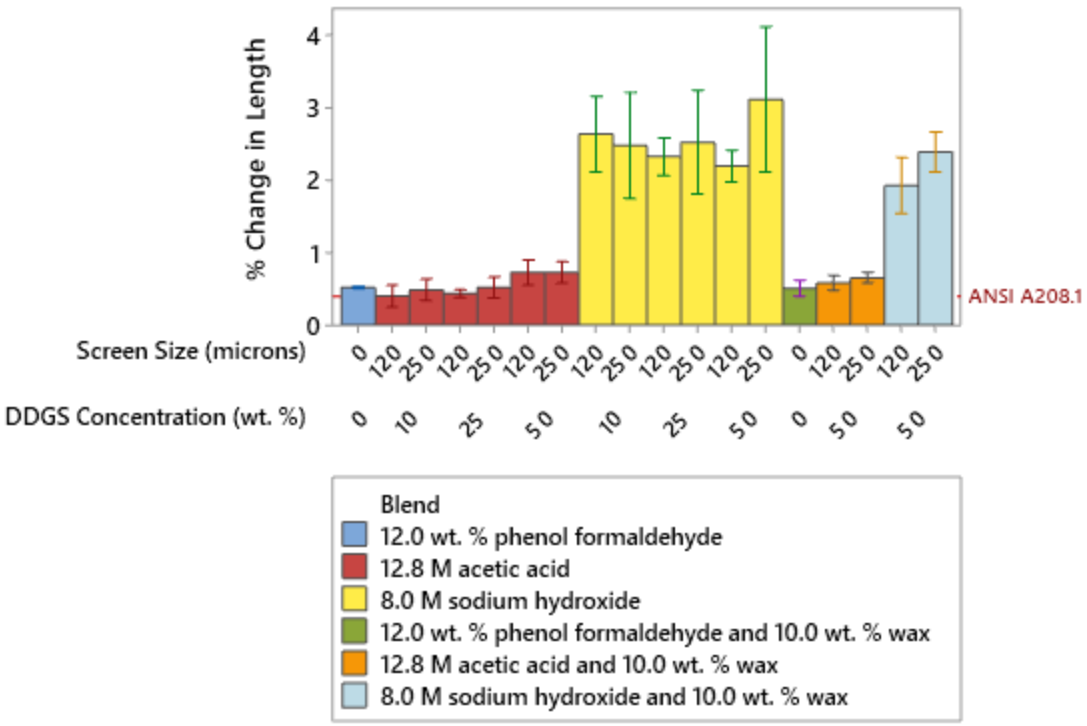

Figure 43. Mean interval plot with interval bars of percentage change in length of particleboards.

The factor information displays the specific blends, screen sizes, and DDGS concentrations performed using a three-way ANOVA model, as shown in Table 30. The three-way interaction between blend, screen size, and DDGS concentration is significant, as shown in Table 31. However, all the other interaction effects in the three-way ANOVA model are not significant, and these are supported by both the weak interactions and parallel profiles in Figure 44. Since the interaction effect is not significant; therefore, the ANOVA test on main effects indicated that screen size and blend are significant and either smaller screen size of 120 microns or 12.8 M acetic acid treatment displays good dimensional stability.

Table 30. Factor information for the three-way ANOVA.

Factor	Levels	Values
Blend	2	12.8 M acetic acid, 8.0 M sodium hydroxide
Screen Size	2	120, 250
DDGS Concentration	3	10, 25, 50

Table 31. A three-way ANOVA for percentage change in length.

Source	DF	SS	MS	F	P
Blend	1	47.938	47.938	568.76	0
Screen Size	1	0.43	0.43	5.1	0.03
DDGS Concentration	2	0.5132	0.2566	3.04	0.06
Blend*DDGS Screen Size	1	0.2067	0.2067	2.45	0.126
Blend*DDGS Concentration	2	0.0823	0.0411	0.49	0.618
Screen Size*DDGS Concentration	2	0.5098	0.2549	3.02	0.061
Blend*Screen Size*DDGS Concentration	2	0.7105	0.3552	4.21	0.023
Error	36	3.0342	0.0843		
Total	47	53.4247			
S	0.29032	**R-sq**	94.32%	**R-sq (adj)**	92.59%

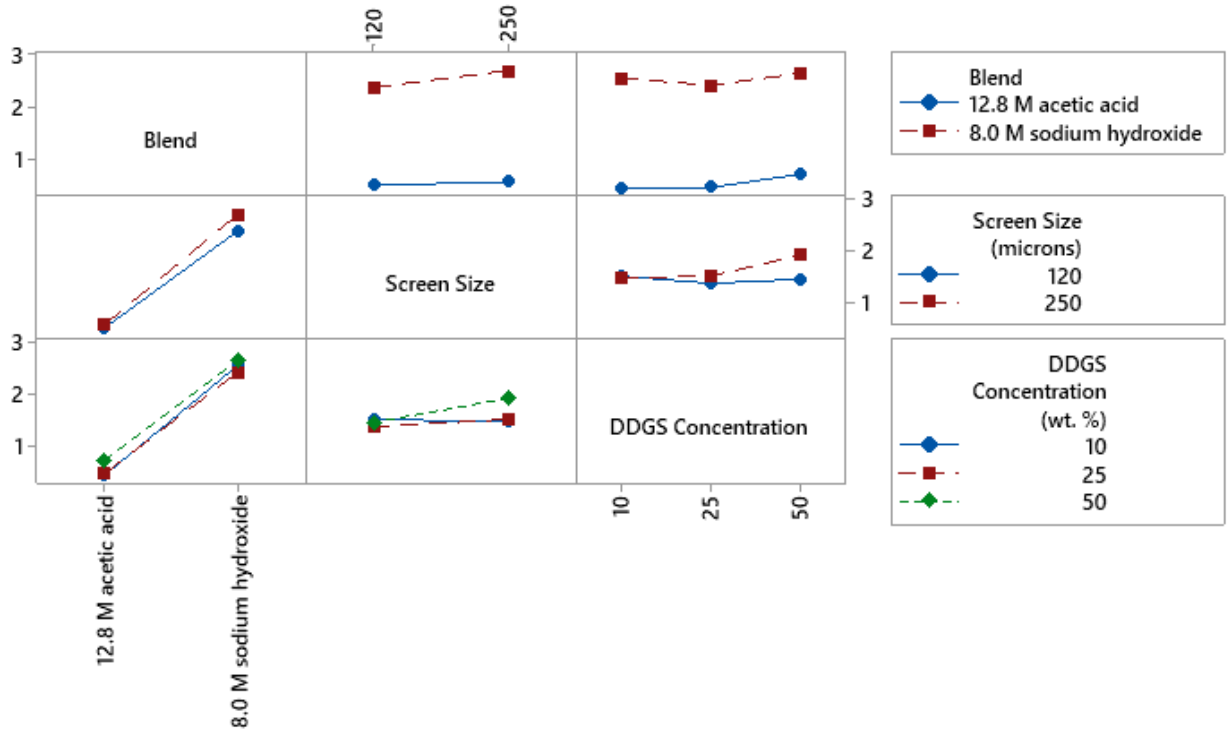

Figure 44. Interaction plot of blend, screen size, and DDGS concentration for percentage change in length.

Some of the blends were not included in the three-way ANOVA model; therefore, a separate ANOVA model was run on blend followed by post hoc Tukey test to determine whether the means are significantly different. The Tukey test revealed that combinations of 8.0 M sodium hydroxide and 10 wt. % wax are significantly different than other blends in Table 32, which means that 8 M sodium hydroxide and 10 wt. % wax combinations performed poorly in dimensional stability compared to the other blends.

Table 32. Tukey pairwise comparison showing the influence of blend on the percentage change in length.

Blend	N	Mean	Grouping		
8 M sodium hydroxide	24	2.5475	A		
8 M sodium hydroxide and 10 wt.% wax	8	2.161		B	
12.88 M acetic acid and 10 wt.% wax	8	0.6173			C
12.88 M acetic acid	24	0.5488			C
12 wt.% phenol formaldehyde	4	0.51797			C
12 wt.% phenol formaldehyde and 10 wt.% wax	4	0.5032			C
Means that do not share a letter are significantly different.					

5.3.4. Static bending results

Static being tests were conducted to determine the flexural properties of the particleboards, specifically on the modulus of rupture and modulus of elasticity.

5.3.4.1. Modulus of rupture

The modulus of rupture of each particleboard was measured and is summarized in Figure 45, where high modulus of rupture is desired. When comparing the modulus of rupture results to the ANSI A208.1-2009 standard, all formulations do not fulfill the standard's requirement of 7.6 MPa.

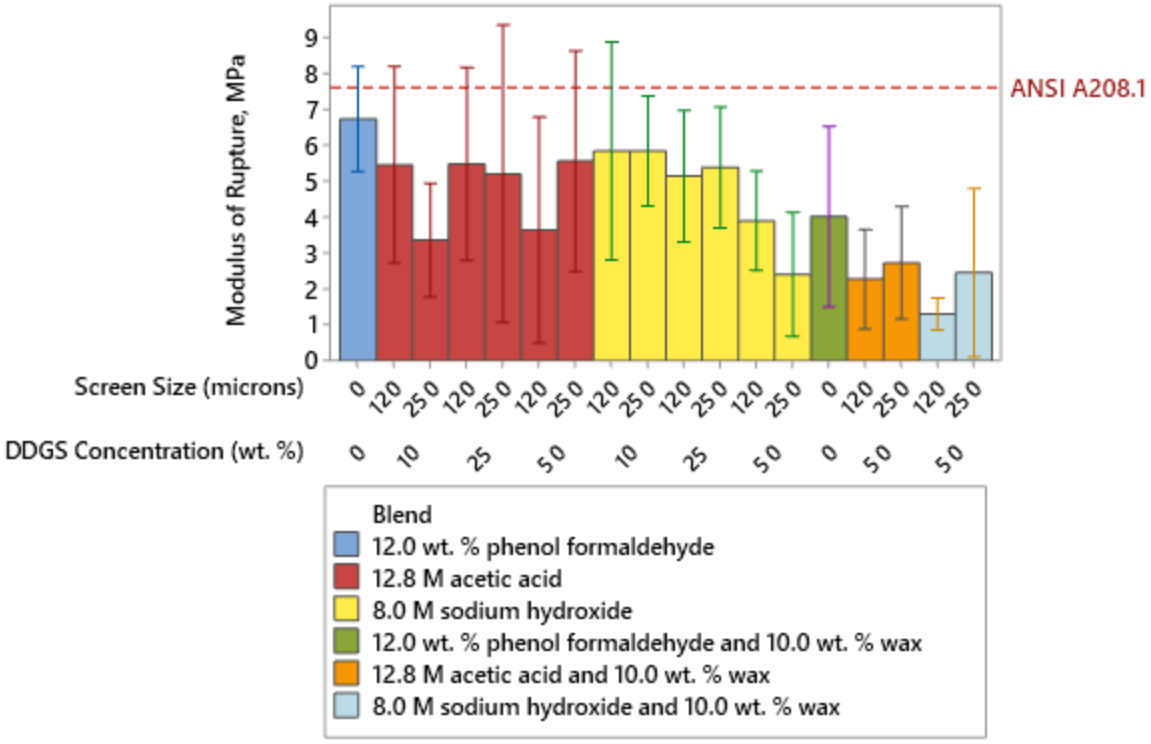

Figure 45. Modulus of rupture of particleboards.

The factor information displays the specific blends, screen sizes, and DDGS concentrations performed using a three-way ANOVA model, as shown in Table 33. The blend*DDGS concentration interaction is significant in Table 34, and this is supported by the intersecting lines in first row and third column in Figure 46. These intersecting lines indicate that the 10 wt. % DDGS concentration samples are superior to the 25 wt. % and 50 wt. % for sodium hydroxide blends, while 12.8 M acetic acid blend shows an increasing trend from 10 wt. % to 25 wt. % DDGS concentration samples than a decreasing trend from 25 wt. % to 50 wt. %. The decrease in flexural strength may be attributed to DDGS aggregates forming at higher DDGS concentrations. Moreover, the low r^2 value of 38.68% in Table 34 may be attributed to the DDGS aggregates that resulted in some variation in modulus of rupture.

Table 33. Factor information for the three-way ANOVA.

Factor	Levels	Values
Blend	2	12.8 M acetic acid, 8.0 M sodium hydroxide
Screen Size	2	120, 250
DDGS Concentration	3	10, 25, 50

Table 34. A three-way ANOVA for modulus of rupture.

Source	**DF**	**SS**	**MS**	**F**	**P**
Blend	1	0.012	0.0125	0	0.944
Screen Size	1	0.957	0.95671	0.38	0.54
DDGS Concentration	2	19.361	9.68061	3.87	0.03
Blend*Screen Size	1	0.211	0.21085	0.08	0.773
Blend*DDGS Concentration	2	16.605	8.30254	3.32	0.048
Screen Size*DDGS Concentration	2	3.572	1.78606	0.71	0.497
Blend*Screen Size*DDGS Concentration	2	16.109	8.05431	3.22	0.052
Error	36	90.095	2.50265		
Total	47	146.922			
S	1.58198	**R-sq**	38.68%	**R-sq (adj)**	19.94%

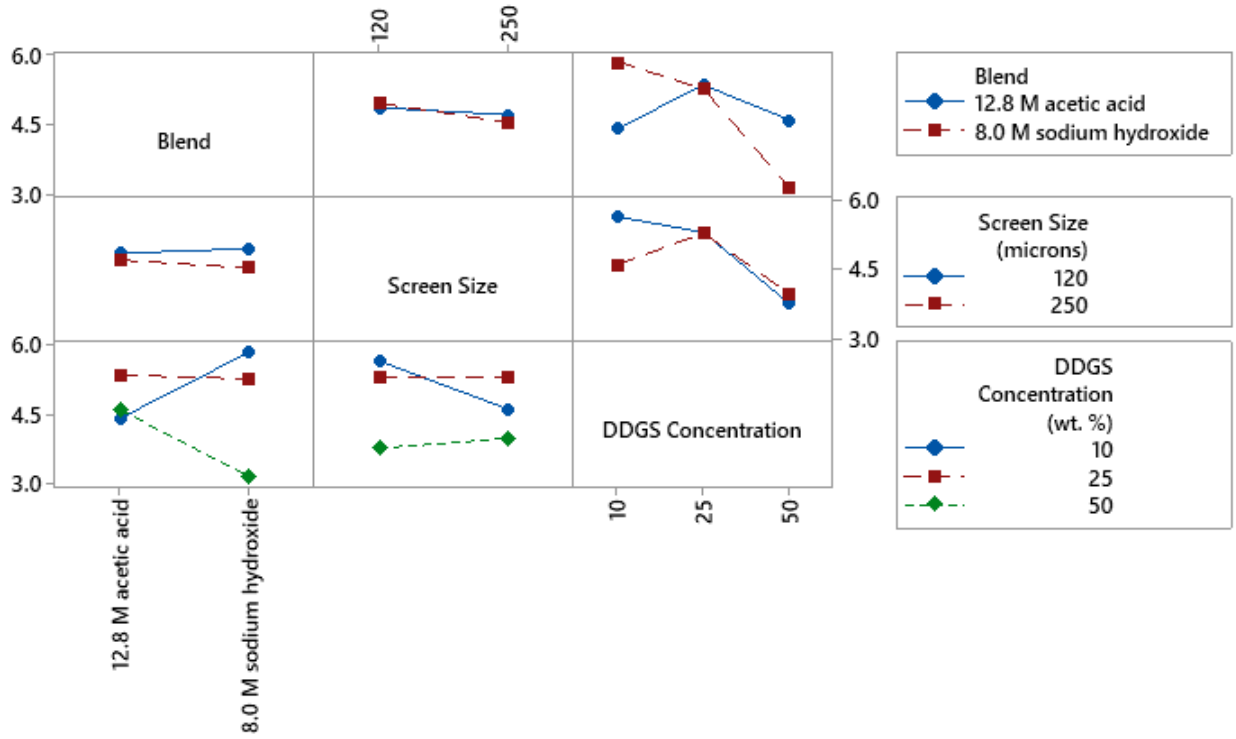

Figure 46. Interaction plot of blend, screen size, and DDGS concentration for modulus of rupture.

Some of the blends were not included in the three-way ANOVA model; therefore, a separate ANOVA model was run on blend-only followed by a post hoc Tukey test to determine whether the means were significantly different. The addition of 10 wt. % wax to both 12.8 M acetic acid and 8.0 M sodium hydroxide is significantly different from those blends without wax, as shown in Table 35. Furthermore, the means of the flexural strengths of these different blends deteriorated with the addition of wax.

Table 35. Tukey pairwise comparison showing the influence of blend on the modulus of rupture.

Blend	N	Mean	Grouping	
12.0 wt.% phenol formaldehyde	4	6.721	A	
12.8 M acetic acid	24	4.782	A	
8.0 M sodium hydroxide	24	4.75	A	
12.0 wt.% phenol formaldehyde and 10.0 wt.% wax	4	4.011	A	B
12.8 M acetic acid and 10.0 wt.% wax	8	2.503		B
8.0 M sodium hydroxide and 10.0 wt.% wax	8	1.881		B
Means that do not share a letter are significantly different.				

5.3.4.2. Modulus of elasticity

The modulus of elasticity of each particleboard was measured and is summarized as in Figure 47, where high modulus of elasticity is desired. When comparing the modulus of elasticity results to the ANSI A208.1-2009 standard, all formulations do not fulfill the standard requirement of 1380 MPa except for sodium hydroxide treated particleboards at 250 microns screen size and 10 wt. % DDGS concentration.

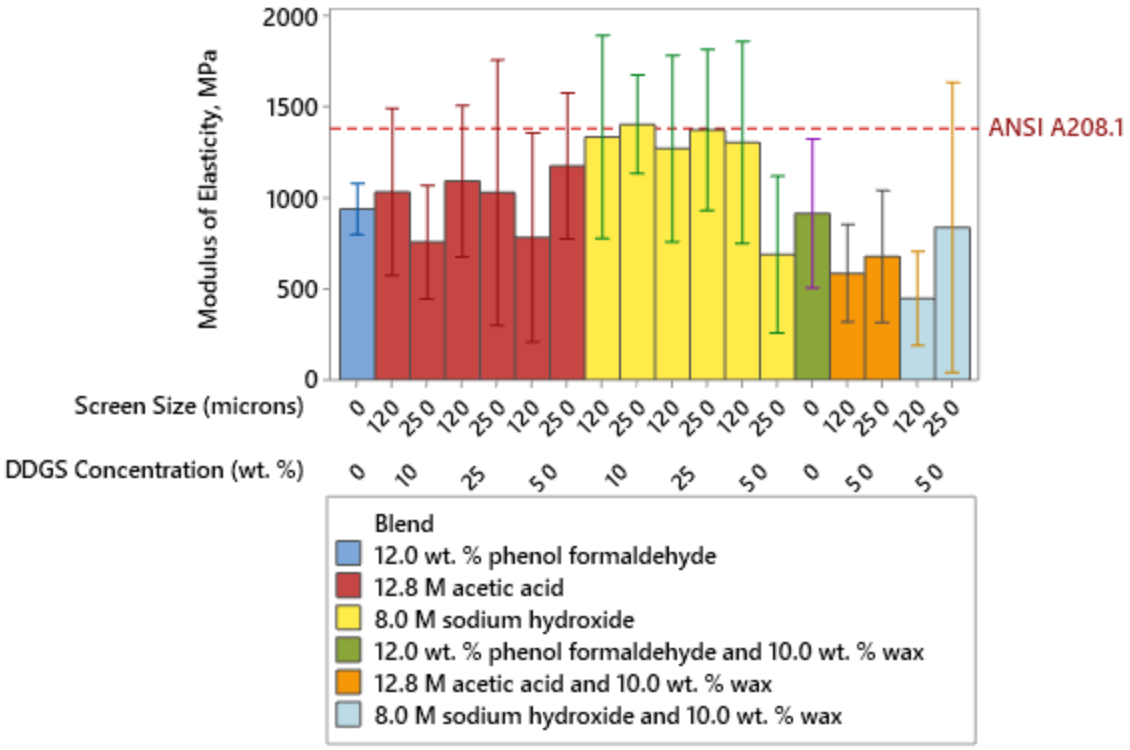

Figure 47. Modulus of elasticity of particleboards.

The factor information displays the specific blends, screen sizes, and DDGS concentrations performed using a three-way ANOVA model, as shown in Table 36. The three-way interaction between blend, screen size, and DDGS concentration was significant, as shown in Table 37. However, all the other interaction effects in the three-way ANOVA model were not significant, and the interaction plot in Figure 48 can be ignored.

Table 36. Factor information for the three-way ANOVA.

Factor	Levels	Values
Blend	2	12.8 M acetic acid, 8.0 M sodium hydroxide
Screen Size	2	120, 250
DDGS Concentration	3	10, 25, 50

Table 37. A three-way ANOVA for modulus of elasticity.

Source	DF	SS	MS	F	P
Blend	1	753885	753885	8.11	0.007
Screen Size	1	50360	50360	0.54	0.466
DDGS Concentration	2	346628	173314	1.87	0.17
Blend*Screen Size	1	82819	82819	0.89	0.351
Blend*DDGS Concentration	2	418327	209163	2.25	0.12
Screen Size*DDGS Concentration	2	42778	21389	0.23	0.796
Blend*Screen Size*DDGS Concentration	2	1073931	536965	5.78	0.007
Error	36	3345435	92929		
Total	47	6114162			
S	304.842	**R-sq**	45.28%	**R-sq (adj)**	28.57%

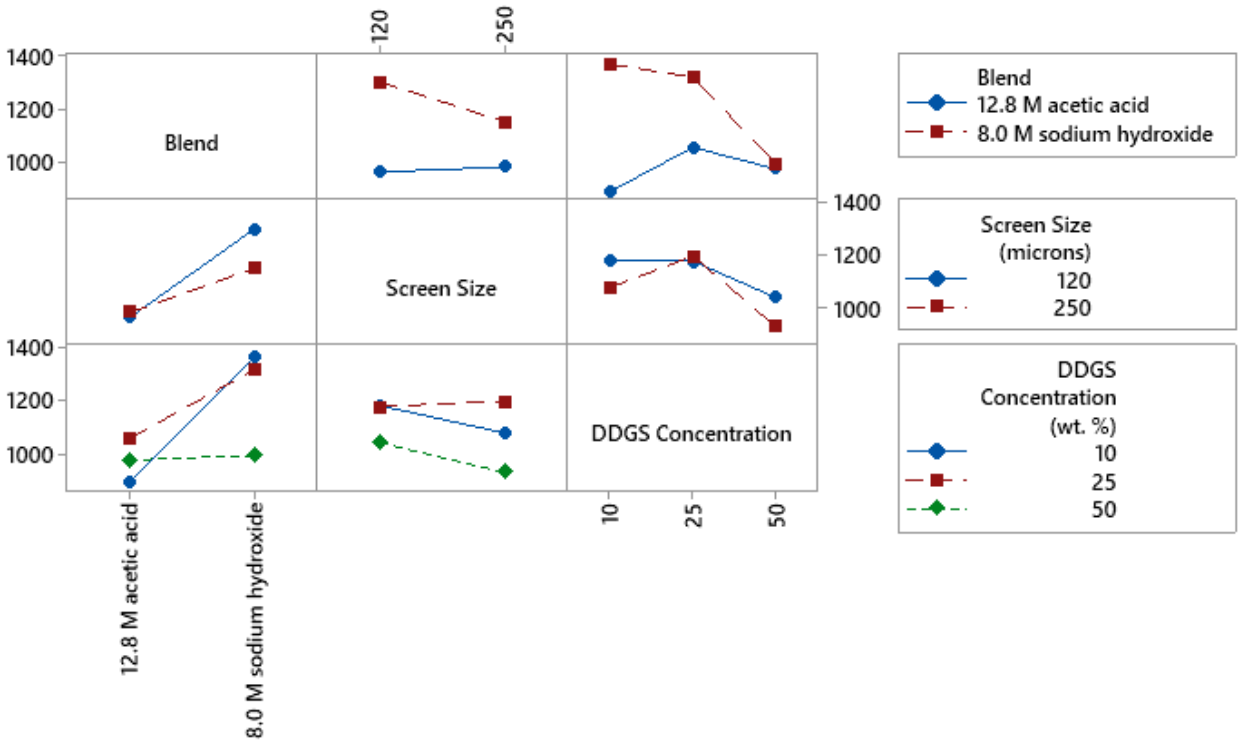

Figure 48. Interaction plot of blend, screen size, and DDGS concentration for modulus of elasticity.

Since the interaction effects are not significant; therefore, a three-way ANOVA test on main effects can be interpreted, where blend is significant. Thus, a separate ANOVA model was run on blend only followed by post hoc Tukey test to determine whether the means are significantly different. The Tukey test revealed that the addition of 10 wt. % wax to 8.0 M sodium hydroxide is significantly different from not adding wax. Adding wax into the particleboards can lead to deterioration in stiffness, as shown in Table 38.

Table 38. Tukey pairwise comparison showing the influence of blend on the modulus of elasticity.

Blend	N	Mean	Grouping	
8.0 M sodium hydroxide	24	1226.3	A	
12.8 M acetic acid	24	975.7	A	B
12.0 wt.% phenol formaldehyde	4	937.3	A	B
12.0 wt.% phenol formaldehyde and 10.0 wt.% wax	4	913	A	B
8.0 M sodium hydroxide and 10.0 wt.% wax	8	640		B
12.8 M acetic acid and 10.0 wt.% wax	8	630		B
Means that do not share a letter are significantly different.				

5.3.5. Internal bond results

The internal bond result shows the cohesive strength of each particleboard and is summarized in Figure 49, where high internal bond strength is desired. When comparing the internal bond results to the ANSI A208.1-2009 standard, all the formulations met the standard requirement of 0.31 MPa.

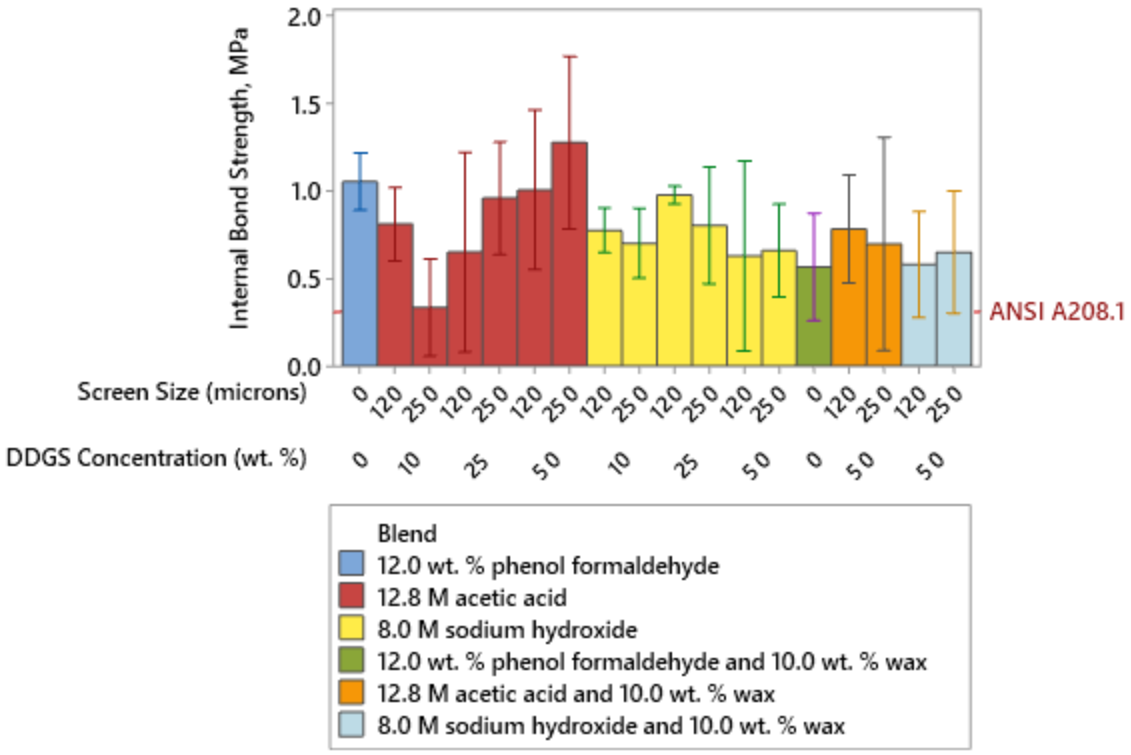

Figure 49. Internal bond strength of particleboards.

The factor information displays the specific blends, screen sizes, and DDGS concentrations that were performed using a three-way ANOVA model, as shown in Table 39. The ANOVA test on a three-way interaction between blend, screen size, and DDGS concentration is significant in Table 40. Moreover, the screen size*DDGS concentration and blend*DDGS concentration interactions are also significant, and these are supported by the strong interaction effects of screen size*DDGS concentration and blend*DDGS concentration in Figure 50. The strong interaction between blend*DDGS concentration is due to the diverging lines at 50 wt. % DDGS concentration in row one and column three, while the interaction between screen size*DDGS concentration is due to the intercepting lines in row two and column three. The internal bond strengths of acetic acid treatment at 50 wt. % DDGS concentration are superior to those at 10 wt. % and 25 wt. %, while 8.0 M sodium hydroxide treatment shows that 10 wt. % and 25 wt. % DDGS concentrations were superior than 50 wt. %. Higher

concentrations of DDGS can lead to higher internal bond strengths, but the non-uniformity of DDGS aggregates at 50 wt. % DDGS concentration of 8 M sodium hydroxide treatment may impede strong bonding between wood flour and DDGS.

Table 39. Factor information for the ANOVA.

Factor	Levels	Values
Blend	2	12.8 M acetic acid, 8.0 M sodium hydroxide
Screen Size	2	120, 250
DDGS Concentration	3	10, 25, 50

Table 40. A three-way ANOVA for internal bond strength.

Source	**DF**	**SS**	**MS**	**F**	**P**
Blend	1	0.08083	0.080834	1.6	0.214
Screen Size	1	0.00439	0.004388	0.09	0.77
DDGS Concentration	2	0.50885	0.254423	5.03	0.012
Blend*Screen Size	1	0.0338	0.033798	0.67	0.419
Blend*DDGS Concentration	2	1.04695	0.523475	10.34	0
Screen Size*DDGS Concentration	2	0.40711	0.203554	4.02	0.027
Blend*Screen Size*DDGS Concentration	2	0.41834	0.209172	4.13	0.024
Error	36	1.82173	0.050604		
Total	47	4.322			
S	0.224953	**R-sq**	57.85%	**R-sq (adj)**	44.97%

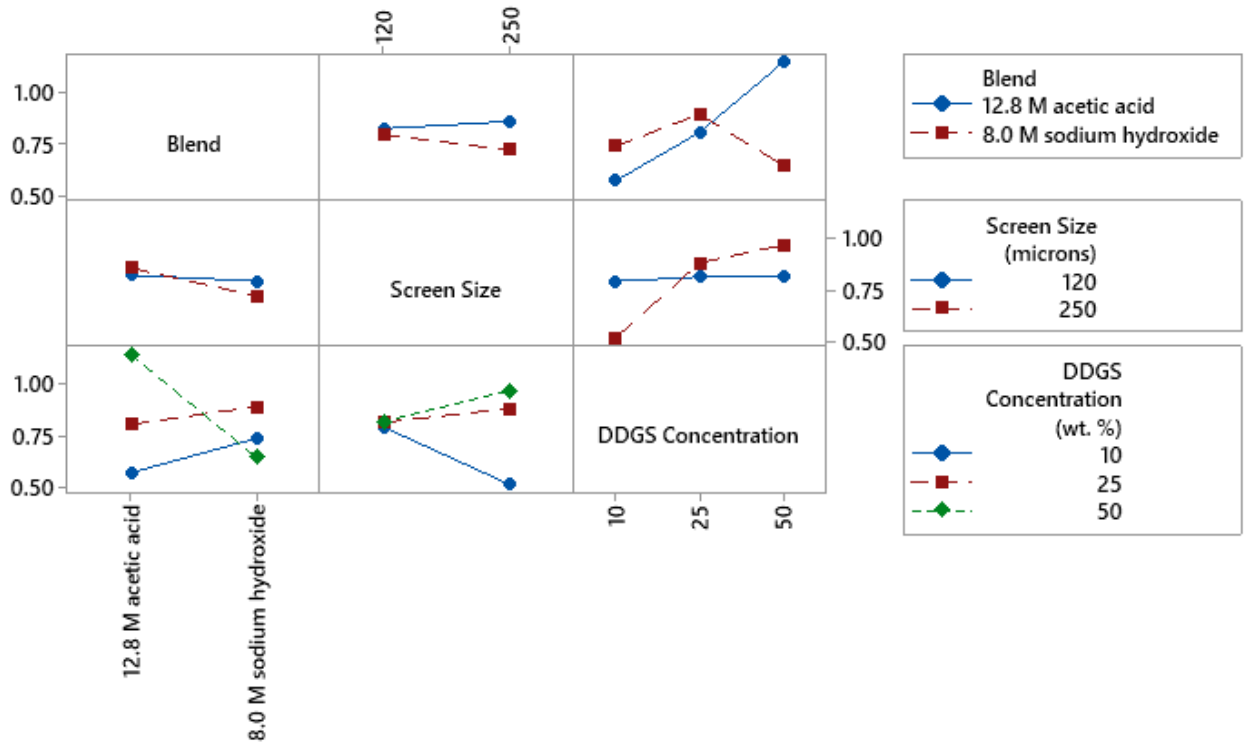

Figure 50. Interaction plot of blend, screen size, and DDGS concentration for internal bond strength.

Some of the blends were not included in the three-way ANOVA model; therefore, a separate ANOVA model was run on blend followed by post hoc Tukey test to see whether the means are significantly different. The results show that all blends are not significantly different from each other in Table 41.

Table 41. Tukey pairwise comparison showing the influence of blend on the internal bond strength.

Blend	N	Mean	Grouping
12 wt. % phenol formaldehyde	4	1.0553	A
12.8 M acetic acid	24	0.8402	A
8.0 M sodium hydroxide	24	0.7581	A
12.8 M acetic acid and 10 wt. %wax	8	0.74	A
8 M sodium hydroxide and wax	8	0.6151	A
Phenol formaldehyde and wax	4	0.5657	A
Means that do not share a letter are significantly different.			

5.3.6. Screw withdrawal results

The screw withdrawal load of each particleboard was measured and is summarized in Figure 51, where high load is desired. When comparing the screw withdrawal results to the ANSI A208.1 standard, all formulations do not fulfill the standard requirement of 800 N. It should be noted that no screw withdrawal value was provided in the standard for medium-density particleboards at grade M-0, thus the higher grade of M-S was used.

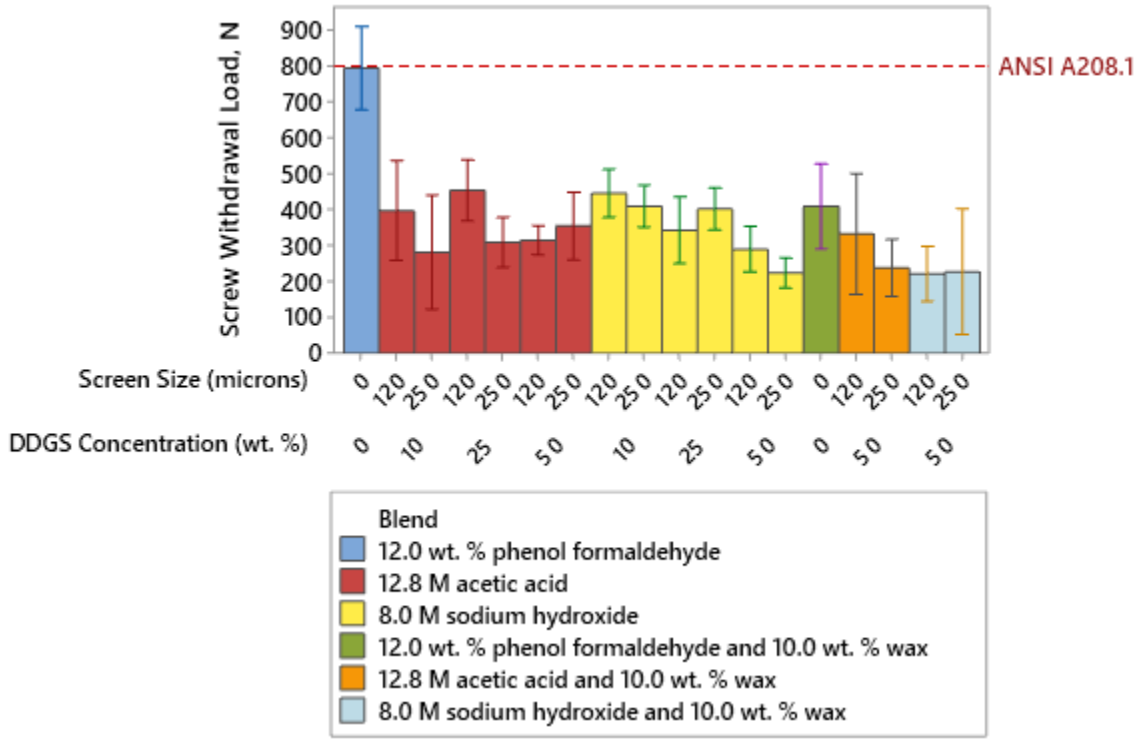

Figure 51. Screw withdrawal load of particleboards.

The factor information displays the specific blends, screen sizes, and DDGS concentrations performed using a three-way ANOVA model, as shown in Table 42. The three-way interaction between blend, screen size, and DDGS concentration is significant in Table 43. Moreover, blend*DDGS concentration interaction is significant, and this is supported by the intercepting lines in Figure 52. The screw withdrawal strengths of 8.0 M sodium hydroxide treatment at 10 wt. % DDGS concentration are superior to those at 25 wt. % and 50 wt. %, while

12.8 M acetic acid samples show an increasing trend from 10 wt. % to 25 wt. % DDGS concentration than a decreasing trend from 25 wt. % to 50 wt. %. Higher concentrations of DDGS lead to poor screw withdrawal strengths, and this may be attributed the DDGS aggregates formed at higher DDGS concentrations. Moreover, the main effect being significant is screen size, which shows that smaller screen size leads to better screw withdrawal resistance of the particleboards.

Table 42. Factor information on three-way ANOVA for screw withdrawal.

Factor	Levels	Values
Blend	2	12.8 M acetic acid, 8.0 M sodium hydroxide
Screen Size	2	120, 250
DDGS Concentration	3	10, 25, 50

Table 43. A three-way ANOVA for screw withdrawal.

Source	**DF**	**SS**	**MS**	**F**	**P**
Blend	1	7	6.8	0	0.963
Screen Size	1	23330	23330.2	7.66	0.009
DDGS Concentration	2	76239	38119.7	12.51	0.000
Blend*Screen Size	1	10718	10717.9	3.52	0.069
Blend*DDGS Concentration	2	55673	27836.3	9.14	0.001
Screen Size*DDGS Concentration	2	7887	3943.6	1.29	0.286
Blend*Screen Size*DDGS Concentration	2	48803	24401.7	8.01	0.001
Error	36	109669	3046.4		
Total	47	332327			
S	55.1939	**R-sq**	67.00%	**R-sq (adj)**	56.92%

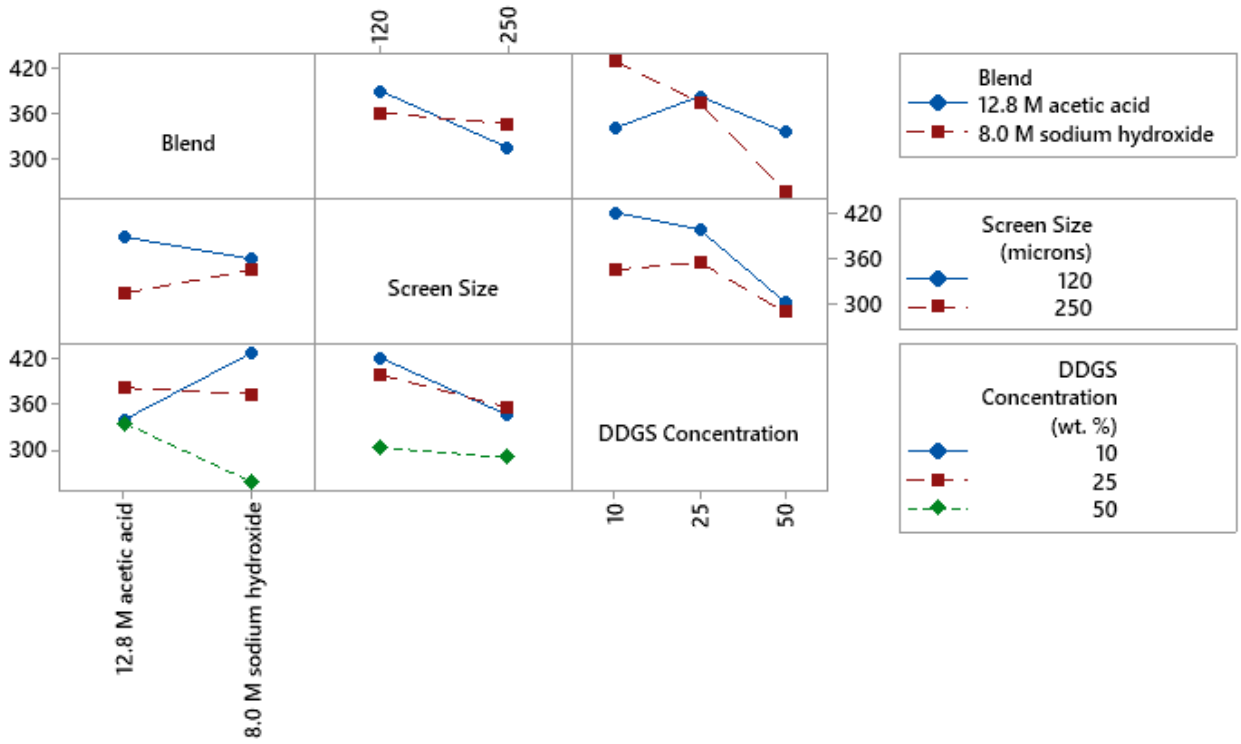

Figure 52. Interaction plot of blend, screen size, and DDGS concentration for screw withdrawal.

Some of the blends were not included in the three-way ANOVA model; therefore, a separate one-way ANOVA model was tested on blend followed by post hoc Tukey test to see whether the means are significantly different. 8.0 M sodium hydroxide and 10 wt. % wax was not significantly different than 12.8 M acetic acid and 10 wt. % wax, as shown in Table 44. Moreover, 12 wt. % phenol formaldehyde shows better screw withdrawal strength as compared to the other blends, and this means that other blends are inferior to the control boards.

Table 44. Tukey pairwise comparison showing the influence of blend on the screw withdrawal.

Blend	N	Mean	Grouping		
12.0 wt. % phenol formaldehyde	4	794.4	A		
12.0 wt. % phenol formaldehyde and 10.0 wt. % wax	4	409.6		B	
8.0 M sodium hydroxide	24	352.9		B	
12.8 M acetic acid	24	352.2		B	
12.8 M acetic acid and 10.0 wt. % wax	8	285.5		B	C
8.0 M sodium hydroxide and 10.0 wt. % wax	8	224.5			C
Means that do not share a letter are significantly different.					

5.3.7. Hardness test results

The hardness of each particleboard was measured and is summarized in Figure 53, where high hardness value is desired. When comparing the hardness results to the ANSI A208.1-2009 standard, some sodium hydroxide formulations do not fulfill the standard requirement of 2225 N. It should be noted that no hardness value was provided in the standard for medium-density particleboards at grade M-0, thus the higher grade of M-3 was used.

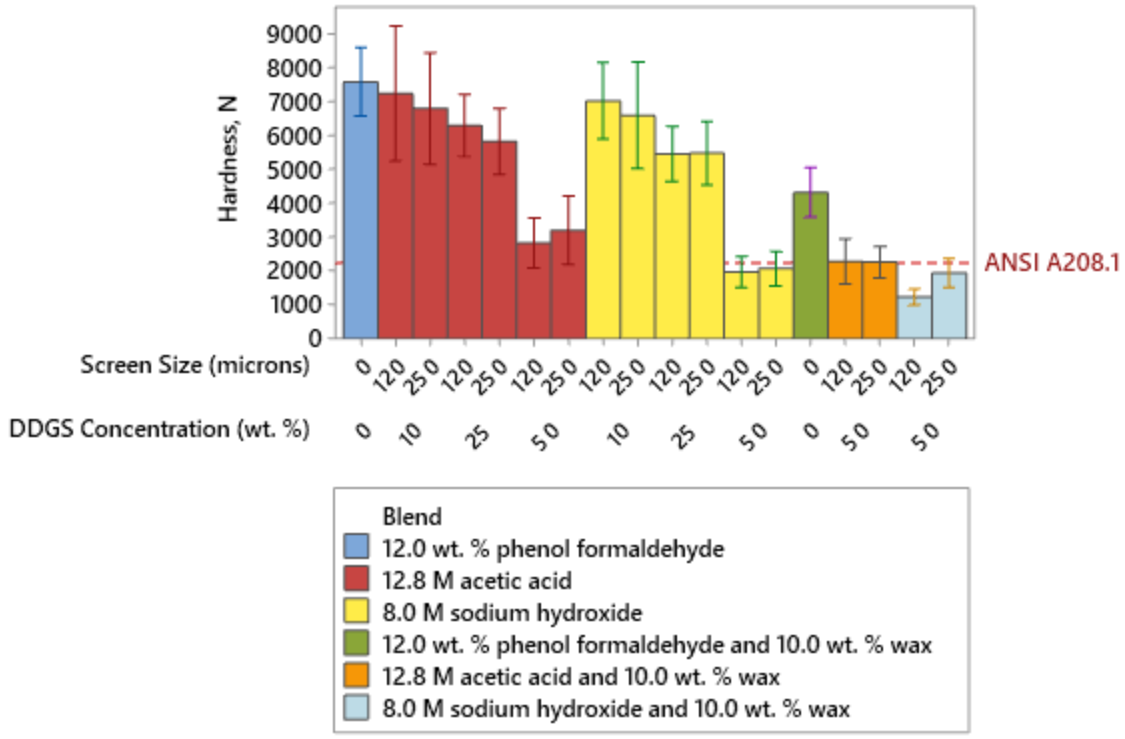

Figure 53. Hardness of particleboards.

The factor information displays the specific blends, screen sizes, and DDGS concentrations that were performed using a three-way ANOVA model, as shown in Table 45. The three-way interaction between blend, screen size, and DDGS concentration is not significant, as shown in Table 46. Moreover, the interaction effects are not significant, and these was supported by both the weak interactions and parallel profiles in Figure 54. Since the interaction effect is not significant; therefore, the ANOVA test on main effect can be interpreted, where DDGS concentration and blend are significant. Thus, DDGS concentration can be interpreted as higher DDGS concentrations lead to lower hardness, and this statement is true for both blends. One possibility is that wood flour has higher ability to resist deformation than DDGS particles.

Table 45. Factor information on three-way ANOVA for hardness.

Factor	Levels	Values
Blend	2	12.8 M acetic acid, 8.0 M sodium hydroxide
Screen Size	2	120, 250
DDGS Concentration	3	10, 25, 50

Table 46. A three-way ANOVA for hardness.

Source	**DF**	**SS**	**MS**	**F**	**P**
Blend	1	8555347	8555347	4.55	0.036
Screen Size	1	492641	492641	0.26	0.610
DDGS Concentration	2	332270746	166135373	88.32	0.000
Blend*Screen Size	1	36862	36862	0.02	0.889
Blend*DDGS Concentration	2	2465652	1232826	0.66	0.522
Screen Size*DDGS Concentration	2	1901682	950841	0.51	0.605
Blend*Screen Size*DDGS Concentration	2	620929	310465	0.17	0.848
Error	84	158005542	1881018		
Total	95	504349401			
S	1371.5	**R-sq**	68.67%	**R-sq (adj)**	64.57%

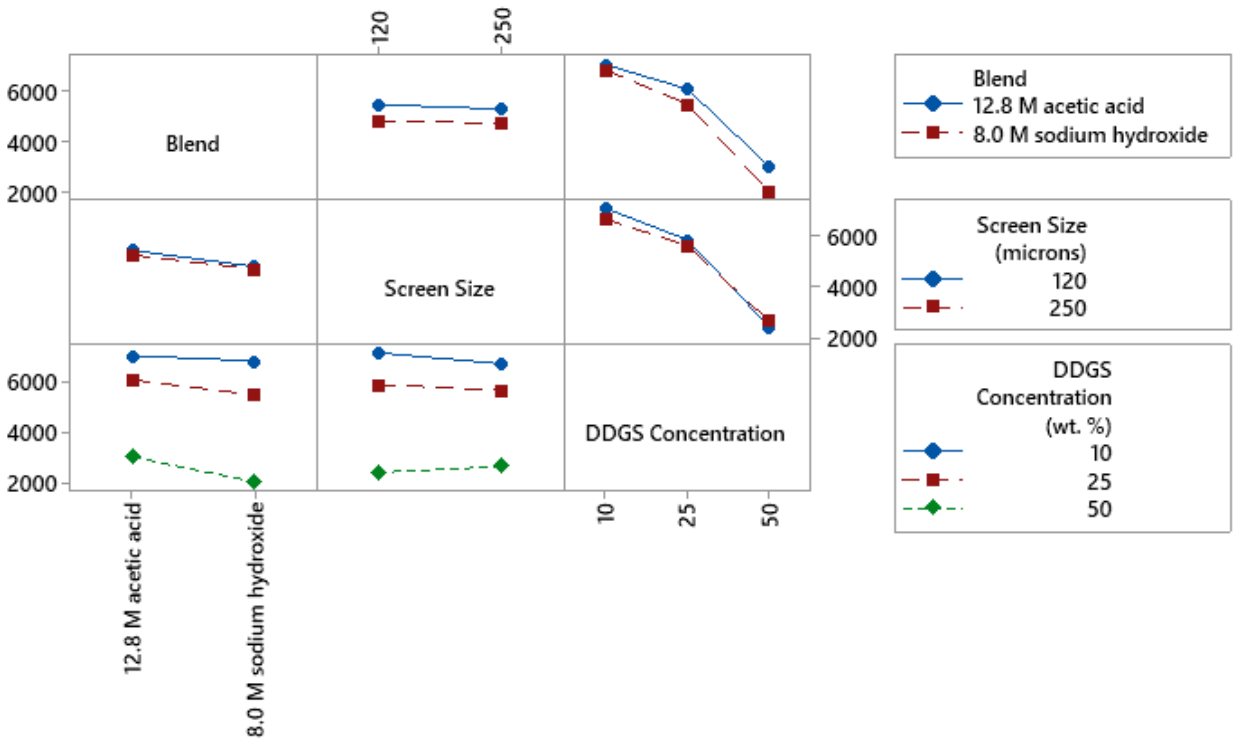

Figure 54. Interaction plot of blend, screen size, and DDGS concentration for hardness.

Since some of the blends were not included in the three-way ANOVA model, a separate one-way ANOVA model was tested on blend followed by post hoc Tukey test to determine whether the means are significantly different. The Tukey test revealed that 12 wt. % phenol formaldehyde is significantly different from all the other blends, while the addition of wax to both 12.8 M acetic acid and 8.0 M sodium hydroxide reduced the hardness load significantly, as shown in Table 47.

Table 47. Tukey pairwise comparison showing the influence of blend on the hardness.

Blend	N	Mean	Grouping			
12 wt. % phenol formaldehyde	8	7587	A			
12.8 M acetic acid	48	5368		B		
8.0 M sodium hydroxide	48	4771		B		
12.0 wt. % phenol formaldehyde and 10.0 wt. % wax	8	4329		B	C	
12.8 M acetic acid and 10.0 wt. % wax	16	2277			C	D
8.0 M sodium hydroxide and 10.0 wt. % wax	16	1590				D
Means that do not share a letter are significantly different.						

5.3.8. Discussion on deviation among mechanical testing

The deviation in results from the mechanical testing might be attributed to three different factors; the DDGS agglomerates, density variation across the board, and differential heat distribution across the mold.

First, the visible agglomerates formed for acetic acid treated DDGS at 50 wt. % in Figure 55, while sodium hydroxide treated DDGS at DDGS concentrations of 25 wt. % and 50 wt. % in Figure 56. These agglomerates led to non-uniform dispersion of DDGS particles in the wood flour matrix that resulted in both lower mechanical properties of the particleboards and variability of the results.

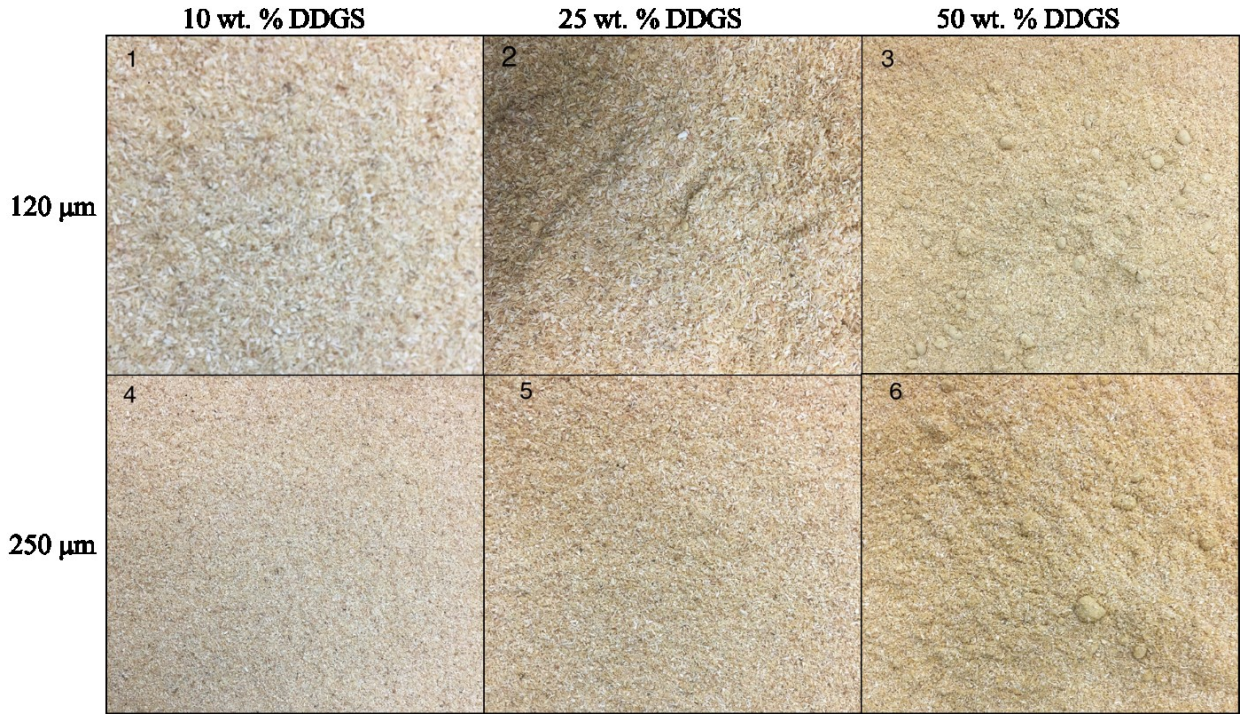

Figure 55. 12.8 M acetic acid treated DDGS composite at various blends.

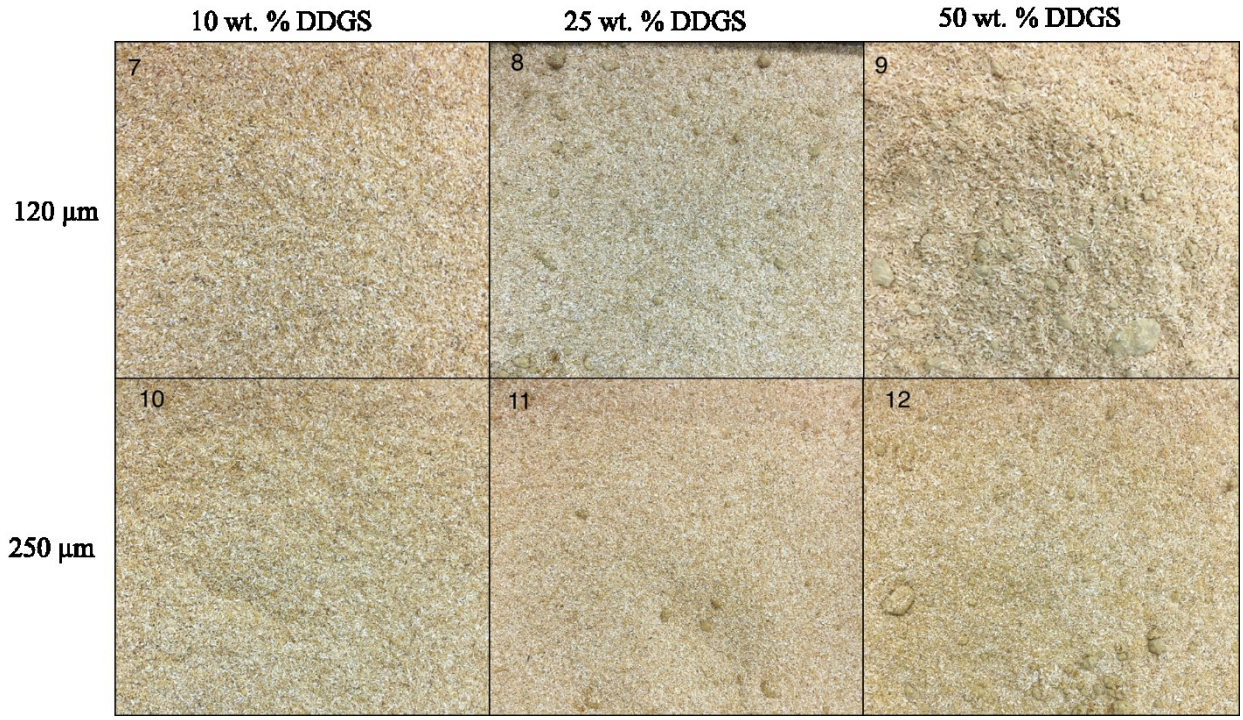

Figure 56. 8.0 M sodium hydroxide treated DDGS composite at various blends.

Figure 57 displays the selected cut out patterns from the preferred formulation to study the impact of density on the internal bond strength of the particleboard and the variation of density across the components of the particleboard.

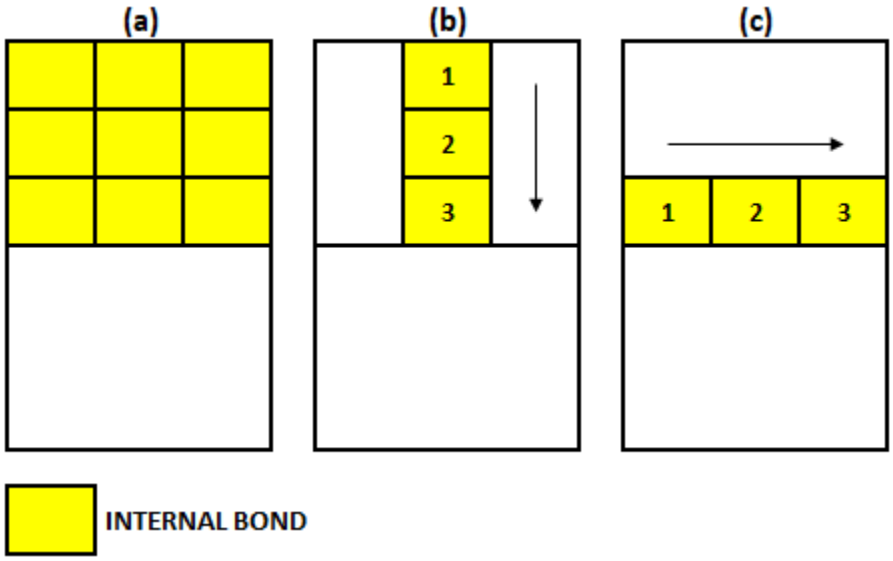

Figure 57. Cut out patterns of the preferred formulation to study (a) the impact of density on the internal bond strength of the particleboard, (b) the variation of density across the vertical component of the particleboard, and (c) the variation of density across the horizontal component of the particleboard.

The correlation between the internal bond strength and the density is determined by the r^2 value. The r^2 value of 0.84 shown in Figure 58 indicates a good fit model, which implies that the particleboard internal bond strength increases with density. This increasing trend correlated to the previous study reported for formaldehyde resin manufactured boards [69]. Since this is a good fit model, equation (33) may give a reasonable estimate to predict the internal bond strength value based of any given density.

$$y = 0.0018x - 1.0292 \tag{33}$$

where y is the internal bond strength in MPa and x is the density in kg/m^3.

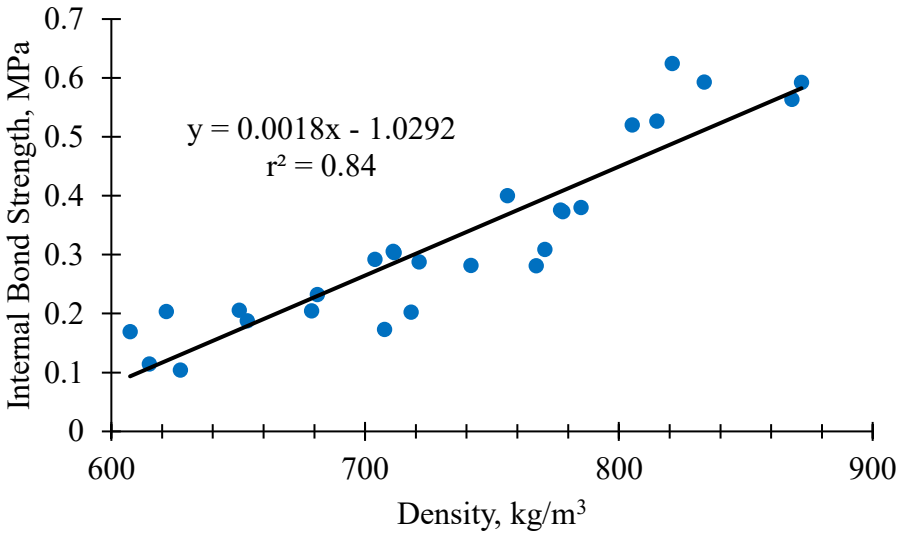

Figure 58. The impact of density on the internal bond strength of the particleboard.

Second, Figure 59 and Figure 60 imply that the density around the center of the panel is denser than the edges, which corresponds to a similar study [57]. The denser center might be attributed to the uneven distribution of load in the hot press, and the load may concentrate mostly around the center of the platen. Though the individual sections of a particleboard may not meet the medium-density requirement, but the aforementioned average densities of the entire particleboard fulfilled the medium-density requirement of between 640 and 800 kg/m^3 as specified by the standard.

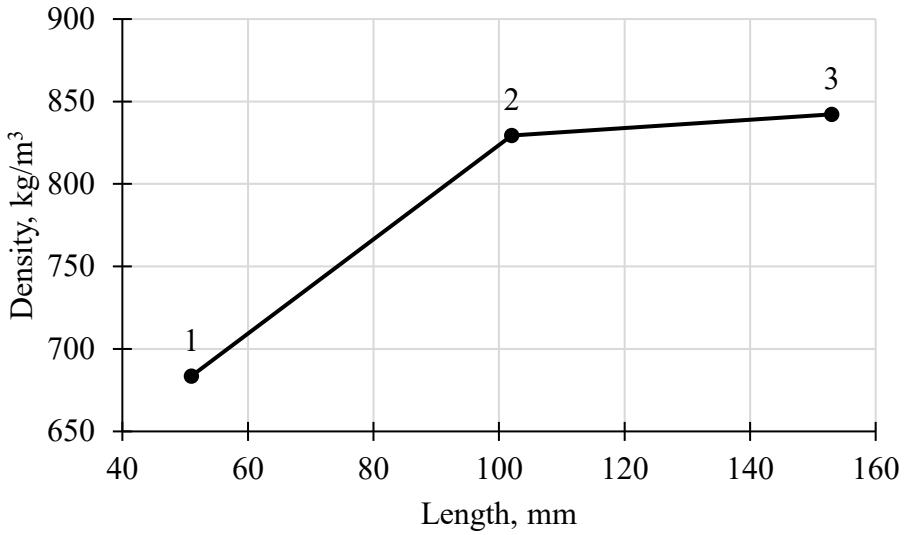

Figure 59. The variation of density across the vertical component of the particleboard.

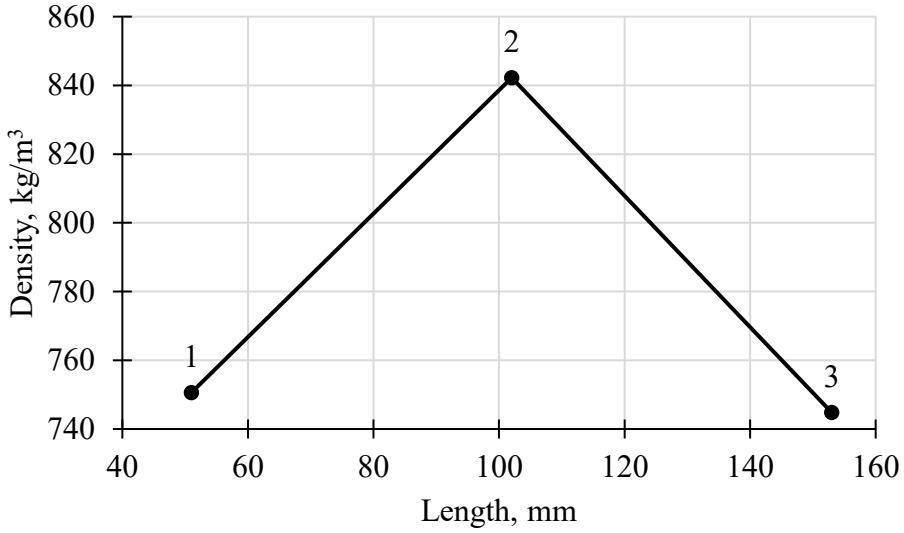

Figure 60. The variation of density across the horizontal component of the particleboard.

Third, to analyze the temperature distribution of the platen, the hot press was heated with the mold at 120 ℃ for at least an hour. Figure 61 shows the temperature distribution of a heated platen, where the center region of the platen is much hotter than the edges.

Figure 61. Heating temperature distribution of a platen.

The mold was removed from the hot press, and the temperature distribution is shown in Figure 62. The thermal image of the mold shows that the upper half of the mold is much hotter than the bottom half of the mold. This is because the upper half of the mold has a higher mass that allow it to store more heat energy and stay at a higher temperature over time, while the lower mass of the bottom half of the mold cools quickly. The differential temperature within both the upper half mold and bottom half mold might be due to uneven distribution of heat in the platen of the hot press that resulted in some cooler regions. The variation in temperature may impede the proper curing and binding process between the DDGS particles and the wood flour, and this variation may have resulted in non-uniform mechanical properties across the panel.

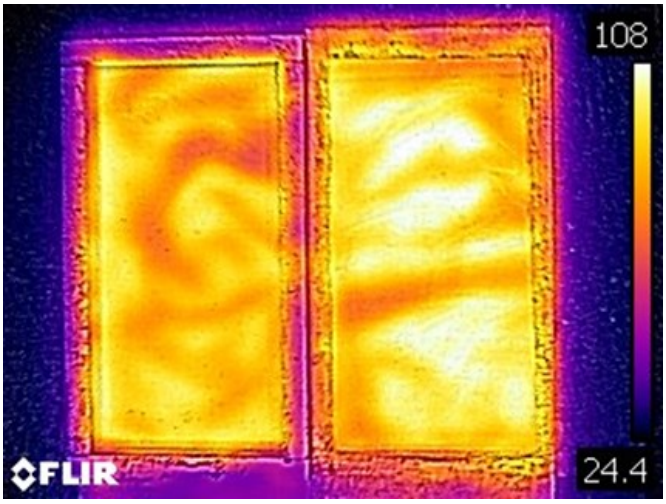

Figure 62. Heating temperature distribution of the bottom half (left) and upper half (right) of a mold.

5.3.9. Discussion on physical and mechanical results

Based on the physical and mechanical testing, the ideal chemical treatment to functionalize DDGS was found to be 12.8 M acetic acid with a favored formulation of DDGS concentration at 25 wt. % and a screen size of 120 μm.

Both the results of the control panel of 12 wt. % phenol formaldehyde and preferred formulation met the ANSI A208.1-2009 standard for both internal bond strengths and hardness but failed to meet the ANSI standard with the other measured properties, as shown in Table 48. The fact that the control panels do not meet the industrial results could be due to the weak dispersion of the particles at higher filler concentrations and the difference in manufacturing processes. Furthermore, in this study, single-layer boards were produced in contrast with the commonly manufactured multi-layer boards in industry with higher mechanical properties. Due to the limitation in facilities such as the unavailability of a forming machine, multi-layer panels could not be produced in this study.

Despite these shortcomings, the preferred formulation displayed improvement in linear expansion and modulus of elasticity when compared with the properties of the control formula.

Though the internal bond strength of the preferred formulation is lower than that of the control formula, the results of the preferred formulation show that the internal bond strength exceeded the requirements of the ANSI standard; this positive outcome indicates that the acid treated DDGS in the preferred formulation has strong potential to be used as a binder to manufacture particleboards. To meet the requirements of the ANSI standard, further investigation on both the feasibility of using lower filler concentration at 5 and 15 wt. % as well as manufacturing multi-layer boards may help to overcome the unnecessary formation of agglomerates and improve the physical and mechanical properties of the particleboards.

Table 48. Comparison of the control panel and the preferred formulation to ANSI A208.1-2009 standard. The bolded and underlined values met the ANSI A208.1-2009 standard.

Property	ANSI standard	Control panel	Preferred formulation
Linear expansion (% change)	0.40	0.52	0.43
Modulus of rupture (MPa)	7.60	6.72	5.48
Modulus of elasticity (MPa)	1380.00	937.27	1088.80
Internal bond strength (MPa)	0.31	**1.06**	**0.65**
Screw withdrawal (N)	800.00	794.35	454.48
Hardness (N)	2225.00	**7587.23**	**6297.87**

5.4. Economic analysis

It is important to assess the economic benefits of using DDGS as a functional material to replace synthetic resin in wood particleboards. The costs of materials used in this experiment are approximated in Table 49 and may vary based upon the bulk purchase prices. The prices of DDGS, wood flour, phenol formaldehyde resin, and wax emulsion were obtained from their respective manufacturers, while the prices of glacial acetic acid and sodium hydroxide were taken from the discounted rate sold by the Department of Chemistry and Biochemistry at North

Dakota State University. From the table, sodium hydroxide, glacial acetic acid, and wax emulsion are the costliest materials in this project.

Table 49. Breakdown of experiment's raw material cost.

Component	Cost per pound (USD/lb)	Cost per kilogram (USD/kg)
DDGS	0.07	0.15
Wood flour	0.25	0.55
Glacial acetic acid	4.48	9.87
Sodium hydroxide	11.34	25.00
Phenol formaldehyde resin	0.63	1.39
Wax emulsion	5.07	11.17

Based on these prices, the cost to manufacture a control panel was calculated at $0.78 per square foot, as shown in Table 50; this cost is without the use of DDGS filler.

Table 50. Cost to manufacture a control panel.

Formulation	Ratio	Component Cost (USD)
100 wt. % wood flour	0.82	0.12
12 wt. % phenol formaldehyde resin	0.10	0.04
10 wt. % wax emulsion	0.08	0.24
Total cost (USD/panel)		0.39
Total cost (USD/ft^2)		0.78
Total cost (USD/m^2)		8.40

The preferred formulation of 25 wt. % DDGS treated with 12.8 M acetic acid was selected based on its performance in physical and mechanical testing. The cost to manufacture this type of particleboard was calculated at $0.98 per square foot as shown in Table 51.

Table 51. Cost to manufacture a preferred formulation of DDGS particleboard.

Formulation	Ratio	Component Cost (USD)
25 wt. % DDGS	0.2	0.01
75 wt. % wood flour	0.6	0.09
12.8 M acetic acid	0.2	0.39
Total cost (USD/panel)		0.49
Total cost (USD/ft^2)		0.98
Total cost (USD/m^2)		10.55

Note that these are the prices calculated based on lab scale, but the prices of boards manufactured in industrial scale are expected to be significantly cheaper due to economy of scale. The cost to manufacture a square foot of control particleboard with phenol formaldehyde resin is $0.20 lower than manufacturing a preferred formulation of DDGS particleboard, which is about 20.4% lower. The higher cost of this treated DDGS particleboard is because of the high cost of acetic acid used to functionalize DDGS, which is costlier than the combined cost of phenol formaldehyde resin and wax emulsion. Although cost is more expensive to manufacture the preferred formulation, there are hidden savings such as addressing the health and environmental issues associated with formaldehyde emissions. Additionally, mechanical properties could be traded off by reducing the acidic concentration, hence, lowering the cost of manufacturing the treated DDGS particleboard. Moreover, replacing acetic acid with less costly acids may be a suitable option, though they need to be tested to evaluate their effects on physical and mechanical properties of the particleboard.

6. CONCLUSIONS

This research was conducted to understand whether chemically treated DDGS particles can act as natural binder in wood panels and would improve the physical and mechanical properties of medium-density particleboards. Overall, this research showed that acid or alkali treated DDGS, and incorporation of higher DDGS concentrations led to detrimental mechanical properties that mainly resulted from DDGS agglomerates but displayed good moisture resistance properties. By evaluating the selected physical and mechanical properties, 12.8 M acetic acid was found to be preferred treatment to functionalize DDGS with a favored blend of DDGS concentration at 25 wt. % and a screen size of 120 μm, as detailed below.

Hypothesis 1: The protein of the DDGS can be functionalized either with acetic acid or sodium hydroxide as a natural binder in medium-density particleboards.

Conclusion 1: The chemically treated DDGS samples were analyzed via DSC, FTIR, and internal bond strength tests. Both DSC and FTIR results indicated DDGS proteins were decoupled through either acetic acid or sodium hydroxide treatment. Moreover, the particleboards met the internal bond strength requirement per ANSI A208.1-2009 standard. These tests verified that the chemically treated DDGS has a potential to act as a natural binder.

Hypothesis 2: Higher DDGS concentrations will improve the physical and mechanical properties of the particleboards.

Conclusion 2: The results from physical testing showed that acetic acid treated DDGS at higher DDGS concentrations led to lower water absorption of the particleboards than acetic acid treated DDGS at lower DDGS concentrations. This is true only for acetic acid treated DDGS, while sodium hydroxide treated DDGS failed the water absorption tests, which could be potentially due to the lower fat and protein contents. To overcome this failure in the water

absorption test, wax was incorporated to the sodium hydroxide treated DDGS formulations. For both acetic acid and sodium hydroxide blends, the linear expansion results remained statistically non-significant regardless of the DDGS concentration. The reason that 8.0 M sodium hydroxide treated DDGS formulations failed is currently unclear and investigating the feasibility of lowering the sodium hydroxide concentration may reveal why the proteins and fat in DDGS were reduced and degraded. By lowering the sodium hydroxide concentration, it may be possible to achieve better water resistance properties of particleboards without the need of wax.

For mechanical testing, screw withdrawal and static bending tests showed acceptable mechanical properties with DDGS concentrations at 10 wt. % for sodium hydroxide treatment, while 10 and 25 wt. % for acetic acid treatment. However, detrimental mechanical properties appeared with DDGS concentrations at 25 wt. % and 50 wt. % for sodium hydroxide treatment as well as at 50 wt. % for acetic acid treatment. The decrease in mechanical properties for screw withdrawal and static bending tests were because noticeable agglomerates formed for sodium hydroxide treated DDGS at DDGS concentrations of 25 wt. % and 50 wt. %, while these agglomerates of acetic acid treated DDGS formed at 50 wt. %. Moreover, hardness results displayed that DDGS particles have lower ability to resist deformation than wood flour, while both screw withdrawal and modulus of rupture results showed that DDGS aggregates may have led to even lower screw withdrawal resistance and lower flexural strength. In contrast to the screw withdrawal, static bending, and hardness tests, the results of the internal bond test of acetic acid treated DDGS did show an increasing trend in internal bond strength with increasing DDGS concentration.

Hypothesis 3: Smaller DDGS particle size will improve the mechanical properties of the particleboards.

Conclusion 3: The results of modulus of rupture, modulus of elasticity, internal bond, and hardness indicated that smaller DDGS particle size is not statistically significant to bigger DDGS particle size, while screw withdrawal results indicated better screw withdrawal resistance of particleboards with smaller DDGS particle size. Most of the mechanical results remained statistically non-significant regardless of the DDGS particle size because smaller particles may have higher potential to agglomerate compared to larger particles.

In conjunction with the good physico-mechanical properties and the environmental benefit of using chemically functionalized corn DDGS in particleboards, these particleboards may have potential in many wood-based panel industries to replace harmful synthetic resin with bio-based material.

REFERENCES

[1] M. Gürü, S. Tekeli, and I. Bilici, "Manufacturing of urea–formaldehyde-based composite particleboard from almond shell," *Mater. Des.*, vol. 27, no. 10, pp. 1148–1151, 2006.

[2] M. Puettmann, E. Oneil, and J. Wilson, "Cradle to Gate Life Cycle Assessment of US Particleboard Production," *CORRIM Rep.*, 2013.

[3] "Wood Based Panel Market Size, Share & Trends Analysis Report By Product, 2018 - 2025," Grand View Research, San Francisco, CA, Market Research Report, 2018.

[4] Y. Zheng, Z. Pan, R. Zhang, B. M. Jenkins, and S. Blunk, "Particleboard quality characteristics of saline jose tall wheatgrass and chemical treatment effect," *Bioresour. Technol.*, vol. 98, no. 6, pp. 1304–1310, 2007.

[5] D. W. Silva, M. V. Scatolino, N. R. T. do Prado, R. F. Mendes, and L. M. Mendes, "Addition of different proportions of castor husk and pine wood in particleboards," *Waste Biomass Valorization*, vol. 9, no. 1, pp. 139–145, 2018.

[6] B. H. Tisserat *et al.*, "Fiberboard Created Using the Natural Adhesive Properties of Distillers Dried Grains with Solubles," *BioResources*, vol. 13, no. 2, pp. 2678–2701, 2018.

[7] H. BuildingNetwork, "Alternative Resin Binders for Particleboard, Medium Density Fiberboard (MDF), and Wheatboard," *Health Build. NetworkMay*, pp. 1–6, 2008.

[8] Y. Li and X. Susan Sun, "Mechanical and thermal properties of biocomposites from poly (lactic acid) and DDGS," *J. Appl. Polym. Sci.*, vol. 121, no. 1, pp. 589–597, 2011.

[9] D. S. Bajwa, J. Otte, and D. Sundquist, "Functionalized Distiller's Dried Grains with Solubles for Improving Impact Properties of Polylactic Acid," *J. Biobased Mater. Bioenergy*, vol. 9, no. 2, pp. 182–187, 2015.

[10] D. J. Sundquist and D. S. Bajwa, “Dried distillers grains with solubles as a multifunctional filler in low density wood particleboards,” *Ind. Crops Prod.*, vol. 89, pp. 21–28, 2016.

[11] R. M. Rowell, *Handbook of wood chemistry and wood composites*. CRC press, 2012.

[12] R. Kumar, V. Choudhary, S. Mishra, I. Varma, and B. Mattiason, “Adhesives and plastics based on soy protein products,” *Ind. Crops Prod.*, vol. 16, no. 3, pp. 155–172, 2002.

[13] R. C. Pettersen, “The chemical composition of wood,” *Chem. Solid Wood*, vol. 207, pp. 57–126, 1984.

[14] H. Chen, *Biotechnology Of Lignocellulose: Theory and Practice*. Springer, 2014.

[15] A. Uzman, *Molecular biology of the cell: Alberts, B., Johnson, A., Lewis, J., Raff, M., Roberts, K., and Walter, P.* Wiley Online Library, 2003.

[16] ASTM International, “ASTM D1554-10 Standard Terminology Relating to Wood-Base Fiber and Particle Panel Materials,” West Conshohocken, PA, 2016.

[17] ASTM International, “ASTM D1038-11 Standard Terminology Relating to Veneer and Plywood,” West Conshohocken, PA, 2011.

[18] ASTM International, “ASTM D7033-14 Standard Practice for Establishing Design Capacities for Oriented Strand Board (OSB) Wood-Based Structural-Use Panels,” West Conshohocken, PA, 2014.

[19] “ANSI A208.1-2009. Particleboard,” National Composite Association, Leesburg, VA, 2009.

[20] R. Neulicht and J. Shular, “Emission factor documentation for AP-42. Section 10.6.2. Particleboard Manufacturing,” Midwest Research Institute, 1998.

[21] M. Hughes, “Wood and Wood Products: Manufacture of wood-based panels,” *Aalto Univ.-Finl.*, p. 63, 2016.

[22] J. Ferra *et al.*, *Wood Composites: Materials, Manufacturing and Engineering*, vol. 6. Walter de Gruyter GmbH, 2017.

[23] A. Ashori and A. Nourbakhsh, "Effect of press cycle time and resin content on physical and mechanical properties of particleboard panels made from the underutilized low-quality raw materials," *Ind. Crops Prod.*, vol. 28, no. 2, pp. 225–230, 2008.

[24] T. Tabarsa, S. Jahanshahi, and A. Ashori, "Mechanical and physical properties of wheat straw boards bonded with a tannin modified phenol–formaldehyde adhesive," *Compos. Part B Eng.*, vol. 42, no. 2, pp. 176–180, 2011.

[25] W. Gul, A. Khan, and A. Shakoor, "Impact of hot pressing temperature on medium density fiberboard (MDF) performance," *Adv. Mater. Sci. Eng.*, vol. 2017, 2017.

[26] W. Gul, A. Khan, and A. Shakoor, "Impact of Hot Pressing Pressure on Medium Density Fiberboard (MDF) Performance," *AAPPS Bull.*, 2017.

[27] T. M. Maloney, "Modern particleboard and dry-process fiberboard manufacturing," 1977.

[28] J. Xu, R. Widyorini, H. Yamauchi, and S. Kawai, "Development of binderless fiberboard from kenaf core," *J. Wood Sci.*, vol. 52, no. 3, pp. 236–243, 2006.

[29] V. Hemmilä, S. Adamopoulos, O. Karlsson, and A. Kumar, "Development of sustainable bio-adhesives for engineered wood panels – A Review," *RSC Adv.*, vol. 7, no. 61, pp. 38604–38630, 2017.

[30] C. A. R. Board, "Airborne toxic control measure to reduce formaldehyde emissions from composite wood products," *Health Saf. Code Title 17 Calif. Code Regul. Sect. 93120–9312012*, 2009.

[31] R. Shukla and M. Cheryan, "Zein: the industrial protein from corn," *Ind. Crops Prod.*, vol. 13, no. 3, pp. 171–192, 2001.

[32] W. Xu, N. Reddy, and Y. Yang, “An acidic method of zein extraction from DDGS,” *J. Agric. Food Chem.*, vol. 55, no. 15, pp. 6279–6284, 2007.

[33] N. Deo, S. Jockusch, N. J. Turro, and P. Somasundaran, “Surfactant interactions with zein protein,” *Langmuir*, vol. 19, no. 12, pp. 5083–5088, 2003.

[34] Q. Wang, W. Xian, S. Li, C. Liu, and G. W. Padua, “Topography and biocompatibility of patterned hydrophobic/hydrophilic zein layers,” *Acta Biomater.*, vol. 4, no. 4, pp. 844–851, 2008.

[35] N. Matsushima, G. Danno, H. Takezawa, and Y. Izumi, “Three-dimensional structure of maize α-zein proteins studied by small-angle X-ray scattering,” *Biochim. Biophys. Acta BBA-Protein Struct. Mol. Enzymol.*, vol. 1339, no. 1, pp. 14–22, 1997.

[36] E. Corradini, P. Curti, A. Meniqueti, A. Martins, A. Rubira, and E. Muniz, “Recent advances in food-packing, pharmaceutical and biomedical applications of zein and zein-based materials,” *Int. J. Mol. Sci.*, vol. 15, no. 12, pp. 22438–22470, 2014.

[37] V. Cabra, R. Arreguin, A. Galvez, M. Quirasco, R. Vazquez-duhalt, and A. Farres, “Characterization of a 19 kDa α-zein of high purity,” *J. Agric. Food Chem.*, vol. 53, no. 3, pp. 725–729, 2005.

[38] U.S. Department Of Energy, “Alternative Fuels Data Center: Maps and Data - Global Ethanol Production,” Oct-2018. [Online]. Available: https://afdc.energy.gov/data/10331. [Accessed: 11-Mar-2019].

[39] S. K. Tanneru and P. H. Steele, “Liquefaction of dried distiller’s grains with solubles (DDGS) followed by hydroprocessing to produce liquid hydrocarbons,” *Fuel*, vol. 150, pp. 512–518, 2015.

[40] V. Cheesbrough, K. A. Rosentrater, and J. Visser, “Properties of distillers grains composites: a preliminary investigation,” *J. Polym. Environ.*, vol. 16, no. 1, pp. 40–50, 2008.

[41] R. Bothast and M. Schlicher, “Biotechnological processes for conversion of corn into ethanol,” *Appl. Microbiol. Biotechnol.*, vol. 67, no. 1, pp. 19–25, 2005.

[42] K. A. Rosentrater, “Some physical properties of distillers dried grains with solubles (DDGS),” *Appl. Eng. Agric.*, vol. 22, no. 4, pp. 589–595, 2006.

[43] K. Liu and K. A. Rosentrater, *Distillers Grains: Production, Properties, and Utilization*. CRC Press, 2011.

[44] R. Bhadra, K. A. Rosentrater, and K. Muthukumarappan, “Cross-sectional staining and surface properties of DDGS particles and their influence on flowability,” *Cereal Chem.*, vol. 86, no. 4, pp. 410–420, 2009.

[45] H. Lin and S. Gunasekaran, “Cow blood adhesive: Characterization of physicochemical and adhesion properties,” *Int. J. Adhes. Adhes.*, vol. 30, no. 3, pp. 139–144, 2010.

[46] N. Parris and L. C. Dickey, “Adhesive properties of corn zein formulations on glass surfaces,” *J. Agric. Food Chem.*, vol. 51, no. 13, pp. 3892–3894, 2003.

[47] G. Qi and X. S. Sun, “Soy protein adhesive blends with synthetic latex on wood veneer,” *J. Am. Oil Chem. Soc.*, vol. 88, no. 2, pp. 271–281, 2011.

[48] Z. He, *Bio-based wood adhesives: preparation, characterization, and testing*. CRC Press, 2017.

[49] S. K. K. Vanga, “Thermal and Electric Field Effects on Peanut Protein Using Molecular Modeling and In-vitro Digestibility,” PhD Thesis, McGill University, 2014.

[50] L. Konermann, “Protein unfolding and denaturants,” *E LS*, 2012.

[51] A. K. Mohanty, Q. Wu, and A. Singh, "Bioadhesive from distillers' dried grains with solubles (DDGS) and the methods of making those," US7837779B2, Nov-2010.

[52] T. J. Anderson and B. P. Lamsal, "Zein extraction from corn, corn products, and coproducts and modifications for various applications: a review," *Cereal Chem.*, vol. 88, no. 2, pp. 159–173, 2011.

[53] A. J. Soulby, J. W. Heal, M. P. Barrow, R. A. Roemer, and P. B. O'connor, "Does deamidation cause protein unfolding? A top-down tandem mass spectrometry study," *Protein Sci.*, vol. 24, no. 5, pp. 850–860, 2015.

[54] ASTM International, "ASTM D1037-12 Standard Test Methods for Evaluating Properties of Wood-Base Fiber and Particle Panel Materials," West Conshohocken, PA, 2012.

[55] ASTM International, "ASTM D2395-17 Standard Test Methods for Density and Specific Gravity (Relative Density) of Wood and Wood-Based Materials," West Conshohocken, PA, 2017.

[56] A. J. Norris, "Epoxidized Sucrose Soyate as a Primary Binder in Particleboard," Master Thesis, North Dakota State University, 2018.

[57] D. J. Sundquist, "Dried Distillers Grains with Solubles as a Multifunctional Filler in Wood Particleboards," Master Thesis, North Dakota State University, 2015.

[58] D. M. Levine, P. P. Ramsey, R. K. Smidt, P. P. Ramsey, and R. K. Smidt, *Applied statistics for engineers and scientists: using Microsoft Excel and Minitab*. Prentice Hall Inc., 2001.

[59] D. C. Montgomery, *Design and analysis of experiments*, 7th ed. John wiley & sons, 2009.

[60] B. S. Blanchard and W. J. Fabrycky, *Systems engineering and analysis*, 5th ed. Prentice Hall International Series in Industrial and Systems Engineering, 2011.

[61] P. Pandey, “Hull Fiber From DDGS and Corn Grain as Alternative Fillers in Polymer Composites with High Density Polyethylene,” PhD Thesis, North Dakota State University, 2018.

[62] R. V. Morey, D. L. Hatfield, R. Sears, D. Haak, D. G. Tiffany, and N. Kaliyan, “Fuel properties of biomass feed streams at ethanol plants,” *Appl. Eng. Agric.*, vol. 25, no. 1, pp. 57–64, 2009.

[63] P. C. Bergman, A. Boersma, R. Zwart, and J. Kiel, “Torrefaction for biomass co-firing in existing coal-fired power stations,” *Energy Cent. Neth. Rep. No ECN-C-05-013*, 2005.

[64] N. Reddy, C. Hu, K. Yan, and Y. Yang, “Acetylation of corn distillers dried grains,” *Appl. Energy*, vol. 88, no. 5, pp. 1664–1670, 2011.

[65] S. Muniyasamy, M. M. Reddy, M. Misra, and A. Mohanty, “Biodegradable green composites from bioethanol co-product and poly (butylene adipate-co-terephthalate),” *Ind. Crops Prod.*, vol. 43, pp. 812–819, 2013.

[66] P. Yu, D. Damiran, A. Azarfar, and Z. Niu, “Detecting molecular features of spectra mainly associated with structural and non-structural carbohydrates in co-products from bioethanol production using DRIFT with uni-and multivariate molecular spectral analyses,” *Int. J. Mol. Sci.*, vol. 12, no. 3, pp. 1921–1935, 2011.

[67] A. Azarfar, A. Jonker, and P. Yu, “Protein structures among bio-ethanol co-products and its relationships with ruminal and intestinal availability of protein in dairy cattle,” *Int. J. Mol. Sci.*, vol. 14, no. 8, pp. 16802–16816, 2013.

[68] P. Harmsen, W. Huijgen, L. Bermudez, and R. Bakker, “Literature review of physical and chemical pretreatment processes for lignocellulosic biomass,” Wageningen UR-Food & Biobased Research, 2010.

[69] A. Istek and H. Siradag, “The effect of density on particleboard properties,” in *International Caucasian Forestry Symposium*, 2013, pp. 932–938.